AD-A044 631 NAVAL SURFACE WEAPONS CENTER WHITE OAK LAB SILVER SP--ETC F/G 7/3
THE EFFECT OF GAS BUBBLE PERCOLATION ON THE CARBONACEOUS MESOPH--ETC(U)
SEP 76 D O RESTER

UNCLASSIFIED NSWC/WOL/TR-76-113 NL

1 OF 2
ADA044631

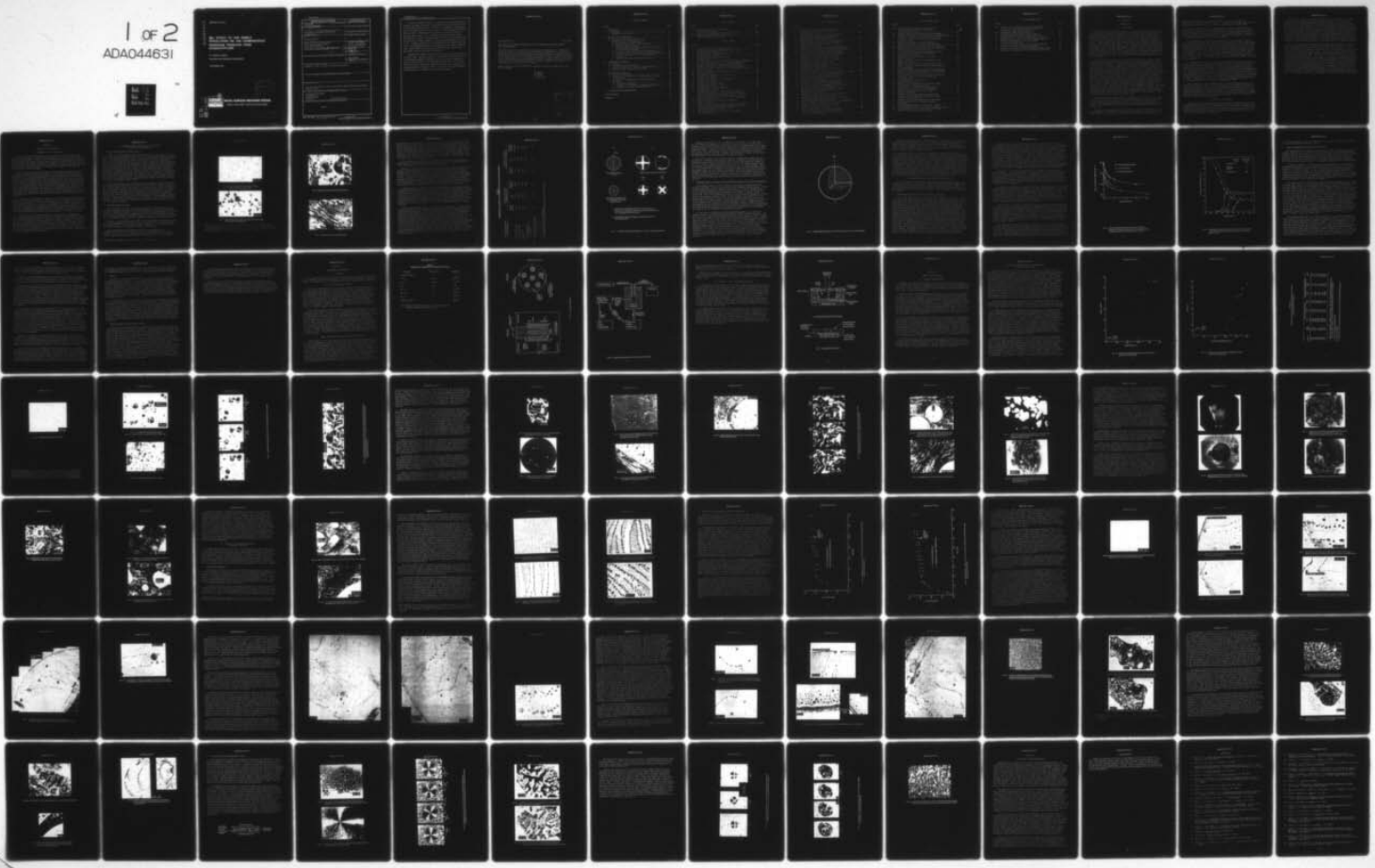

NSWC/WOL TR 76-113

THE EFFECT OF GAS BUBBLE PERCOLATION ON THE CARBONACEOUS MESOPHASE PRODUCED FROM ACENAPHTHYLENE

BY DENNIS O. RESTER

RESEARCH AND TECHNOLOGY DEPARTMENT

1 SEPTEMBER 1976

NAVAL SURFACE WEAPONS CENTER

Dahlgren, Virginia 22448 • Silver Spring, Maryland 20910

UNCLASSIFIED

SECURITY CLASSIFICATION OF THIS PAGE *(When Data Entered)*

REPORT DOCUMENTATION PAGE	READ INSTRUCTIONS BEFORE COMPLETING FORM
1. REPORT NUMBER: NSWC/WOL/TR-76-113 (14) ✓	2. GOVT ACCESSION NO. / 3. RECIPIENT'S CATALOG NUMBER
4. TITLE *(and Subtitle)*: (6) The Effect of Gas Bubble Percolation on the Carbonaceous Mesophase Produced from Acenaphthylene	5. TYPE OF REPORT & PERIOD COVERED / 6. PERFORMING ORG. REPORT NUMBER
7. AUTHOR(s): (10) Dennis O. Rester	8. CONTRACT OR GRANT NUMBER(s) (16)
9. PERFORMING ORGANIZATION NAME AND ADDRESS: Naval Surface Weapons Center ✓ White Oak Laboratory White Oak, Silver Spring, Maryland 20910	10. PROGRAM ELEMENT, PROJECT, TASK AREA & WORK UNIT NUMBERS: 62761N; SEASF54-594; SF54594501; WR3501; (17)
11. CONTROLLING OFFICE NAME AND ADDRESS (12) 92 p. (11)	12. REPORT DATE: 1 Sept 76 / 13. NUMBER OF PAGES: 126
14. MONITORING AGENCY NAME & ADDRESS *(if different from Controlling Office)*	15. SECURITY CLASS. *(of this report)*: UNCLASSIFIED / 15a. DECLASSIFICATION/DOWNGRADING SCHEDULE

16. DISTRIBUTION STATEMENT *(of this Report)*

Approved for public release; distribution unlimited

17. DISTRIBUTION STATEMENT *(of the abstract entered in Block 20, if different from Report)*

18. SUPPLEMENTARY NOTES

This technical effort is part of the Reentry Vehicle Materials Technology (REVMAT) Program

19. KEY WORDS *(Continue on reverse side if necessary and identify by block number)*

Carbonaceous Mesophase
Acenaphthylene
Liquid Crystals
Pyrolysis
Hot stage microscopy

20. ABSTRACT *(Continue on reverse side if necessary and identify by block number)*

(Over)

DD FORM 1 JAN 73 1473 EDITION OF 1 NOV 65 IS OBSOLETE
S/N 0102-014-6601

UNCLASSIFIED

SECURITY CLASSIFICATION OF THIS PAGE *(When Data Entered)*

391 596

A study of mesophase formation in acenaphthylene was undertaken in an attempt to determine the effect of gas bubble percolation during pyrolysis on the mesophase microstructure. Samples of acenaphthylene approximately 20 g in size were pyrolyzed in test tubes to various temperatures between 400°C and 500°C. Examination of the pyrolysis residues revealed that mesophase spheres up to 14 μm in diameter were formed during heating acenaphthylene to 404°C. During heating to 450°C, the spheres grew in size and coalesced to produce regions of fluid coalesced mesophase up to 2 mm in size. Complete conversion to the mesophase occurred between 466°C and 500°C. The mesophase produced from acenaphthylene was found to contain a small amount (<20%) of the fine fibrous microstructure characteristic of good needle cokes used in graphite manufacture.

Acenaphthylene samples about 20 mg in size were pyrolyzed on a microscope hot stage. Mesophase formation, coalescence, and deformation due to gas bubble percolation was observed directly at pyrolysis temperatures between 413°C and 455°C. After mesophase formation began at 413°C, gas bubble percolation through the sample was found to cause coalescence of mesophase droplets, formation of defect structures in coalesced droplets, and deformation or stretching of the coalesced mesophase.

NSWC/WOL/TR 76-113 1 Sept 1976

THE EFFECT OF GAS BUBBLE PERCOLATION ON THE CARBONACEOUS MESOPHASE PRODUCT FROM ACENAPHTHYLENE

This report presents the results of a study of the formation of the carbonaceous mesophase during the pyrolysis of the hydrocarbon acenaphthylene. The work was primarily directed toward determination of the influence of gas bubble percolation on mesophase formation and coalescence of mesophase droplets. A literature survey of the characteristics of the carbonaceous mesophase is also included in the report. Both the literature survey and experimental work was submitted by the author to the University of Maryland Graduate School as a thesis in partial fulfillment of the requirements for a Master of Science degree.

Support for this study was provided by the Naval Sea Systems Command under Task No. SF 54594501.

J. DIXON
By direction

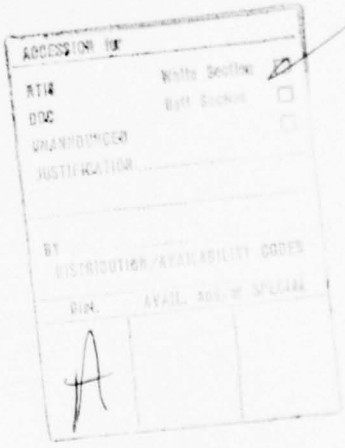

TABLE OF CONTENTS

Chapter		Page
I.	INTRODUCTION	1
	A. Background	1
	B. Statement of the Problem	2
II.	REVIEW OF THE LITERATURE	5
	A. Importance of the Fluid State	5
	B. Mesophase Sphere Formation and Growth During Pyrolysis of Hydrocarbons	6
	1. General Microstructural Characteristics	6
	2. Mesophase Sphere Structure	6
	3. Mesophase Sphere Coalescence and the Microstructure of the Coalesced Mesophase	12
	C. Factors Which Control the Mesophase Microstructure	14
	1. Temperature, Heat Treatment Time, and Rate of Heating	14
	2. Chemical Composition of the Precursor Material	18
	3. Pressure	20
	4. Insoluble Particles and Material Surfaces	20
III.	EXPERIMENTAL TECHNIQUES	23
	A. Reagents	23
	B. Test Tube Pyrolysis Methods	23
	C. Sample Preparation for Polarized Light Microscopy	23
	D. Pyrolysis Using a Microscope Hot Stage	27
IV.	RESULTS AND DISCUSSION	29
	A. General Considerations	29
	B. Mesophase Transformation in Acenaphthylene Pyrolyzed in Test Tubes	30
	C. Pyrolysis of Acenaphthylene Using a Microscope Hot Stage	50
	1. Preliminary Experiments	50
	2. Influence of Gas Bubbles on Mesophase Formation	55
	3. Formation of Fibrous Extinction Crosses	78
V.	CONCLUSIONS AND RECOMMENDATIONS	87
ACKNOWLEDGEMENTS		88
REFERENCES		R-1

LIST OF TABLES

Table		Page
I.	Comparison of Properties of Mesophase from Various Precursors	10
II.	Properties of Acenaphthylene Used in This Study	24
III.	Chemical Analysis Data on Acenaphthylene Samples Pyrolyzed in Test Tubes	33

LIST OF FIGURES

Figure		Page
1.	Initial Formation of Mesophase Spheres	7
2.	Growth and Coalescence of Mesophase Spheres Due to Increases in Temperature	7
3.	Advanced Stages of Sphere Coalescence	8
4.	Completely Coalesced Mesophase	8
5.	The Molecular Arrangement in an Ideal Mesophase Sphere	11
6.	Mesophase Sphere with an "Onion Skin" Molecular Arrangement.	13
7.	Heat Treatment Temperature - Time Curves Showing the Conditions Necessary for Mesophase Sphere Formation	16
8.	Mesophase Formation as a Function of Temperature for Three Coker Feedstocks Heated at 5°C/hr from 360°C to 510°C.	17
9.	Pyrolysis Furnace	25
10.	Control Equipment for the Pyrolysis Furnace	26
11.	Microscope Hot Stage	28
12.	Acenaphthylene Weight Loss as a Function of Pyrolysis Temperature	31
13.	C/H Ratio as a Function of Acenaphthylene Pyrolysis Temperature	32
14.	Acenaphthylene Heated to 404°C	34
15.	Acenaphthylene Heated to 426°C	35
16.	Acenaphthylene Heated to 450°C	35
17.	Mesophase Spheres Formed by Heating Acenaphthylene to 450°C	36
18.	Acenaphthylene Heated to 450°C Showing Extinction Contour Changes Due to Rotating the Plane of Polarized Light (Crossed Polarizers) Clockwise from 0° to 60°	37
19.	Reflected Polarized Light Photomicrograph of Mesophase Sphere Coalescence	39
20.	Reflected Light Photomicrograph of Mesophase Sphere Coalescence	39
21.	Reflected Light Photomicrograph of Micron Size Mesophase Spheres Formed During Heating Acenaphthylene to 450°C	40
22.	Coalesced Mesophase and Mesophase Spheres in Acenaphthylene Heated to 450°C	40
23.	Fibrous Microstructure in the Coalesced Mesophase from Acenaphthylene	41

LIST OF FIGURES (Cont)

Figure		Page
24.	Coalesced Mesophase with a Coarse Isotropic Microstructure Formed During Pyrolysis of Acenaphthylene to 450°C	42
25.	Coarse Fibrous Microstructure (Region B) Near a Gas Pore in the Coalesced Mesophase Formed During Heating Acenaphthylene to 450°C	43
26.	Higher Magnification of Region B in Figure 25	43
27.	Reflected Light Photomicrograph of an Extracted Sample of Mesophase Produced During Heating Acenaphthylene to 450°C	44
28.	Extracted Mesophase Spheres and Coalesced Mesophase Particles Observed with a Scanning Electron Microscope	44
29.	Mesophase Spheres Separated by Extraction and Photographed Using a Scanning Electron Microscope	46
30.	Scanning Electron Photomicrograph of Mesophase Spheres Isolated by Extracting a Sample of Acenaphthylene Which Was Pyrolyzed to 450°C	47
31.	Higher Magnification of Region A in Figure 30	47
32.	Mesophase Growth and Coalescence in an Acenaphthylene Sample Heated to 466°C	48
33.	Completely Coalesced Mesophase in a Sample of Acenaphthylene Heated to 500°C	49
34.	Acenaphthylene Completely Transformed into the Coalesced Mesophase at 500°C	49
35.	Fibrous Microstructure in Acenaphthylene Pyrolyzed to 500°C.	51
36.	Fine Fibrous Microstructure Around a Gas Pore in an Acenaphthylene Sample Heated to 500°C	51
37.	Mesophase Droplet Formation During Hot Stage Pyrolysis of Acenaphthylene	53
38.	Strings of Coalesced Mesophase Droplets Formed During Hot Stage Pyrolysis of Acenaphthylene	53
39.	Gas Bubble Tracks in the Mesophase Produced During Hot Stage Pyrolysis of Acenaphthylene	54
40.	Mesophase Droplet Coalescence Caused by Bubble Percolation in an Acenaphthylene Sample Pyrolyzed on a Hot Stage	54
41.	Temperature - Time Cycle for Hot Stage Pyrolysis of Acenaphthylene, Maximum Heating Rate	56
42.	Temperature - Time Cycle for Hot Stage Pyrolysis of Acenaphthylene, Minimum Heating Rate	57
43.	Initial Formation of Mesophase Droplets in Acenaphthylene Heated to 421°C on the Microscope Hot Stage	59
44.	Strings of Coalesced Droplets of Mesophase Formed by Gas Bubble Percolation	60
45.	Higher Magnification of Region A in Figure 44	60
46.	Accelerated Coalescence of Mesophase Droplets Due to Gas Bubble Percolation During Hot Stage Pyrolysis of Acenaphthylene	61

LIST OF FIGURES (Cont)

Figure		Page
47.	Coalesced Mesophase Droplets Outlining the Path of Gas Bubbles Which Formed During Acenaphthylene Pyrolysis	61
48.	Composite Photograph Showing Strings of Mesophase Droplets Formed by Gas Bubble Percolation During Pyrolysis	62
49.	Gas Bubble (C) Trapped in a Bubble Track by Rapid Cooling of a Sample of Acenaphthylene Pyrolyzed On the Hot Stage	63
50.	Composite Photograph of Mesophase Droplets Ordered During Pyrolysis by Gas Bubble Movement	65
51.	Higher Magnification of Regions A and B in Figure 48	66
52.	Mesophase Droplets Showing a Torn Surface with Only Partial Contact with the Cover Glass	67
53.	Coalesced Mesophase Droplets Outlining One Side of a Gas Bubble Which Formed During Hot Stage Pyrolysis of Acenaphthylene	69
54.	Photograph of the Bottom Side of the Area Shown in Figure 53	69
55.	Bands of Coalesced Mesophase at the Edge of the Sample Cover Glass	70
56.	Bands of Coalesced Mesophase Which Formed at the Edge of the Liquid Sample During Hot Stage Pyrolysis of Acenaphthylene	71
57.	Coalesced Mesophase with an Isotropic Microstructure Formed During Heating Acenaphthylene to Approximately 455°C on the Microscope Hot Stage	72
58.	Coalesced Mesophase Formed by Gas Bubble Percolation Through an Acenaphthylene Sample Pyrolyzed on the Hot Stage	73
59.	Untransformed Pitch Entrapped in the Coalesced Mesophase	73
60.	Region of Coalesced Mesophase Containing a High Concentration of Extinction Crosses	75
61.	Large Droplet of Coalesced Mesophase Formed During Hot Stage Pyrolysis of Acenaphthylene	75
62.	Stretched Out Extinction Crosses in the Coalesced Mesophase	76
63.	Extinction Crosses Deformed to Produce Nearly Parallel Lines in the Coalesced Mesophase from Pyrolysis of Acenaphthylene	76
64.	Mesophase Droplets Stretched and Torn Apart Due to Stresses Caused By Gas Bubble Formation and Movement	77
65.	Fibrous Extinction Crosses Observed in a Sample of Acenaphthylene Pyrolyzed on the Microscope Hot Stage	79
66.	Single Extinction Cross Illustrating the Fibrous Nature of the Extinction Cross Brushes	79

LIST OF FIGURES (Cont)

Figure		Page
67.	Changes in the Orientation of Fibrous Extinction Crosses Due to Clockwise Rotation of the Plane of Polarized Light (Crossed Polarizers)	80
68.	Transmitted Light Photomicrograph of Acenaphthylene Pyrolyzed on the Hot Stage	81
69.	Reflected Polarized Light (Crossed Polarizers) Photomicrograph of the Same Region Shown in Figure 68	81
70.	Polished Cross Section of an Ideal Mesophase Sphere Sectioned Perpendicular to Its Axis Above or Below the Median Plane	83
71.	Co-rotating (A) and Counter-Rotating (B) Extinction Crosses in a Droplet of Coalesced Mesophase	84
72.	Extinction Crosses in Coalesced Mesophase Formed During Pyrolysis of Acenaphthylene on the Microscope Hot Stage . . .	85

CHAPTER I

INTRODUCTION

A. BACKGROUND

The importance of manufactured graphite as a high temperature material is due to its combination of metallic and nonmetallic properties, and the large variety of properties obtainable through variations in the microstructure. Manufactured graphite materials are "polycrystalline", since they are composed of areas with a near perfect graphite crystal structure (these areas are called crystallites) connected by areas of amorphous carbon. The crystallites are composed of parallel layers of carbon atoms. Each layer contains carbon atoms arranged in a hexagonal pattern. The term "amorphous carbon" is used to describe the many disordered forms of carbon whose structure and properties are intermediate between the two extremes represented by natural graphite and diamond. Amorphous carbon may also consist of small groups and in some cases ribbons of carbon layer planes of varying sizes with little three-dimensional order. The properties of polycrystalline or manufactured graphites are determined by the size, shape, orientation, and defect structure of the crystallites, and the nature of the amorphous carbon regions holding the crystallites together.

The polycrystalline structure of manufactured graphites is developed during heating certain carbon based (organic) materials such as petroleum pitches to temperatures as high as 2800°C. This heating process is called "graphitization", and it results in the formation of crystallites whose three-dimensional structure is similar to that of the ideal graphite crystal structure. Since the graphitization process produces a polycrystalline material, it is necessary to define a method to distinguish betwen materials whose crystallites have different degrees of disorder. The term "degree of graphitization" is used to indicate the relative degree to which the crystallite structure developed during graphitization approaches the ideal structure of single crystal graphite. An ideal graphite crystal has an interlayer spacing[1] (crystal semilattice spacing) of 0.3350 nm. Interlayer spacings from 0.3350 to 0.3354 nm have been reported[2,3] for natural graphite. Organic materials which develop an average interlayer spacing less than 0.3360 nm during graphitization (heating to 2800°C) usually considered[2] to be "graphitizing organics". A graphitizing organic is said to form a "well ordered graphitic structure" on heating to 2800°C or to have a high "graphitizability". In contrast to the above discussion, an organic heated to 2800°C which develops an average interlayer spacing greater than 0.3360 nm may be classified as a "non-graphitizing" organic, since the higher interlayer spacing indicates a large number of defects in the crystallites. Such a material would have a low degree of graphitization.

The average stacking height of the layer planes in crystallites is also used as an indication of the relative degree of graphitization. For example, acenaphthylene is a graphitizing organic. It produces a graphitized material with an average interlayer spacing of 0.3356 nm[4] and an average crystallite height of about 45 nm.[5] Non-graphitizing organics usually have an average crystallite height of 5 nm or less.

Pyrolysis and carbonization are two additional terms used frequently in the carbon industry. Carbonization is defined as the process of converting an organic into carbon by heat treatment. This process is 99% complete after heating to

1000°C, and carbonization is generally referred to as a heat treatment to temperatures in the range of 1000 - 1200°C. Pyrolysis, on the other hand, is used to describe the heat treatment of organics to temperatures less than 500°C.

It must be remembered that the classification of terms as described above is arbitrary, and based on the average properties of a sample. Due to the nature of polycrystalline materials, a manufactured graphite contains small regions which could be classified as amorphous carbon (no three-dimensional order). Likewise, an organic classified as non-graphitizing may also form a small number of nearly perfect graphite crystallites during heating to 2800°C.

The development of polycrystalline graphites has been empirical in nature, since the fabrication procedure involves the carbonization of complex carbon based materials (pitches and cokes) of unknown chemical composition. As a result, little progress has been made in developing a scientific basis for control of the microstructure, and therefore the properties, of graphitic materials. However, it has recently been shown[6] that the microstructure and properties of graphitic materials are determined by the characteristics of an ordered fluid which is formed during the pyrolysis of certain pitches and hydrocarbons used as precursors for manufactured graphite. This ordered fluid forms in the 370 - 500°C temperature range, has many of the properties of a nematic liquid crystal, and has been termed the "carbonaceous mesophase".

The carbonaceous mesophase is observed initially[6-9] as optically anisotropic spheres of micron size. These spheres grow in size and coalesce with increases in heat treatment time and temperature to produce an optically anisotropic fluid, referred to as the coalesced mesophase. The coalesced mesophase is composed of nearly parallel layers of large planar aromatic molecules, with no three-dimensional order and numerous stacking defects. This ordering of planar aromatic molecules is the beginning of the development of the graphite crystal structure. The number and kinds of stacking defects in the coalesced mesophase at the temperature of mesophase solidification determines the type of graphitic crystallites formed during heating to 2800°C. Therefore, the properties of manufactured graphites are controlled by the ordering developed in the coalesced mesophase below 500°C.

The following study deals primarily with the general characteristics of the carbonaceous mesophase produced during the pyrolysis of acenaphthylene, and the affect of gas bubble percolation on the mesophase microstructure. A review of our current understanding of the physical and microstructural characteristics of the carbonaceous mesophase is given in Chapter II. This review illustrates the importance of the mesophase in determining the microstructure and properties of graphitic materials, and discusses those factors which are known to affect the ordering of molecules in the carbonaceous mesophase.

B. STATEMENT OF THE PROBLEM

Decomposition and dehydrogenation reactions which occur during the pyrolysis of mesophase forming organics at atmospheric pressure are known to produce large volumes of volatile organics. Since the mesophase is fluid, the formation of gas bubbles in the mesophase-untransformed pitch mixture and the stirring action of the these bubbles as they move through the mesophase would be expected to have some influence on the mesophase microstructure.

Both Dubois, et al.[10] and White, et al.[11-13] have reported that gas bubble percolation in the completely coalesced mesophase produces a fine texture of extinction contours around pores formed by the gas bubbles. This fine texture represents both stacking defects in the molecular layers and folded layers in the mesophase. Thus, the microstructure near a pore produced by gas bubble formation in the coalesced mesophase has a structure entirely different from regions at some distance from the pore. Nucleation, growth, and percolation of gas bubbles through the coalesced mesophase was reported[10,11,12] to increase the density of molecular layer stacking defects and folds by several orders of magnitude when compared to samples of freshly coalesced mesophase. It was postulated that since the coalesced mesophase is a viscous fluid, gas bubble percolation results in plastic flow and deformation of the coalesced mesophase. The strains produced increase the number of defects in the ideal layer structure of the molecules in the coalesced mesophase.

White and Price have also reported[14] that bubble percolation in a fluid coalesced mesophase just prior to mesophase solidification (see Chapter II, Section C.2) is responsible for formation of the fine fibrous microstructure. The fine fibrous microstructure is important because it is the characteristic microstructure found in highly graphitizing needle cokes. However, the studies mentioned above are all based on polarized light observation of mesophase samples cooled to room temperature. There is no direct evidence which shows the influence of gas bubbles on the mesophase microstructure. This study is an attempt to determine by direct observation the affect of gas bubble formation and percolation on mesophase spheres and on the microstructure of the coalesced mesophase produced from acenaphthylene. Acenaphthylene was selected for study since it is known to form the mesophase[15,16] and produces a well ordered graphite[4] on heating to 2800°C. Since the chemical reactions which occur during the pyrolysis of acenaphthylene are known,[4] interpretation of the results will be more meaningful. It is hoped that the results will identify some additional factors which determine the characteristics of the mesophase microstructure. Control of the microstructure of the coalesced mesophase will allow one to control or tailor the properties of manufactured graphitic materials.

not solidify immediately after complete coalescence produce a well ordered graphitic

CHAPTER II

REVIEW OF THE LITERATURE

A. IMPORTANCE OF THE FLUID STATE

It has long been recognized that pitches, polymers, and hydrocarbons may be divided into two groups: (1) those which graphitize or form three-dimensional order on heat treatment to 2800°C, and (2) those which do not graphitize. Materials which graphitize are known to exhibit regions of optical anisotrophy when observed under polarized light after carbonization. Ramdohr[17] was one of the first investigators to report in detail on the optical anisotropy of graphitizing materials which had been heat treated above 500°C. He used the term "mosaic" to describe the observed microstructural features.

After Ramdohr's paper in 1928, numerous investigators described the optical anisotropy of graphitizing materials (mostly coals) which had been heat treated above 500°C. However, little progress was made in relating the microstructural characteristics of graphitizing materials to the processes which occur during carbonization until Mackowsky's[18] work was published in 1951. She observed that the size of the optically anisotropic regions in thermally treated coals was dependent upon the degree of plasticity which developed during heating from room temperature to 550°C. Although numerous papers were published describing the "mosaic" structure of carbonized materials, little interest was developed in the microstructural changes which occur during the heat treatment of graphitizing materials in the temperature range below 500°C. The importance of the microstructural changes which occur during this temperature range, and the potential of microscopy as a method of documenting these changes was not fully realized until the late Fifties and early Sixties.[19]

In a series of investigations by Kipling, et al.,[20] and later by Kipling and Shooter,[21,22,23] the significance of the existence of a fluid state during carbonization was established. Polymers and hydrocarbons which could be classified as graphitizing were shown to be optically anisotropic after a 700°C heat treatment, indicating that some degree of molecular orientation had occurred during the early stages of carbonization. The existence of the fluid state during carbonization was postulated by Kipling and co-workers and later by Ihnatowicz, et al.[24] to permit the molecular orientation necessary for the development of a graphitic structure.

The existence of a fluid state during the early stages of carbonization (400 - 500°C) is necessary if the material is to develop a highly graphitic structure on heat treatment to 2800°C.[25] The extent or degree of molecular mobility in the 400 - 500°C temperature range determines the extent of formation of crystalline preorder, and therefore, the graphitizability of the material. Organic materials which do not go through a state of fusion during pyrolysis at 400 - 500°C produce non-graphitizing or disordered carbons. There are exceptions (i.e., materials which do not fuse but graphitized on heat treatment to 2800°C); but in each case reported, either metal catalysts were present or some form of "stress carbonization" or "stress graphitization" was employed.

B. MESOPHASE SPHERE FORMATION AND GROWTH DURING PYROLYSIS OF HYDROCARBONS

1. General Microstructural Characteristics

In 1961, Taylor[26] discovered that graphitizing organics can exist in a state whose structure is intermediate between that of an isotropic fluid and a crystalline solid. This ordered fluid was found to exist in the 400 - 500°C temperature range, and was investigated in detail by Brooks and Taylor[6-9] during the pyrolysis of organics such as naphthacene and coke oven pitches. Samples of organics heated to 400 - 500°C were cooled to room temperature, sectioned, polished, and observed using polarized light microscopy. The observations made on samples heated to different temperatures may be described as follows. As the temperature was increased, the organic material melted to form an isotropic fluid which developed a pitch-like nature due to decomposition of the starting material. Molecular rearrangements and condensation reactions occurred to form large polynuclear aromatics. At temperatures above 400°C, optically anisotropic spheres of micron size began to appear in the isotropic pitch (see Figure 1). The temperature required for sphere formation varied with the original chemical composition of the organic being pyrolyzed, but was usually in the range of 400 - 450°C.

Increases in heating time or temperature of the material in which the spheres had formed resulted in nucleation of new spheres and growth of spheres. When two or more spheres made contact, coalescence of spheres occurred in three dimensions to give a more complex structure (see Figure 2). Crowding and coalescence of spheres caused deviations from the spherical shape when the transformation to the ordered fluid was more than 50% complete. As coalescence of spheres became extensive, growth of the ordered fluid occurred primarily around the edges of large regions of coalesced spheres as shown in Figure 3, page 8 instead of through sphere nucleation and growth. The process of sphere growth and coalescence was continued until the isotropic fluid pitch had been completely converted into a viscous "mosaic" structure (see Figure 4, page 8).

2. Mesophase Sphere Structure

The ordered fluid observed by Brooks and Taylor[6-9] during the pyrolysis of graphitizing organics has many of the characteristics of certain types of "liquid crystals". Therefore the term "carbonaceous mesophase" or "mesophase"* was selected to describe the spheres and the complex mosaic structure formed by sphere coalescence. Both the spheres and the mosaic represent a state of aggregation with properties intermediate between those of an isotropic liquid and a crystalline solid.

Elemental analysis,[9-16] infrared[9,16,27] and ultraviolet[9,27] absorption spectroscopy, mass spectroscopy,[28-31] nuclear magnetic resonance,[16] and molecular weight determinations[9,16,27] have provided conclusive evidence that the mesophase spheres are composed primarily of polynuclear aromatic hydrocarbons.

These results along with studies by Lewis, Singer, Edstrom, and co-workers[2,27,32-38] on the carbonization of pure hydrocarbons have led to the following explanation of the chemical changes which produce mesophase formation. Organics which form the mesophase undergo a continuous series of decomposition,

*(Gk. "meso" - intermediate; and "phasis' - state or phase)

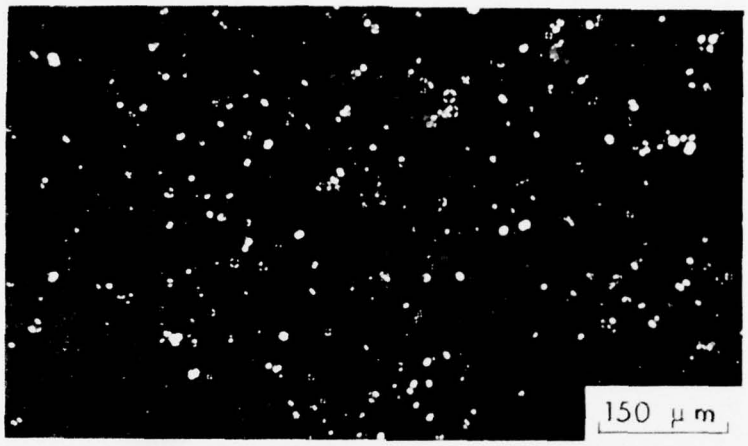

FIG. 1*. INITIAL FORMATION OF MESOPHASE SPHERES
(Black Background is Isotropic Pitch)

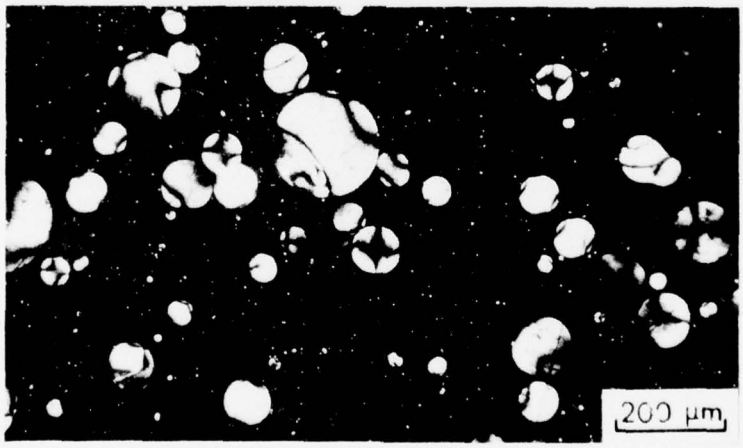

FIG. 2. GROWTH AND COALESCENCE OF MESOPHASE SPHERES DUE TO INCREASES IN TEMPERATURE

*Figures 1 - 4 are reflected polarized light photomicrographs of polished samples of pyrolyzed acenaphthylene. However, these figures may be used to illustrate the general characteristics of mesophase formation, growth, and coalescence which occurs during the pyrolysis of any highly graphitizing organic material.

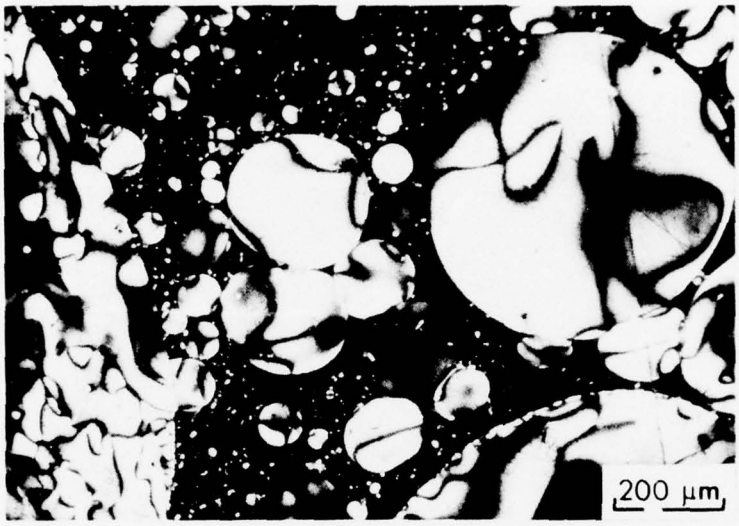

FIG 3. ADVANCED STAGES OF SPHERE COALESCENCE

FIG. 4. COMPLETELY COALESCED MESOPHASE

dehydrogenation, rearrangement, and condensation reactions during heating to 400 - 500°C. These reactions produce a pitch material composed of tens to hundreds of different aromatic ring systems, even when the starting material is a pure hydrocarbon. Dehydrogenation results in the formation of planar aromatic free radicals,[39] and is followed by rearrangement and condensation reactions which steadily increase the size of the aromatic molecules and the C/H ratio. Thus, large aromatics are formed by a process which may be described as a free radical polymerization. Continuation of the temperature-time cycle leads to formation of aromatic molecules of sufficient size to form mesophase spheres.

Since mesophase spheres[40] and the coalesced mesophase[14,24] are insoluble in organic solvents such as pyridine and quinoline, they may be separated from the untransformed pitch using solvent extraction techniques.

Results of studies on individual spheres indicate that molecules with molecular weights in the range of 900[16] to 1700[8] (about 25 to 50 rings) are necessary for mesophase sphere formation (see Table I). Table I illustrates that the sphere formation process separates the heavier molecules from the lower molecular weight species. As a result, mesophase spheres have a density of 1.4 to 1.5 g/cm^3 compared to about 1.3 g/cm^3 for the organics not converted into the mesophase. Mesophase spheres also contain a high concentration of free radicals,[16] and condensation reactions continually increase the molecular size of the planar aromatic molecules in the mesophase. As the pyrolysis continues, essentially all the organics are converted into large planar molecules which are ordered into the mesophase.

Although aliphatic components have been identified in the mesophase produced during pyrolysis of petroleum and coal tar pitches,[41,42,43] it is believed that any aliphatic character present is due to aliphatic side chains attached to the aromatic ring systems. Heterocyclics have also been identified in the mesophase produced from coal tar pitch pyrolysis. Apparently, the mesophase may contain small amounts of non-aromatic species, depending on the original chemical composition of the organic being pyrolyzed. Yamada[40] has reported that the mesophase produced from an asphalt may contain more aliphatic character than aromatic (see Table I). This report[40] is the only known example of a mesophase composed primarily of aliphatic compounds.

Although the mesophase spheres are fluid at the temperature of formation, they solidify on cooling to room temperature and may be polished for observation under polarized light microscopy. *Brooks and Taylor*[6-9] found that an ideal mesophase sphere has a lamellar structure as shown in Figure 5 with an axis of symmetry perpendicular to the lamellae. This structure was suggested by the nature of the extinction contours observed under polarized light (see Figure 5), and the electron diffraction patterns obtained from a single sphere. The extinction contours observed on polished cross-sections of mesophase spheres represent points where the edges of the large planar aromatic molecules in the spheres are either perpendicular or parallel to the plane of polarized light. In an ideal mesophase sphere, the layers of aromatic molecules are about 0.35 nm[9] apart and are curved in a manner such that they are approximately normal to the surface of the sphere. The structure of mesophase spheres discussed above has also been confirmed by White, et al.[11,12], Dubois, et al.[10], and Honda, et al.[44] in their studies of pyrolysis of a variety of different pitches.

TABLE I
COMPARISON OF PROPERTIES OF MESOPHASE FROM VARIOUS PRECURSORS

Material Pyrolyzed and Reference	Insoluble Fraction (Mesophase) (b)			Soluble Fraction (Uncoverted Organics)		
	Density g/cm^3	C/H	Molecular Weight	Density g/cm^3	C/H	Molecular Weight
Coke Oven Pitch[8]	1.4	(a)	1700	(a)	(a)	400-470
Coal Tar Pitch[40]	1.46	2.45	(a)	1.30	1.79	(a)
Asphalt[40]	1.47	1.80	(a)	1.21	1.05	(a)
Acenaphthylene[16] (50% Conversion to Mesophase)	1.5	2.23	900	1.32	1.81	900
Acenaphthylene, This Work (Coalesced Mesophase)	1.5	(a)	(a)	(a)	(a)	(a)

(a) Not reported or not determined
(b) Separated from non-mesophase material by solvent extraction.

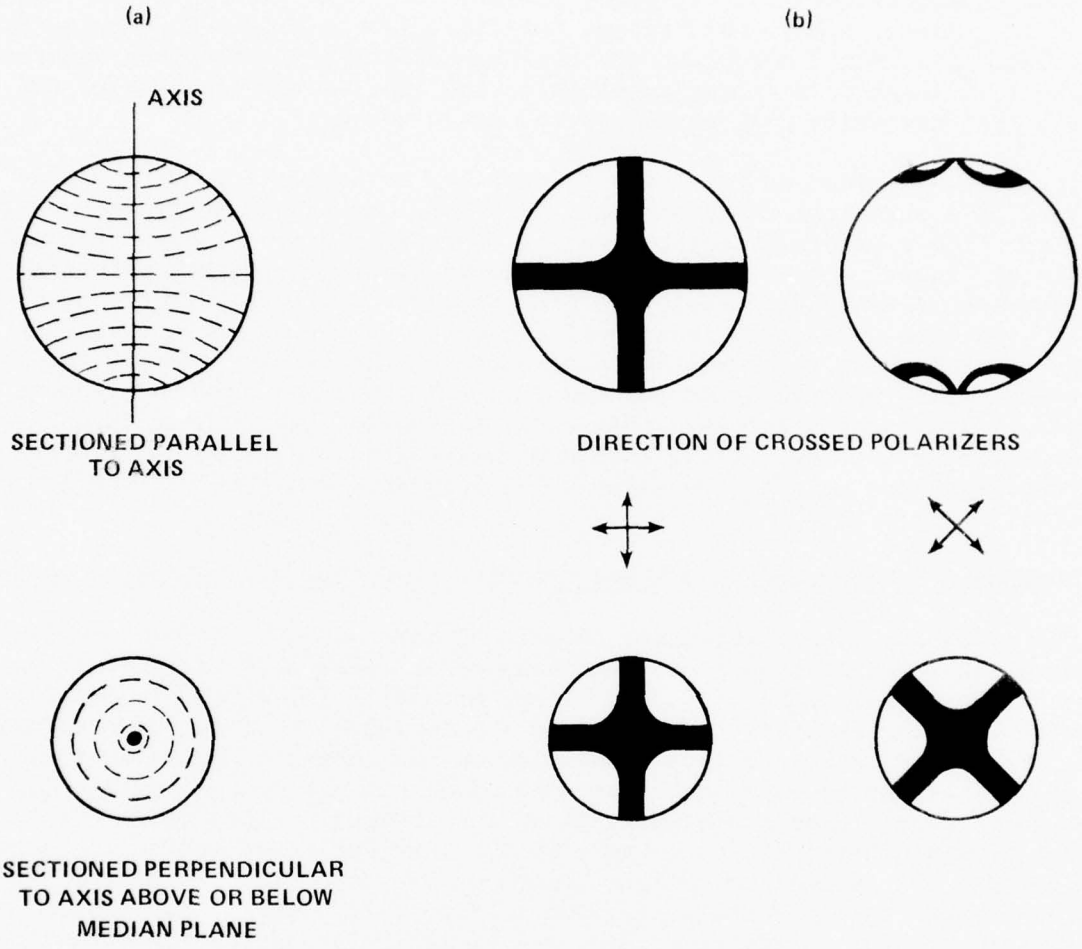

(a) DASHED LINES REPRESENT EDGES OF LARGE AROMATIC MOLECULES. AN IDEAL SPHERE HAS THE OPTICAL PROPERTIES OF A UNIAXIAL POSITIVE CRYSTAL.

(b) EXTINCTION CONTOURS OBSERVED UNDER REFLECTED POLARIZED LIGHT.

FIG. 5. THE MOLECULAR ARRANGEMENT IN AN IDEAL MESOPHASE SPHERE

Mesophase formation is a type of demixing of two fluids. It is the result of: (1) the increasing probability of alignment of planar molecules as their size increases (due to van der Waals forces) and (2) the increased mobility of the large planar molecules as the heat treatment temperature is increased to the 400 - 500°C temperature range. Spheres are formed initially due to differences in surface tension between the liquid mesophase and the untransformed liquid pitch material.[9] The spherical shape is required to minimize the interfacial exposure of the large planar aromatics, which also minimized the surface energy.

Only one exception to the initial formation at atmospheric pressure of the mesophase in a spherical shape has been reported. Mesophase particles separated by extraction from a partially carbonized coal tar pitch were observed by Yamada, et al.[41] to be "lemon" shaped if less than 5 μm in size. The common spherical shape was observed for mesophase particles larger than 5 μm. In related studies, Honda, et al.[45] reported that carbonization of a coal tar pitch to which 5% carbon black was added resulted in the formation of mesophase spheres with a different molecular arrangement than reported by Brooks and Taylor.[9] This new mesophase sphere type consists of layers of molecules arranged in an "onion skin" manner (see Figure 6). An onion skin arrangement of the layers of molecules in a mesophase sphere has also been reported[78] for mesophase spheres which form around micron size carbon black particles.

3. Mesophase Sphere Coalescence and the Microstructure of the Coalesced Mesophase

The mesophase sphere structure (Figure 5) determined by Brooks and Taylor represents an ideal case near the beginning of the mesophase transformation. Growth of these spheres may occur in either of two methods: (1) direct incorporation of molecules into the mesophase spheres, and (2) coalescence of two or more spheres. In the first case, sphere growth is similar to the growth of nematic liquid crystals.[46] It may be represented as a physical process which involves the ordering of the large aromatic molecules present in the isotropic fluid pitch.[28,47] The physical growth process can occur only if large aromatics of sufficient size and concentration are formed thermally. Mesophase sphere coalescence may occur when two or more spheres come in contact as shown in Figure 2, page 7. Samples cooled to room temperature for observation after the beginning of sphere formation frequently show numerous examples of spheres in various stages of coalescence. Both mechanisms of sphere growth are regulated to some extent by the viscosity of the mesophase-pitch mixture at the temperature of sphere formation.[10]

In the absence of interference from neighboring spheres, the coalescence process produces a new spherical shaped region of complex internal structure. The molecules in the newly formed sphere which results from coalescence tend to undergo structural rearrangement in an attempt to form the ideal sphere structure. However, this rearrangement is slow due to the high viscosity of the mesophase,[10] and may be hindered by the beginning of the coalescence process with other spheres. As the number and size of spheres increase, coalescence of spheres produces large irregular shaped mesophase droplets greater than 100 μm in size. White, Dubois, and co-workers[10-12] reported that rearrangement of molecules in these droplets of mesophase is much slower than the structural changes brought about by additional coalescence. As a result, a defect structure is developed in the large mesophase droplets. The most common types of defect structures due to layer plane stacking faults have been classified by White, et al.[11,12] and more recently by Honda, et al.[44]

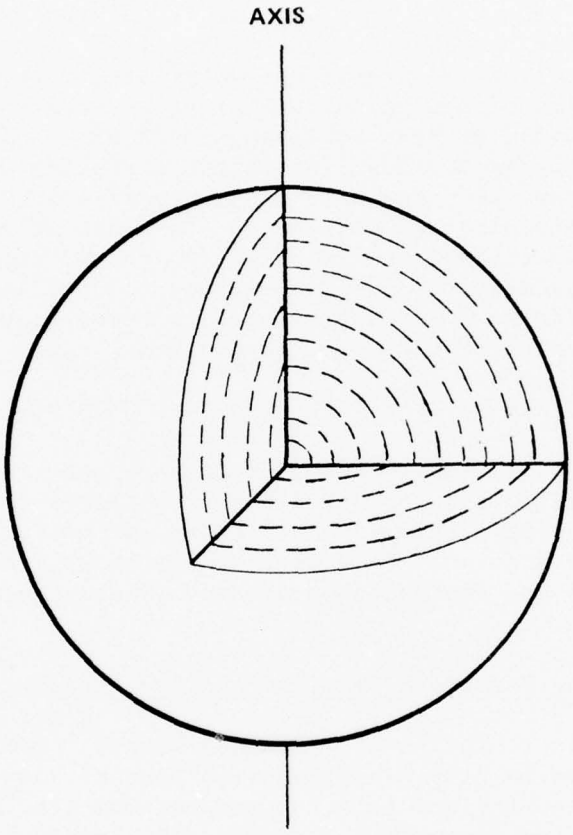

FIG. 6. MESOPHASE SPHERE WITH AN "ONION SKIN" MOLECULAR ARRANGEMENT

Growth of mesophase droplets continues until the isotropic pitch is completely converted into the anisotropic "bulk" or "completely coalesced" mesophase (see Figure 4, page 8). Heat treatment of the coalesced mesophase to about 500°C converts the viscous mesophase into a solid coke. At this point, the microstructure of the coalesced mesophase is frozen and except for shrinkage cracks, remains relatively unchanged on heat treatment to 2800°C.

The microstructure of the coalesced mesophase is important because it is a direct result of the extent and type of ordering of the large planar aromatic molecules which make up the mesophase. This ordering of planar aromatics is the beginning of the development of the graphite crystal structure, and the degree of preorder developed in the coalesced mesophase just prior to hardening determines the type of graphitic material formed on heat treatment to 2800°C. All organics which form the mesophase during pyrolysis develop a graphitic structure to some degree during heating to 2800°C. However, they may not all be classified as graphitizing. The degree of ordering of the molecules and the number and kinds of stacking defects in the coalesced mesophase determines the extent to which the graphitic crystal structure is formed on heat treatment to 2800°C. Factors which affect the microstructure of the coalesced mesophase must be controlled or altered in order to control or tailor the microstructure and properties of the resultant graphitic material.

C. FACTORS WHICH CONTROL THE MESOPHASE MICROSTRUCTURE

The previously described process of mesophase sphere formation, growth, and coalescence is generally true for any aromatic hydrocarbon, or other organic material which develops a highly graphitic structure on heat treatment to 2800°C. However, several factors are known to affect sphere growth and coalescence, as well as the microstructure of the coalesced mesophase. These factors will be discussed in this section.

1. Temperature, Heat Treatment Time, and Rate of Heating

The general characteristics of mesophase sphere formation, growth, and coalescence due to increases in temperature or time have already been presented. A more detailed account of the influence of the temperature-time cycle on the mesophase is given below. It must be remembered, however, that microstructural changes produced in the mesophase due to specific heating conditions are different for materials of different chemical composition. Both the temperature and time required during pyrolysis for formation of large planar aromatics of size and concentration sufficient for mesophase sphere formation is dependent upon the original chemical composition of the organic being pyrolyzed. As a result, different starting materials require a different temperature for initial formation of mesophase spheres.[9] This temperature is usually in the 380 - 430°C range. Not only is a certain temperature required for formation of the molecules which comprise the mesophase, but the viscosity of the liquid must also be low enough to allow movement and ordering of molecules into the layered mesophase structure. The viscosity of mesophase forming hydrocarbons is temperature dependent and has been found to decrease to a minimum in the 350 - 420°C temperature range.[9,42] After sphere formation begins, increases in heating time or temperature produce more planar aromatics of a larger size which cause mesophase growth and a rapid increase in the viscosity.[42] The rate of formation of the large aromatic molecules, and the extent and rate of ordering (the mobility) of these molecules into the mesophase are time-temperature dependent.

Microstructural changes give only a qualitative indication of the affect of heat treatment on the mesophase (see Figures 1-4, pages 7, 8). Since the mesophase is insoluble in many hydrocarbon solvents at room temperature, the weight percent of insoluble material may be used as a quantitative indication of the amount of mesophase formed as a function of temperature or heating time.[13,24,48,51] For example, Honda, et al.[48,49] and Sanada, et al.[50] used the quinoline insoluble content to determine the weight percent mesophase formed in a coal tar pitch as a function of heating time at constant temperature. The results illustrate that increases in time at a constant temperature produces a slower mesophase transformation than increases in temperature. Several other researchers have also reported that sphere growth and coalescence occurs at a faster rate with temperature increases than with increases in time at a fixed temperature.[8,15,42] The time required for the complete conversion of an organic into the coalesced mesophase depends upon the heating temperature and the chemical composition of the material being pyrolyzed.[13,14,42]

Temperature and time are complementary in the mesophase transformation. As shown in Figure 7, sphere formation in a naphtha tar pitch occurs after 20 hours at 350°C or on heating to 400°C at 3°C/min. Following the onset of mesophase sphere formation, sphere growth, coalescence, and complete conversion to the coalesced mesophase may be achieved by temperature increases or increases in time at a fixed temperature.[48-50] Similar results were noted by Horne[15] for acenaphthylene and cinnamylideneindene, and by Whittaker and Grindstaff[42] in their study of mesophase formation in coker feedstocks.

Mesophase formation has been studied in the 380 - 500°C temperature range using heating rates of 0.3°C/min,[47] 0.5°C/min,[24] 2°C/min,[47] and 5°C/hr.[13,14] The results indicate that the weight percent mesophase formed during pyrolysis is a linear function of temperature in the range of approximately 20 to 85% conversion of the organics into the mesophase (see Figure 8). Small changes in heating rate (0.3 to 2°C/min)[47] do not appear to significantly alter the amount of mesophase formed as a function of temperature. It has also been reported[52] that the reaction order and activation energy of the mesophase transformation in a coal tar pitch are independent of heating rates in the range of 1.1 to 5.4°C/min.

After complete conversion of a material into the mesophase, continued heating of the fluid coalesced mesophase produces dehydrogenation and condensation reactions which rapidly increase the mesophase viscosity.[10,24,42,53] Finally, the coalesced mesophase solidifies and the ordered structure with its discontinuities, folds, and various stacking defects is frozen. The microstructure of the solidified mesophase remains essentially unchanged on heating to 2800°C, except for the formation of shrinkage cracks.[11,12] Shrinkage crack formation, sharpening of folds or bends in layers, and layer plane displacements relative to one another reduce the disorder in layer stacking sequences and lead to the formation of highly graphitic regions during heating to 2800°C.

The temperature required for complete conversion into the mesophase depends on the time-temperature cycle and the chemical composition. It has been observed to occur as low as 420°C and as high as 470°C[13,14] during pyrolysis of coker feedstocks at 5°C/hr. Although the exact solidification temperature may not be important, the viscosity of the coalesced mesophase and the time required for solidification of the coalesced mesophase determine the size and structure of the larger regions of molecular order. Therefore, materials which produce a highly fluid mesophase which does

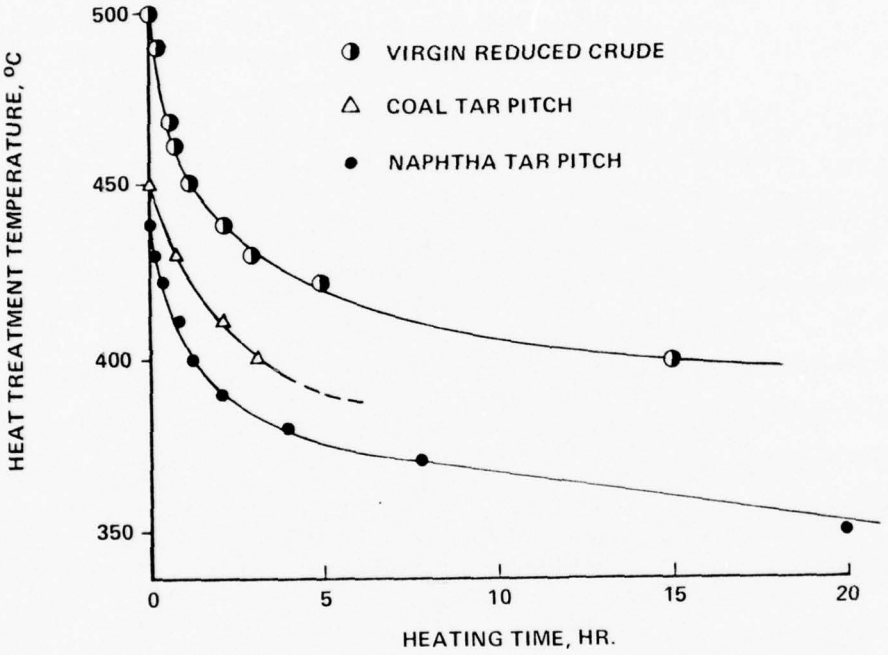

FIG. 7. HEAT TREATMENT TEMPERATURE - TIME CURVES[50] SHOWING THE CONDITIONS NECESSARY FOR MESOPHASE SPHERE FORMATION (HEATING RATE OF 3°C/MIN)

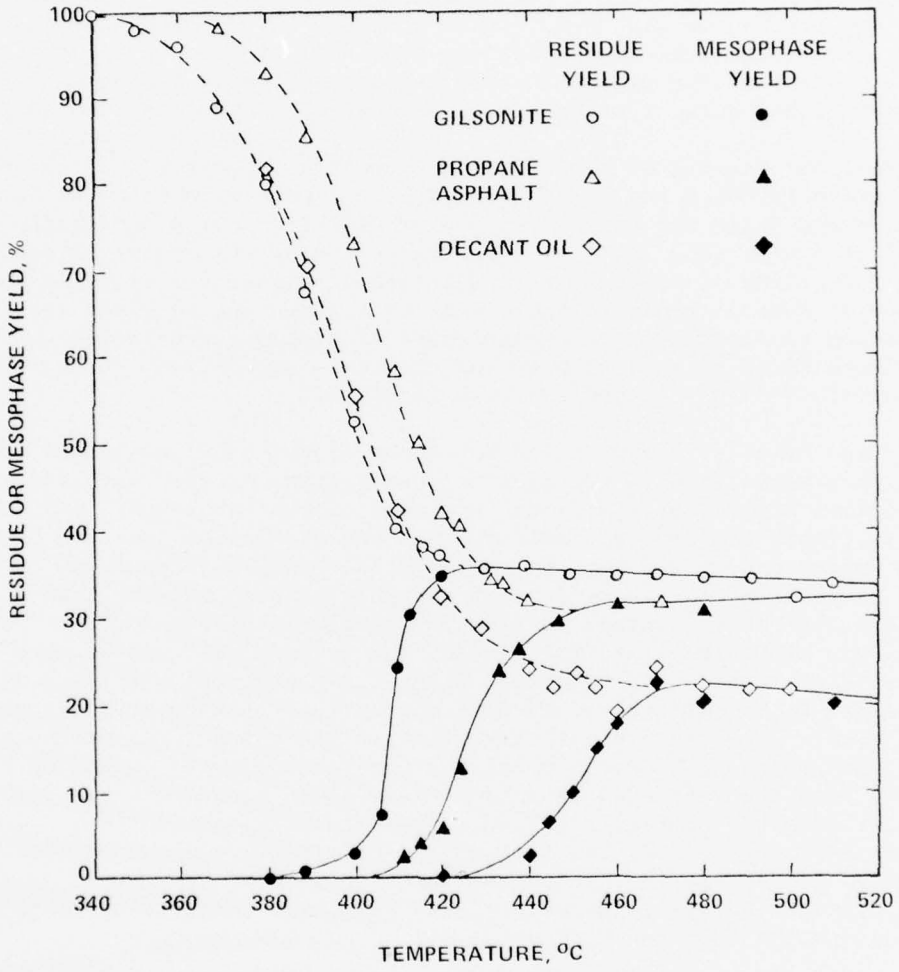

FIG. 8. MESOPHASE FORMATION[14] AS A FUNCTION OF TEMPERATURE FOR THREE COKER FEEDSTOCKS HEATED AT 5°C/HR FROM 360°C TO 510°C

not solidify immediately after complete coalescence produce a well ordered graphitic crystal structure during heating to 2800°C.

2. Chemical Composition of the Precursor Material

The single greatest influence on the coalesced mesophase microstructure is the chemical composition of the organic material which was used to form the mesophase. As demonstrated by Horne, Smith, and co-workers,[15,54-60] proper selection of starting materials and the use of mixtures of pure compounds will enable one to vary the microstructure of the coalesced mesophase from well ordered to almost isotropic. Therefore, control of the microstructure and properties of graphitic materials cannot be accomplished without control of the chemical composition of the raw materials.

An excellent example of the affect of chemical composition on the coalesced mesophase microstructure has been provided by the work of Dubois, et al.,[10] Price and White,[51] and White and Price.[13,14] Five different coker feedstocks were pyrolyzed[13,14] at 5°C/hr from 360°C to 510°C to determine the amount of mesophase formed as a function of temperature and chemical composition (see Figure 8). The temperature of sphere formation, the range of temperature required for the mesophase transformation to occur, and the temperature of complete conversion to the coalesced mesophase were found to be a function of chemical composition. Other studies of pitch pyrolysis[24,42,47,48] confirm these findings.

White and Price[13,14] identified six types of coalesced mesophase microstructure resulting from variations in the chemical composition of the coker feedstocks. The two most common classes of microstructure were called "isotropic" and "fibrous". The term isotropic was used to indicate that the extinction contours of the coalesced mesophase appear random and have no preferential order on a scale of 50 to 100 μm. A fibrous microstructure was defined as a region of size greater than 100 to 200 μm in which the estinction contours are nearly parallel to one another. Types of microstructure were also classified in terms of the average distance between the extinction contours observed under polarized light. For example, a fibrous microstructure with polarized light extinction contours spaced less than 10 μm apart was defined as "fine" fibrous. Both the fibrous and isotropic microstructures were present in different amounts in each of the pyrolyzed coker feedstocks. Organics completely transformed into the coalesced mesophase below 430°C such as an air blown asphalt are of lower aromatic character and form predominately the isotropic microstructure. In each feedstock pyrolyzed, the isotropic microstructure formed almost entirely below 430°C. It is also the predominate microstructural type found in coalesced mesophase prepared by pyrolysis of organics with high concentrations (5 wt % or more) of oxygen, sulfur, and heterocyclics.

The fibrous microstructure is a major component in the coalesced mesophase formed above 430°C as in the decant oil (see Figure 8, page 17). It results from the pyrolysis of highly aromatic compounds and produces a more graphitic structure than the isotropic mesophase on heating to 2800°C. The relationship between the mesophase microstructure and molecular structure is not well understood. It is known that the fine isotropic microstructure is a result of rapid solidification of coalesced spheres which have not grown to a size larger than a few micrometers. This prevents the development of extended regions of molecular order. In contrast, fibrous microstructures result from coalescence of larger spheres which are formed above 430°C with the particular heating cycle used.[14] The important difference, however, is that mesophase formed above 430° remains fluid for some time after

coalescence. This allows molecular rearrangements to occur and produces regions several hundred micrometers in size in which nearly parallel molecular stacking exists. In addition, deformation of the fluid mesophase by gas bubbles is thought to play a major role in forming the fibrous microstructure.[14]

Changes in the time-temperature cycle may alter the mesophase transformation curves (see Figure 8, page 17) and the temperature of sphere formation. However, the trend of formation and rapid solidification of the less ordered isotropic microstructure first is expected to occur regardless of the heating conditions.

Numerous other studies also have shown that different chemical species form the mesophase at different temperatures and produce different degrees of molecular order in the coalesced mesophase. Pyrolysis of a mixture of pure hydrocarbons[31,43,61,62] may produce two or more distinctly different types of coalesced mesophase microstructure, each of which may be obtained by pyrolysis of the pure compounds separately. Apparently each type of organic in a mixture may undergo a different sequence of pyrolysis reactions. If the free radical intermediates from each component in the mixture do not interact or are produced at different temperatures, the coalesced mesophase will contain different microstructural types.[28,29,63] Favorable interaction of intermediates also occurs in some cases,[64-68] and results in a more ordered mesophase than that obtained by separate pyrolysis of each of the components in a mixture.

Oxygen present in an organic originally[20,22,24] or added during pyrolysis[69] produces nonplanar free radicals which crosslink the pyrolysis products. As a result, the viscosity is increased,[22,24,70] the molecular mobility is reduced, the temperature range during which the mesophase is fluid is reduced, and the formation of large regions of order in the coalesced mesophase is prevented. Observable changes in the microstructure of the mesophase usually occur if more than 5% by weight of oxygen is present in the material being pyrolyzed. Oxygen contents greater than 5% by weight reduce the mesophase sphere size, prevent normal sphere coalescence, and reduce the graphitizability of the material. Similar observations have been made during pyrolysis of pure hydrocarbons,[69] coker feedstocks,[42] coal tars,[71] coal tar pitches,[24] and fusible coals.[64,71] However, one cannot generalize these results, since examples[58,65,66] are known in which the addition of oxygen or oxygen containing compounds has actually increased the degree of molecular order developed in the mesophase.

The affect of sulfur on mesophase formation in pure hydrocarbons[5,58,72] and pitches[50,72,73] is similar to that described above for oxygen. Sulfur does not influence the mesophase microstructure as long as the primary reaction during pyrolysis is dehydrogenation of hydrocarbons with release of H_2S.[72] Heterocyclic compounds and other non-graphitizing organics[43,64-68] also begin to reduce the molecular order in the mesophase if present in amounts greater than about 5% by weight.

In reality, it is not the original molecular structure but the structure, reactivity, and fluidity of the thermally formed intermediates which determines the microstructure of the coalesced mesophase. Heating time and temperature influence the mesophase microstructure only in terms of the types of chemical species produced and the rate of production of these species in the 400 - 500°C temperature range. Any chemical process which alters the normal build-up of large planar aromatics as discussed in Chapter II, Section B.2 may reduce the molecular ordering in the mesophase and produce a less graphitic material on heating to 2800°C. The formation of

crosslinked or nonplanar intermediates,[69] steric effects,[2,25,33] and the presence of non-graphitizing organics (for example, biphenyl[62,74]) hinder the formation of a well ordered mesophase, and in the extreme case may prevent mesophase formation.

3. Pressure

Two groups of investigators[29,61,64-68] have reported on mesophase microstructural changes caused by pyrolysis of pure hydrocarbons at pressures from 34 to 300 MN/m^2 (5000 to 43,500 psi). High pressure pyrolysis of organics such as anthracene,[28,75] phenanthrene,[74] and acenaphthylene[43] at 550°C produces only uncoalesced mesophase spheres less than 20 μm in size. Since these spheres do not fuse or coalesce, large regions of ordered molecules cannot form to produce a highly graphitic material on heating to 2800°C. Pyrolysis of anthracene under various pressure-temperature cycles has also been shown to produce a mesophase composed of "cylindrical"[43] and "spaghetti shaped"[28,43] anisotropic units. The spaghetti shaped units are thought to be a result of partial coalescence along one axis of the mesophase spheres.

It is well known that any increase in pressure above atmospheric will increase the char yield during pyrolysis of pitches and hydrocarbons. It should also decrease any changes in the mesophase microstructure which result from gas bubble percolation. Pressure increases during pyrolysis affect the reaction medium, the atmosphere of the pyrolyzing material, the reaction path, the type of intermediates formed, and the overall rate of pyrolysis. Pressures above 30 to 50 NM/m^2 are thought to significantly increase the viscosity of the liquid being pyrolyzed and may reduce the mobility of molecules which form mesophase spheres. Apparently, one major influence of high pressure pyrolysis is to change the chemical composition of the pyrolyzing material. In some cases this produces a more graphitic material, while in others crystallite size and interlayer spacing data indicates a less graphitic material is produced.[25]

4. Insoluble Particles and Material Surfaces

Both coal tar and petroleum pitches are known to contain particles similar to carbon blacks which are insoluble in quinoline. Some pitches may contain as much as 20% by weight of these particles which are usually less than 2 μm in size. These particles are referred to as "insolubles" or "quinoline insolubles". Studies conducted to date indicate that insoluble carbon particles of a size less than 5 μm either present in the pitch originally[42,48,49] or added prior to pyrolysis[64-67] alter the mesophase microstructure. Insoluble carbon particles present in concentrations greater than two or three percent by weight (1) accumulate on the mesophase sphere surface or are pushed along the mesophase surfaced-isotropic pitch interface as the spheres grow in size,[9,76-78] (2) reduce the average mesophase sphere size[64-67] and restrict growth of mesophase spheres[9] (possibly by decreasing molecular diffusion and increasing viscosity), (3) produce an irregular mesophase sphere shape and surface characteristics,[9,48,49] (4) restrict or hinder normal coalescence, and (5) produce a three-dimensional network of incompletely coalesced mesophase spheres surrounded by a three-dimensional network of insoluble particles.[10] Additions of a few percent of micron size metal oxide particles[9,77] to pitches prior to pyrolysis also have the same influence on mesophase sphere growth and coalescense as noted for quinoline insoluble carbon particles.

The insolubles prevent normal sphere coalescence and reduce the formation of large regions of molecular order in the bulk mesophase. As a result, the graphitizability of the material is decreased. The extent to which the mesophase microstructure and the resulting graphitic microstructure is altered by insolubles is determined by the size and percent of insolubles present in the organic prior to pyrolysis.

When particles of natural flake graphite, needle coke, pyrolytic carbon, or graphite fibers are present in a pitch being pyrolyzed, the molecules in the mesophase align themselves parallel to the layered structure in the particles.[9,10,79] Graphite fibers[79] have been reported to definitely be a preferred site for mesophase sphere nucleation. It is possible that large insoluble molecules and solid surfaces in general are nucleation sites for mesophase formation. However, mesophase growth and coalescence after the nucleation process occurs is different in each case.

CHAPTER III

EXPERIMENTAL TECHNIQUES

A. REAGENTS

The acenaphthylene used in this study (see Table II) was obtained from Aldrich Chemical Company, (catalog number A80-5) and was stated to be 99% pure. The major impurity in acenaphthylene is acenaphthene, which will vaporize during pyrolysis.[37]

B. TEST TUBE PYROLYSIS METHODS

Samples of approximately 20 g in size were pyrolyzed in 25 mm diameter by 300 mm long pyrex test tubes in the furnace shown in Figure 9, page 25. Test tubes containing samples were placed in six separate holes in a heated copper block. This technique allowed removal of individual samples at different points in the time-temperature cycle for study at room temperature using polarized light microscopy. A uniform temperature was produced in all samples due to the high conductivity of the copper block. The samples were heated to various temperatures between 350°C and 500°C using a heating rate of 100°C/hr to 200°C, followed by 20°C/hr to the desired temperature. Each sample was heated under refluxing conditions in an atmosphere of the pyrolysis gases. No attempt was made to rigorously exclude air from the samples during pyrolysis.

A Data Trak Programmer, Model FGE 5110, from Research Incorporated was used to program the heating rate (see Figure 10). The Data Trak output signal established a temperature set point in a Barber Colman Model 541B solid state controller. Furnace temperature was measured with a chromel-alumel thermocouple which also produced an input signal to the 541B controller. The difference between the actual and desired temperature was translated by the 541B controller into a direct current output signal. Power in proportion to this signal was supplied to the furnace by means of a Barber Colman solid state Power Controller, Model 621A. The temperature of the copper block was reported as the sample temperature. It was measured using a chromel-alumel thermocouple and a potentiometer, and recorded as a function of time with a Brown Electronik recorder. Heating rates above 200°C were reproducible to within ± 2°C/hr. The temperature of the samples in the copper block were all uniform within 5°C. Temperature measurements using the potentiometer were accurate to ± 4°C at 450°C.

C. SAMPLE PREPARATION FOR POLARIZED LIGHT MICROSCOPY

Samples heated in test tubes were removed from the copper block and allowed to cool to room temperature. The pyrolysis residues were sectioned using a circular saw with a diamond-tipped blade. EPON 82B epoxy resin (Shell Chemical Co.) with 8% by weight diethylenetriamine as the curing agent was used to mount the samples in 3.2 cm diameter bakelite ring forms from Buehler, Ltd. A vacuum of approximately 1 mm of mercury was applied during the mounting procedure to remove air bubbles and impregnate the open porosity in the sample with epoxy resin. After an overnight cure at room temperature, the samples were ground on silicon carbide grinding paper using grit sizes of 240, 320, and 600 in successive steps on a grinding wheel (180 RPM). Polishing was accomplished in three stages with 9.5, 1, and 0.05 μm aluminum oxide powder from Buehler, Ltd. The first two stages were conducted on a wheel (180 RPM) covered with Metcloth (Buehler Ltd.). Final polishing by hand using

TABLE II
PROPERTIES OF ACENAPHTHYLENE USED IN THIS STUDY

Property	Theoretical	Measured
Chemical Formula		---
WT. % C	94.702	94.43[(a)]
WT. % H	5.298	5.28[(a)]
C/H	1.50	1.50
WT. % N	0	0.01[(a)]
WT. % O	0	0.18[(a)]
WT. % S	0	0.12[(a)]
Melting Point, °C	---	86-90

(a) Average of determinations on 3 different samples by Galbraith Laboratories, Knoxville, Tn.

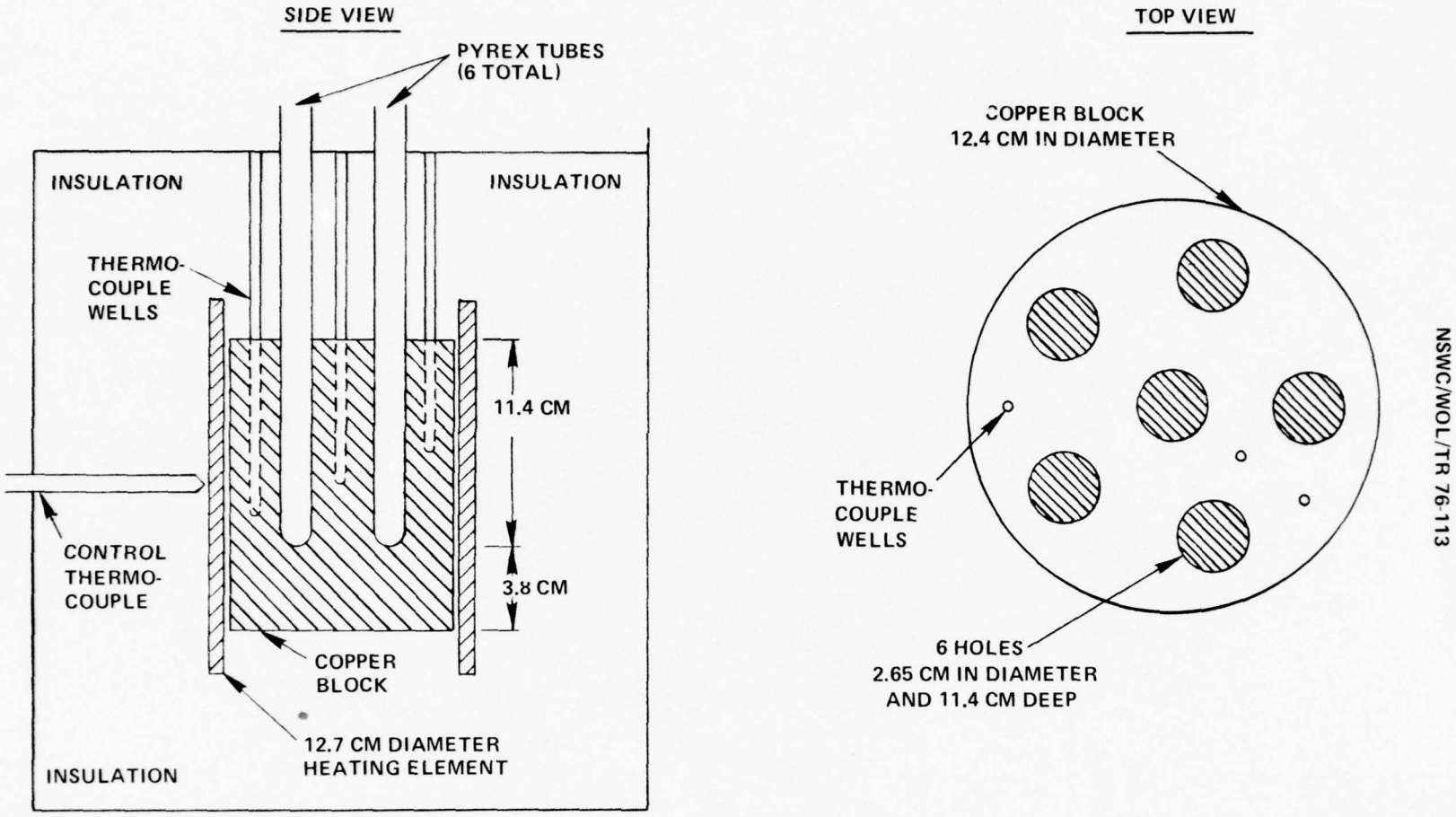

FIG. 9. PYROLYSIS FURNACE

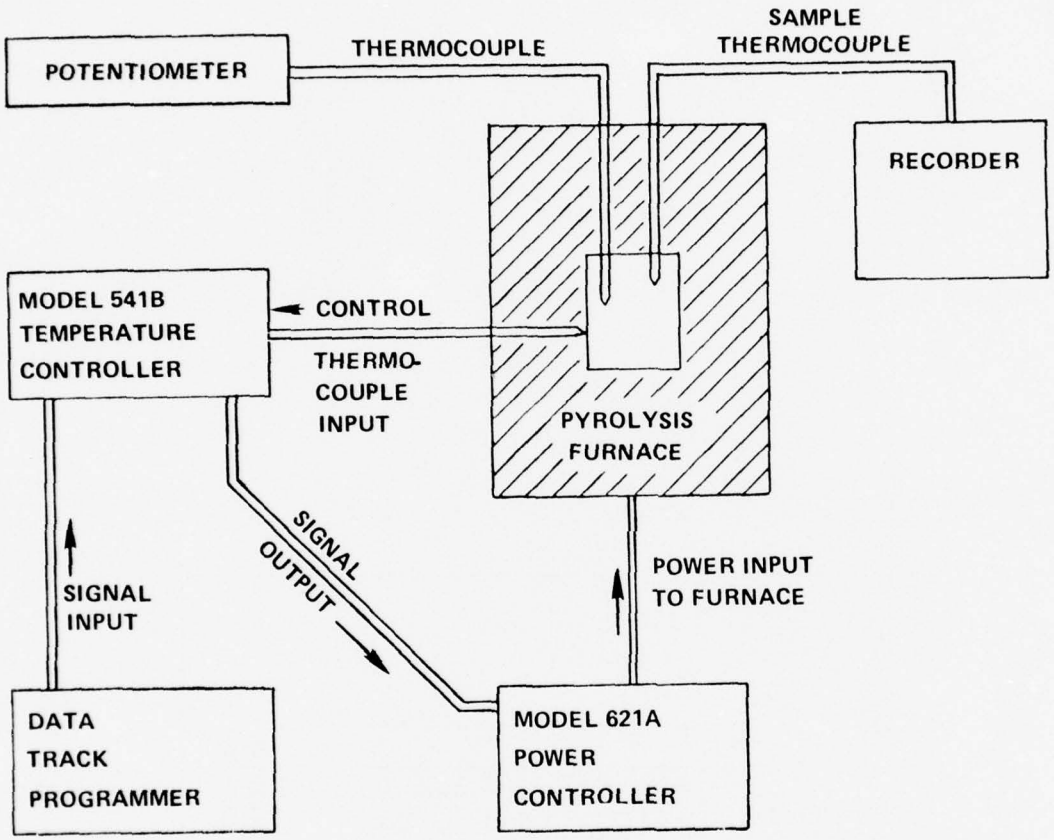

FIG. 10. CONTROL EQUIPMENT FOR THE PYROLYSIS FURNACE

0.05 μm aluminum oxide on Rayvel cloth (Buehler Ltd.) provided a surface for microscopy relatively free of scratches. A solution of methanol in water (50/50 by volume) was used in each step as a lubricant.

Samples were examined for relative degree of conversion into the mesophase with a Zeiss Universal microscope equipped with reflected polarized light optics. Photographs were made with a Polaroid sheet film holder (10 by 12.5 cm) and type 52 black and white film.

D. PYROLYSIS USING A MICROSCOPE HOT STAGE

A microscope hot stage was built to pyrolyze samples of approximately 20 mg in size (see Figure 11). The samples were placed between two microscope cover slides (Corning Number 1) and heated rapidly in air to 370°C in 40 minutes. After a 25-minute hold at about 370°C, the samples were heated at 0.6 to 1.3°C/min to temperatures between 413°C and 455°C. A variac was used to control the temperature-time cycle. After the samples melted, a liquid film about 50 μm to 70 μm thick formed between the 18 mm diameter cover glasses. Continued heating to about 413°C resulted in mesophase sphere formation. Since the mesophase wets glass surfaces, it could be observed directly at temperature through the top cover glass using reflected polarized light microscopy. This experimental technique allowed direct observation of the coalescence and deformation of mesophase droplets as a result of gas bubble movement in the sample.

A chromel-alumel thermocouple touching the bottom cover glass was used to measure temperature. Due to the lack of insulation on the top cover glass directly below the microscope objective, a severe temperature gradient existed from the bottom to the top cover glass. Calibration of the hot stage using melting point standards indicated the temperature measurements may have been as much as 30°C higher than the actual sample temperature at 400°C. However, since the purpose of this study was to determine by direct observation the influence of gas bubbles on mesophase spheres and the coalesced mesophase, the actual temperature is not important in the hot stage experiments.

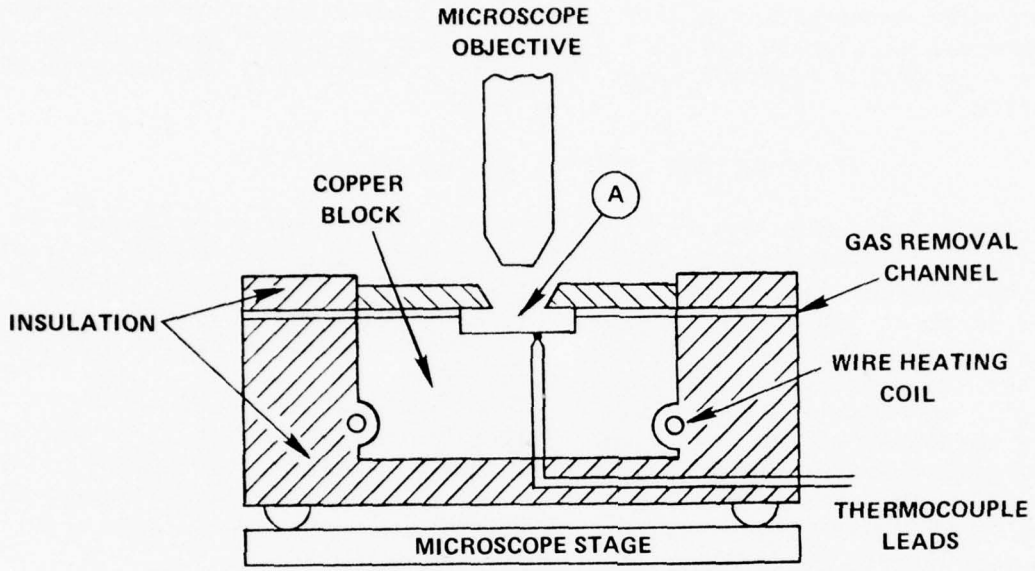

ENLARGED CROSS SECTION OF REGION A

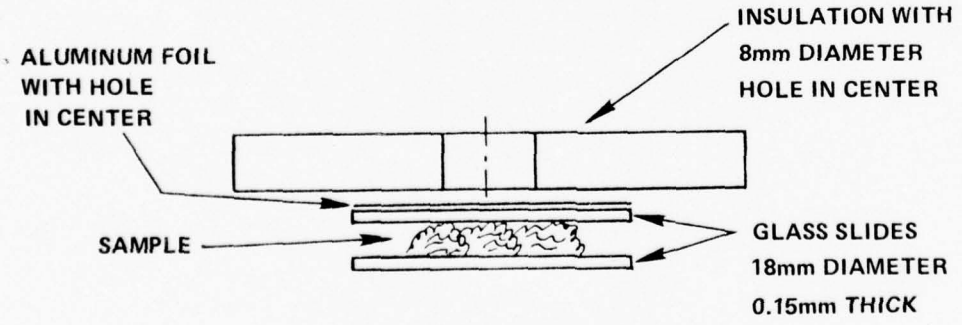

FIG. 11. MICROSCOPE HOT STAGE

CHAPTER IV

RESULTS AND DISCUSSION

A. GENERAL CONSIDERATIONS

Although the sequence of the major chemical reactions which occur during acenaphthylene pyrolysis have been known for years, a brief review of the chemistry involved during the heating of acenaphthylene to 500°C is considered important at this point. Such a review will provide an understanding of the chemical processes which result in mesophase formation.

Numerous studies have been made on the pyrolysis of acenaphthylene. However, the work of Lewis and co-workers[3,16,37,38] has provided much of the information describing the chemical processes which occur during pyrolysis of acenaphthylene. Acenaphthylene begins to undergo a thermally induced vinyl polymerization at temperatures in the range of 185°C to 200°C.[4,5,37] The resulting polymer has an average molecular weight[27,34,37] corresponding to twelve acenaphthylene units at 300°C. X-ray diffraction studies[80] have indicated that the acenaphthylene polymer has a helical structure with three to five acenaphthylene units per turn. Between 300°C and 400°C the polymer begins to thermally degrade[3,16,38] and produces a complex mixture of dimers, trimers, and tetramers of acenaphthylene. Many of these species are free radicals. The acenaphthylene polymer is degraded to an average size of six acenaphthylene units at 360°C.[27,34]

Most of the monomer free radicals formed as a result of polymer decomposition undergo rapid hydrogen transfer reactions to produce acenaphthene.[3] Approximately 50% by weight of the pyrolyzed sample is lost as volatile acenaphthene[27] between 320°C and 410°C. Acenaphthene radicals may combine to form biacenaphthylidene, fluorocyclene, and decacyclene.[16,38] These compounds are also known to form during polymer degradation reactions. The dimer biacenaphthylidene is a major component of the pyrolysis residue[3] and undergoes rearrangement to form zethrene,[4,38] a six ring aromatic hydrocarbon, in the temperature range of 360°C to 400°C. Condensation of two or more zethrene units[3,80] results in the formation of large aromatic molecules in the 400°C to 500°C temperature range. It is these large aromatic molecules which produce mesophase formation.

The above discussion represents one major mechanism for formation of large aromatics during acenaphthylene pyrolysis. This mechanism has been verified in part by other studies.[5,30,81,82] However, it must be remembered that several reaction mechanisms are probably taking place at the same time, and the relative importance of each mechanism is dependent upon the specific pyrolysis conditions.

B. MESOPHASE TRANSFORMATION IN ACENAPHTHYLENE PYROLYZED IN TEST TUBES

The characteristics of the mesophase transformation in acenaphthylene were determined at relatively slow rates of heating (20°C/hr) during pyrolysis of samples in test tubes. Table III gives a list of a series of samples of acenaphthylene which were pyrolyzed to different temperatures from 306°C to 500°C. The 3% weight loss up to 306°C is probably due to evaporation of acenaphthylene.[27] Above 306°C an additional 52-53% of the original sample weight was lost due primarily to vaporization of acenaphthene as discussed in Section A of this chapter. Plots of weight loss and the atomic C/H ratio as a function of temperature are given in Figures 12 and 13, pages 31 and 32 respectively. The rapid weight loss between 300°C and 400°C occurs as the C/H ratio increases from 1.52 to 2.10. A change in the residue appearance from yellow-orange to a black pitch-like material takes place during this temperature range as the acenaphthylene polymer is converted to large planar aromatics. The C/H ratio of 2.1 at 494°C (see Table III) and the molecular weight data given in references 27 and 37 indicate the formation of aromatic molecules of approximately 30 rings in size at 404°C. Larger molecules would be expected to be present if the sample is held at this temperature for long periods of time.

There are no major differences between the C/H ratios and weight loss data given in Table III and those reported in the literature[37,38] for pyrolysis of acenaphthylene at 10°C/min in argon. However, pyrolysis in air does permit the incorporation of small amounts of oxygen into the pyrolysis residue (see Table III, page 33).

Polished sections of each sample listed in Table III, page 33, were observed at room temperature using reflected polarized light microscopy to determine the general characteristics of the mesophase transformation as a function of pyrolysis temperature. Mesophase spheres were first observed in samples of acenaphthylene heated to 404°C (see Figure 14). The spheres were randomly dispersed throughout the sample and varied in size up to a maximum of 14 μm in diameter. For the particular heating cycle used in this study, the actual temperature of formation of micron size spheres is probably in the 390°C to 404°C temperature range. There was no optical anisotropy in samples heated in 306°C and 351°C. Continued heating to 426°C resulted in sphere growth and coalescence as illustrated in Figure 15, page 35. Mesophase spheres as large as 200 μm in diameter were observed in this sample. Figure 15 confirms earlier work[15] which concluded that large spheres are formed primarily by sphere coalescence during acenaphthylene pyrolysis. After heating to 426°C, a random distribution of spheres was found.

Heat treatment of acenaphthylene to 450°C produced nucleation of new spheres and additional growth of spheres formed at lower temperatures (see Figures 16-18, pages 35-37). Sphere growth occurred as a result of direct incorporation of molecules from the isotropic fluid pitch and sphere coalescence. As shown in Figure 18, page 37, coalesced spheres as large as 500 - 600 μm were observed. The larger spheres usually show a complex arrangement of extinction contours when observed using crossed polarizers due to numerous coalescence processes which occur faster than rearrangement of molecules to produce the ideal sphere structure. The increase in viscosity which occurs as the mesophase forms also tends to hinder molecular rearrangements. Coalescence of spheres does not necessarily start to occur as soon as two spheres come in contact. Examples of mesophase spheres which are in contact

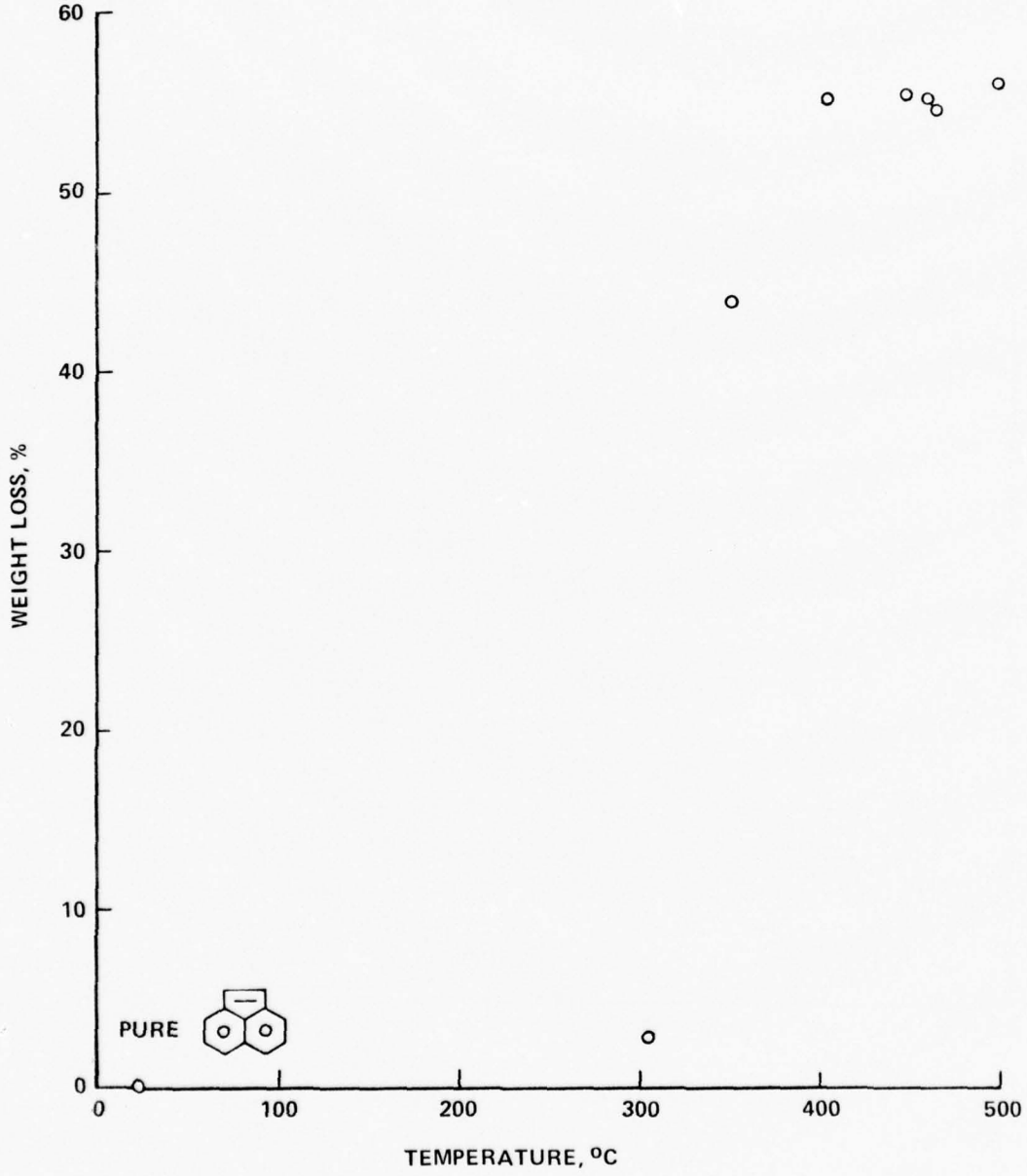

FIG. 12. ACENAPHTHYLENE WEIGHT LOSS AS A FUNCTION OF PYROLYSIS TEMPERATURE

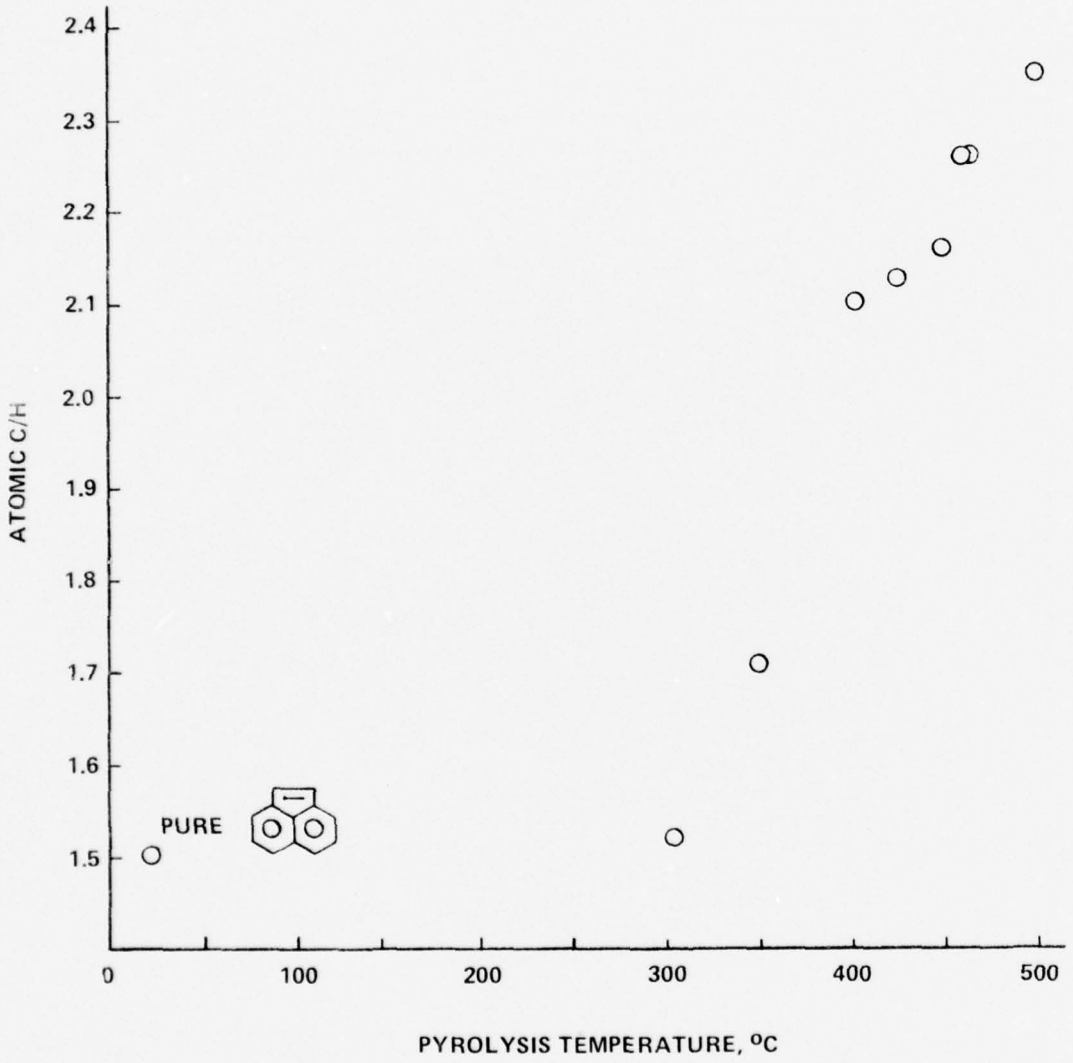

FIG. 13. C/H RATIO AS A FUNCTION OF ACENAPHTHYLENE PYROLYSIS TEMPERATURE

TABLE III

CHEMICAL ANALYSIS DATA ON ACENAPHTHYLENE SAMPLES PYROLYZED IN TEST TUBES[a]

HTT[b]	% WT LOSS	FIRST DETERMINATION WT % C	FIRST DETERMINATION WT % H	FIRST DETERMINATION WT % O	SECOND DETERMINATION WT % C	SECOND DETERMINATION WT % H	C/H[d]
306	3.0	93.53	5.16	1.18	(c)	(c)	1.52
351	43.6	93.47	4.58	1.88	(c)	(c)	1.71
404	55.1	96.04	3.87	0.10	95.57	3.79	2.10
426	(c)	94.95	3.74	0.65	(c)	(c)	2.13
450	55.5	95.22	3.74	0.97	95.59	3.70	2.16
462	55.0	95.52	3.54	0.90	(c)	(c)	2.26
466	54.4	95.38	3.47	1.13	95.71	3.65	2.26
500	56.0	95.57	3.40	1.02	95.56	3.42	2.35

(a) HEATED AT 100°C/HR TO 200°C FOLLOWED BY 20°C/HR TO THE DESIRED TEMPERATURE. ANALYSIS CONDUCTED BY GALBRAITH LABORATORIES, KNOXVILLE, TENNESSEE.

(b) HEAT TREATMENT TEMPERATURE.

(c) NOT DETERMINED.

(d) AVERAGE VALUE FOR CASES INVOLVING ANALYSIS OF TWO DIFFERENT SAMPLES.

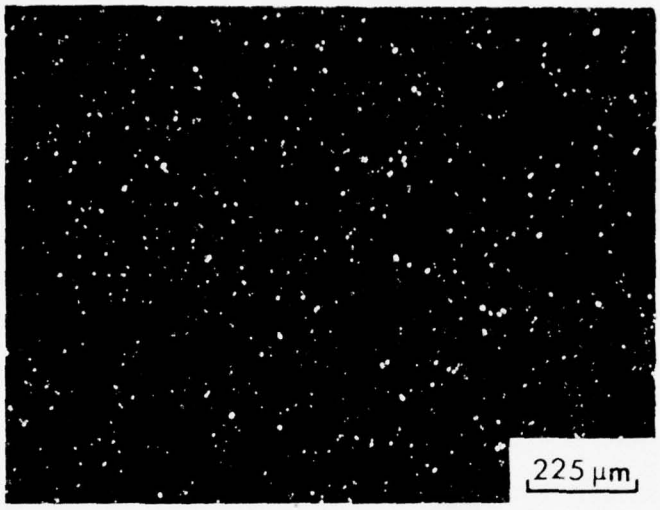

FIG. 14*. ACENAPHTHYLENE HEATED TO 404°C

*All photomicrographs given in Chapter IV, Section B, were taken at room temperature using reflected polarized light (crossed polarizers) unless stated otherwise. The black background in photographs such as Figures 14 and 15 is untransformed pitch which is optically isotropic. The straight lines across the photographs in random directions as shown in Figures 15 (page 35) and 18 (page 37) are polishing scratches.

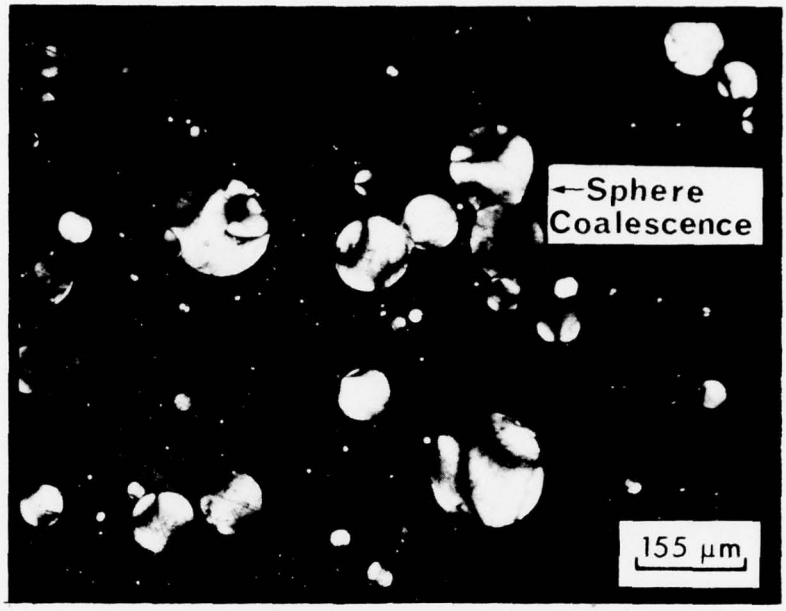

FIG. 15. ACENAPHTHYLENE HEATED TO 426°C
(Note: the examples of sphere coalescence and the range of sphere sizes)

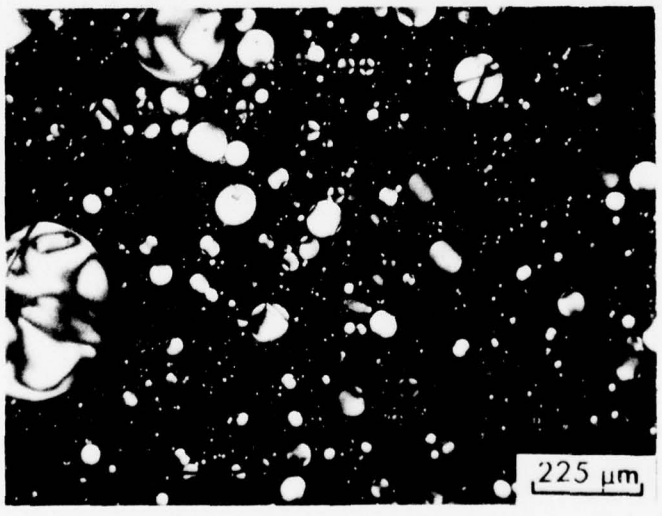

FIG. 16. ACENAPHTHYLENE HEATED TO 450°C

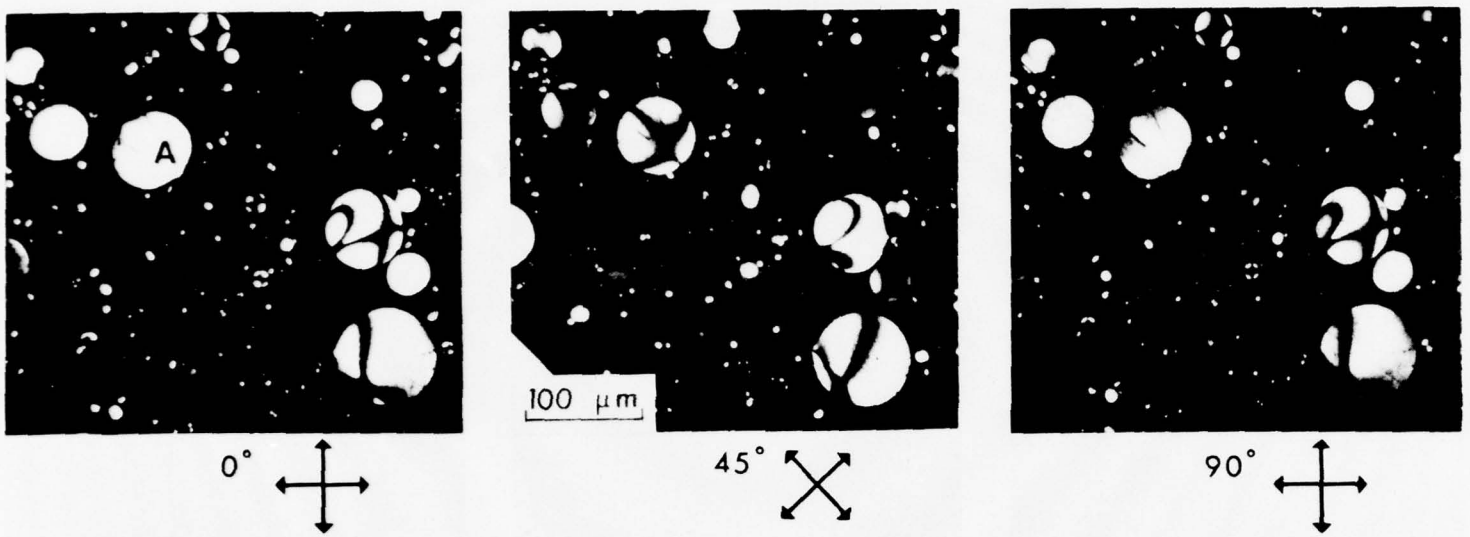

FIG. 17. MESOPHASE SPHERES FORMED BY HEATING ACENAPHTHYLENE TO 450°C

FIG. 18. ACENAPHTHYLENE HEATED TO 450°C SHOWING EXTINCTION CONTOUR CHANGES DUE TO ROTATING THE PLANE OF POLARIZED LIGHT (CROSSED POLARIZERS) CLOCKWISE FROM 0° TO 60°

but have not begun growing together are shown in Figure 18, page 37 and Figures 19 and 20. Figures 19 and 20 are photomicrographs of the same area at different magnifications. After the reflected polarized light photomicrograph was made (Figure 19), the polished surface of the sample was etched for about 10 seconds in acetone. The untransformed pitch is more soluble than the mesophase and is preferentially etched away; producing a sharp line at the mesophase sphere-untransformed pitch interface which may be observed under reflected light (see Figure 20). This technique is useful to indicate sphere coalescence as shown in Figure 20, and makes it possible to detect micron size mesophase spheres in pyrolyzed samples (see Figure 21, page 40).

The sample heated to 450°C also contained regions larger than 2 mm in size in which spheres had grown together to produce the coalesced mesophase (see Figures 22-25, pages 40-43). Figures 16 through 25, pages 35-43, represent different areas in the same sample, and illustrate the inhomogeneous nature of the mesophase formed during heating acenaphthylene to 450°C. White and Price[14] have classified several types of coalesced mesophase microstructures which are known to form during the pyrolysis of petroleum pitches. Some of these microstructural types also formed during acenaphthylene pyrolysis. Using the terminology of White and Price,[14] Figure 24, page 60 would represent a coalesced mesophase region with a "course isotropic" microstructure. In contrast to the isotropic structure, Figures 22 and 23, pages 40 and 41 give examples of the coalesced mesophase with a "fibrous" microstructure. Fibrous microstructures[14] have been classified as "fine fibrous" if the distance between the extinction contours observed under polarized light microscopy is less than 10 μm. As shown in Figures 25 and 26, page 43, the fibrous structures found in the coalesced mesophase from acenaphthylene heated to 450PC would be classified as "course."

Figure 24, page 42 shows several types of nodes and crosses which were observed using crossed polarizers. They are commonly observed in the coalesced mesophase and in large coalesced spheres (see Figure 18, page 37). These nodes and crosses are produced by the coalescence of ideal mesophase spheres[12,44] and represent defects in the stacking of the large aromatic molecules which comprise the mesophase. Various types of nodes and crosses represent particular stacking defects which have been characterized for nematic liquid crystals[83] and also for the coalesced mesophase.[12,44]

Using boiling quinoline in a soxhlet extractor, a sample of acenaphthylene previously heated to 450°C was extracted for ten hours. This procedure was used to separate the insoluble mesophase from the untransformed pitch material which is quinoline soluble. After extraction, mesophase spheres were obtained and examined using reflected light (see Figure 27). Single spheres were easily fractured when a slight stress was applied with a probe. The fracturing process often resulted in hemispheres, confirming that the layer structure of the molecules in an ideal sphere is a plane of weakness.

Samples of extracted mesophase were also glued to an aluminum sample holder, coated with a gold film about 50 nm thick in a vacuum evaporator, and observed using scanning electron microscopy (SEM). As shown in Figure 28, the extracted sample contained spheres and pieces of coalesced mesophase. Examples of single mesophase spheres and clusters of spheres are given in Figures 29-31, pages 46 and

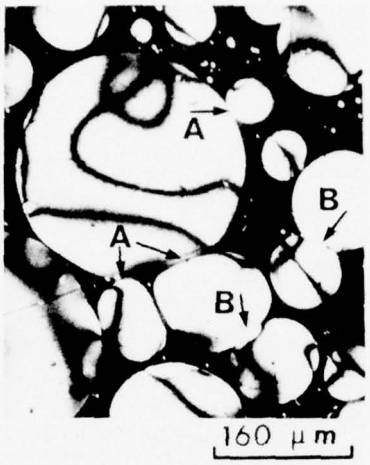

FIG. 19. REFLECTED POLARIZED LIGHT PHOTOMICROGRAPH OF MESOPHASE SPHERE COALESCENCE

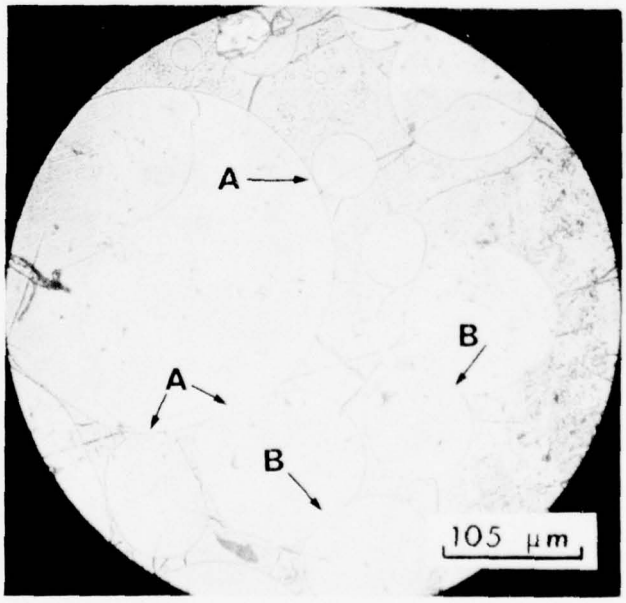

FIG. 20. REFLECTED LIGHT PHOTOMICROGRAPH OF MESOPHASE SPHERE COALESCENCE

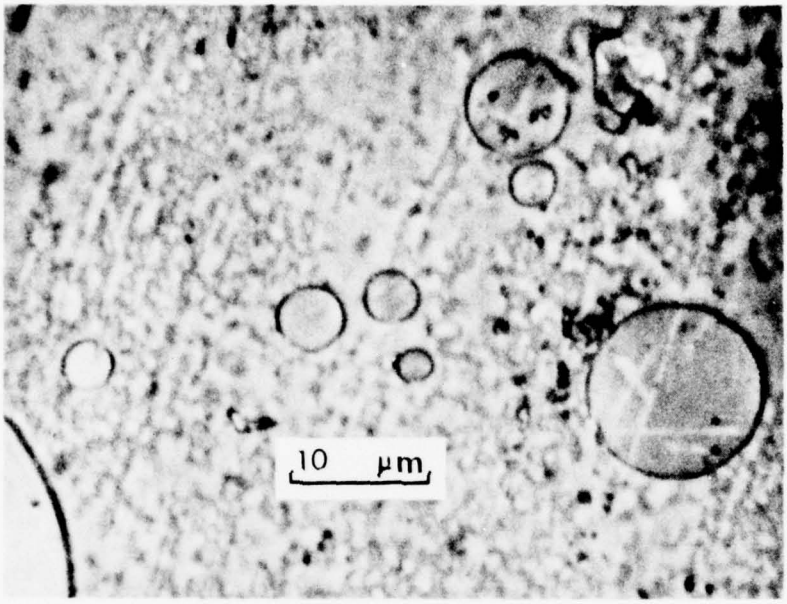

FIG. 21. REFLECTED LIGHT PHOTOMICROGRAPH OF MICRON SIZE MESOPHASE SPHERES FORMED DURING HEATING ACENAPHTHYLENE TO 450°C

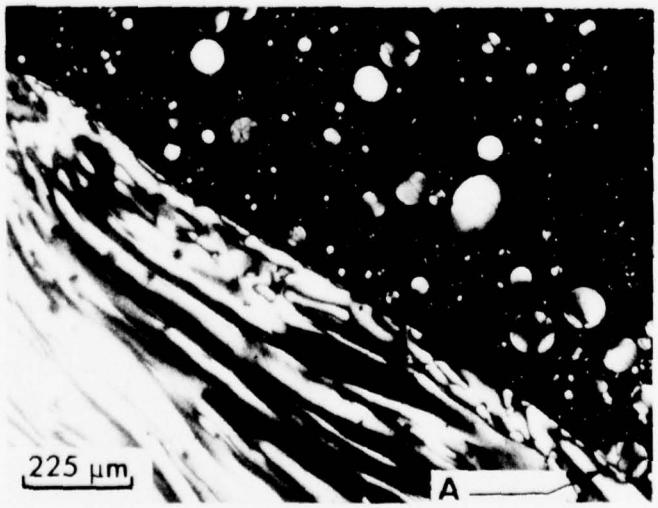

FIG. 22. COALESCED MESOPHASE AND MESOPHASE SPHERES IN ACENAPHTHYLENE HEATED TO 450°C

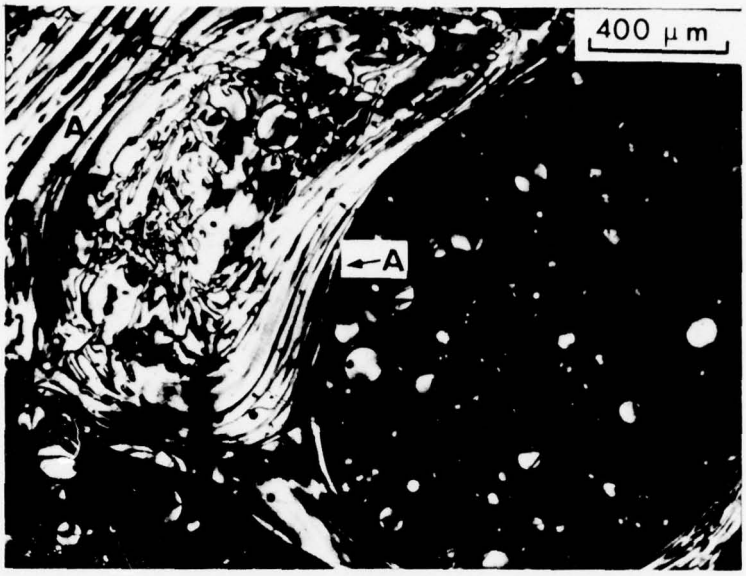

FIG. 23. FIBROUS MICROSTRUCTURE IN THE COALESCED MESOPHASE FROM ACENAPHTHYLENE

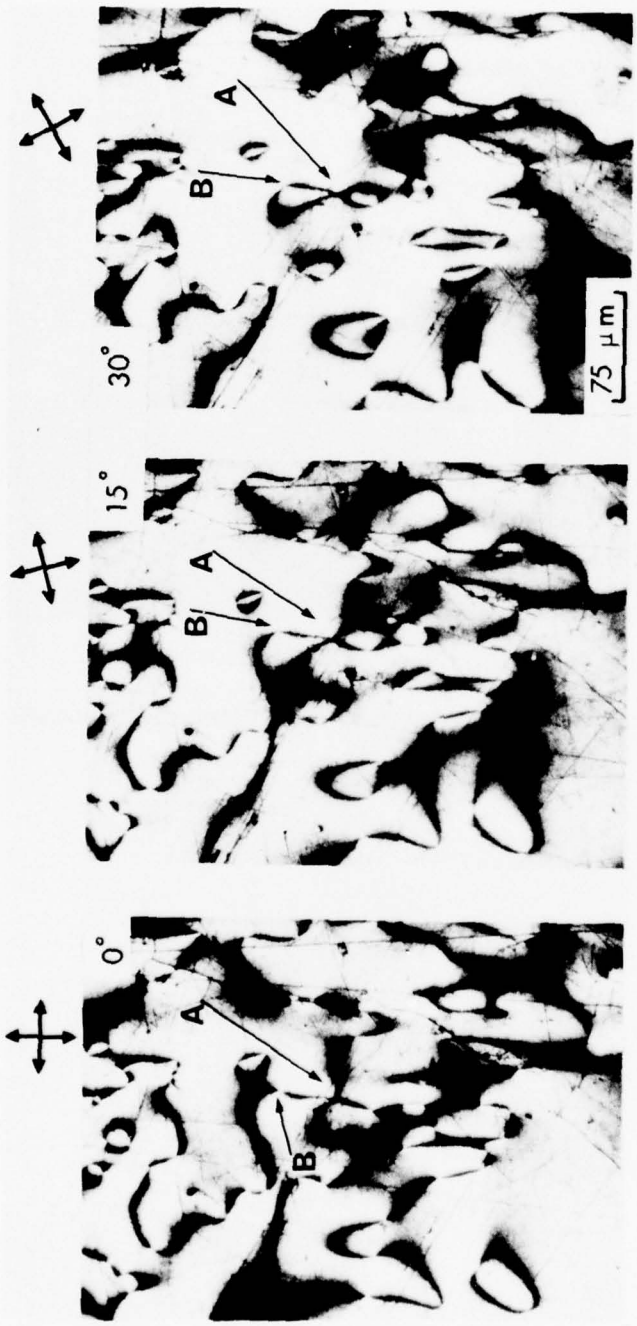

FIG. 24. COALESCED MESOPHASE WITH A COARSE ISOTROPIC MICROSTRUCTURE FORMED DURING PYROLYSIS OF ACENAPHTHYLENE TO 450°C

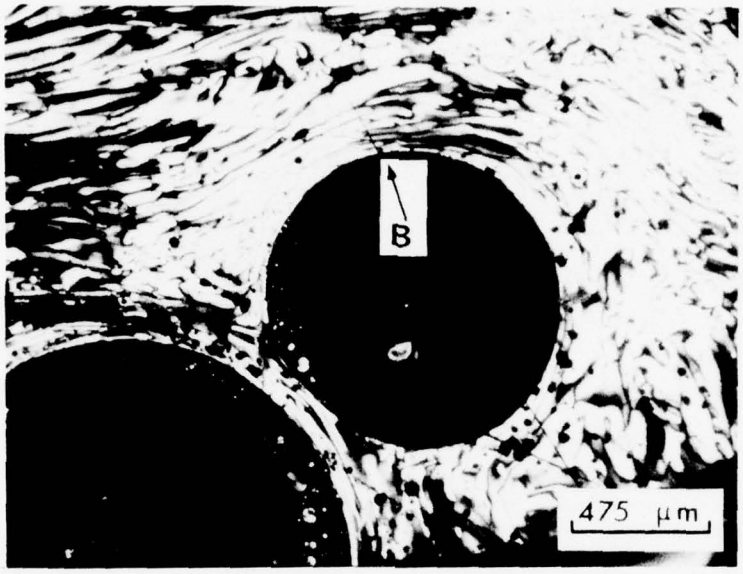

FIG. 25. COARSE FIBROUS MICROSTRUCTURE (REGION B) NEAR A GAS PORE IN THE COALESCED MESOPHASE FORMED DURING HEATING ACENAPHTHYLENE TO 450°C

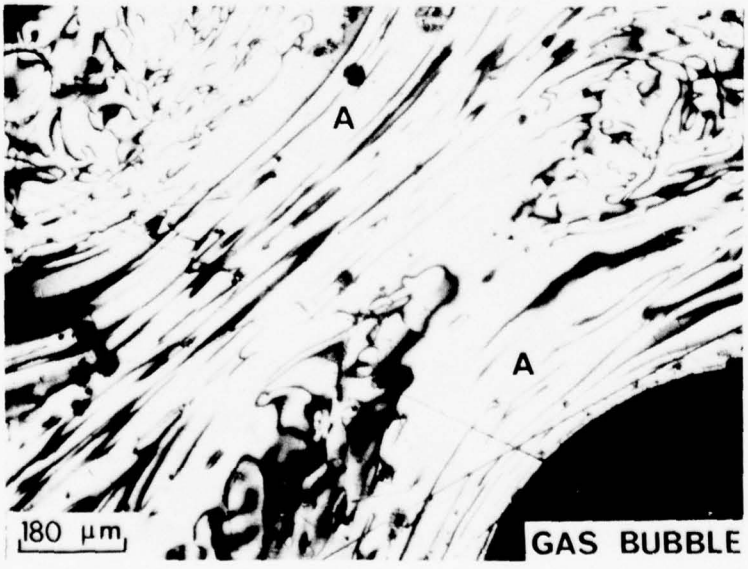

FIG. 26. HIGHER MAGNIFICATION OF REGION B IN FIGURE 25

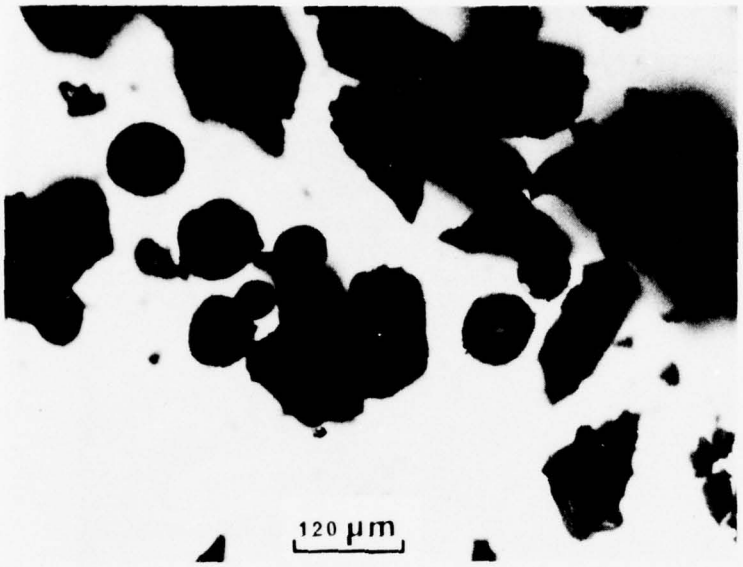

FIG. 27. REFLECTED LIGHT PHOTOMICROGRAPH OF AN EXTRACTED SAMPLE OF MESOPHASE PRODUCED DURING HEATING ACENAPHTHYLENE TO 450°C

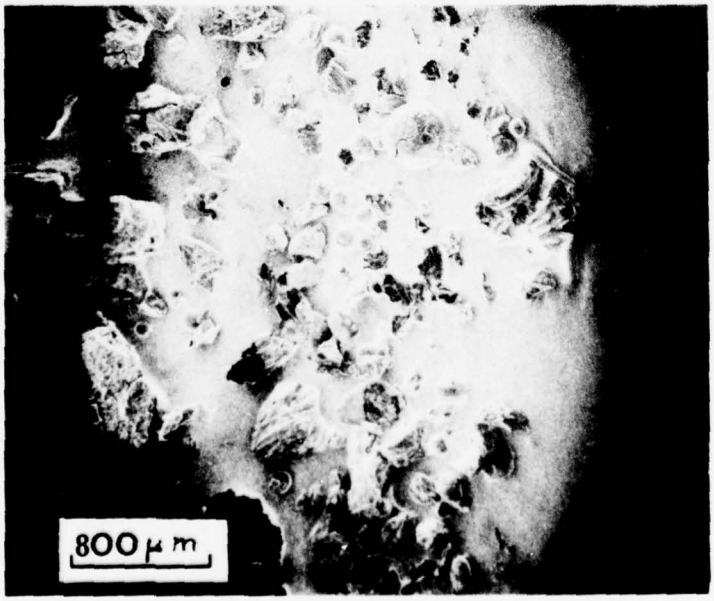

FIG. 28. EXTRACTED MESOPHASE SPHERES AND COALESCED MESOPHASE PARTICLES OBSERVED WITH A SCANNING ELECTRON MICROSCOPE

47. These photomicrographs illustrate a range of sphere sizes from less than 5 μm to about 500 μm. Figures 29-31 indicate that extracted spheres larger than about 15 μm in diameter usually were cracked. The harsh extraction conditions are believed to be responsible for the cracks in spheres. Heating of extracted spheres to 500°C on a microscope hot stage produced no evidence of melting or softening of the spheres. Apparently extraction removed some of the low molecular weight hydrocarbons in mesophase spheres which are responsible for the fluid nature of the spheres at the temperature of sphere formation. This would explain the cracks in extracted spheres, and would make them infusible.

A density gradient column composed of toluene and 1, 1, 2, 2 - tetrabromoethane (ASTM standard D1505) was used to determine the density of extracted mesophase spheres. Spheres and 0.5 mm diameter particles of coalesced mesophase were found to vary in density from 1.40 g/cm^3 to 1.52 g/cm^3. Lewis and Singler[16] reported a value of 1.52 g/cm^3 for the density of mesophase spheres formed during heating acenaphthylene at 400°C for 12 hours. Mesophase spheres separated from pyrolyzed pitches (see Table I, page 10) are known to be more dense than the isotropic unconverted pitch and have been reported [10,24,48] to sink to the bottom of the pyrolysis vessel during heating. However, the samples observed in this study did not show any conclusive evidence of the mesophase sinking to the bottom of the test tubes. Convection currents and stirring of the mesophase-pitch mixture by volatile pyrolysis by-products may have prevented mesophase spheres from sinking to the bottom of the test tubes.

After heating to 466°C, acenaphthylene was more than 50% converted into the ordered mesophase. The microstructure of the 466°C heated sample was very similar and just as inhomogeneous as that of the 450°C pyrolyzed sample described above. Regions containing mesophase spheres and coalesced mesophase were present (see Figure 32), but the extent of formation of the completely coalesced mesophase was much greater than in the acenaphthylene sample pyrolyzed to 450°C.

Between 466°C and 500°C, acenaphthylene was completely converted into the coalesced mesophase, producing a microstructure as shown in Figures 33 and 34. At 500°C the mesophase had solidified and the microstructure or molecular ordering became fixed. The microstructure developed at this point will not change significantly on heating to graphitization temperatures (2800°C).[11,12]

Horne[15] has reported that pyrolysis of acenaphthylene below the temperature of depolymerization for long periods of time (14 hrs. at 300°C) will result in a pitch which undergoes mesophase sphere formation as low as 370°C. This acenaphthylene pitch was completely converted into the coalesced mesophase after heating for 18 hrs. at 400°C in argon. A 50% by weight conversion of acenaphthylene into the mesophase was found after heating at 400°C for 12 hours.[16] Singer and Lewis[39] reported that acenaphthylene pyrolyzed in an argon atmosphere to 430°C produced mesophase spheres up to 100 μm in size. In the current study, spheres as large as 200 μm were observed in samples pyrolyzed to 426°C. These different studies illustrate the wide range of temperature-time conditions which produce sphere formation in acenaphthylene and complete conversion into the coalesced mesophase. Complete conversion of acenaphthylene into uncoalesced spheres is also known to occur if the pyrolysis is conducted at high pressures (260 MN/m^2).[65,66]

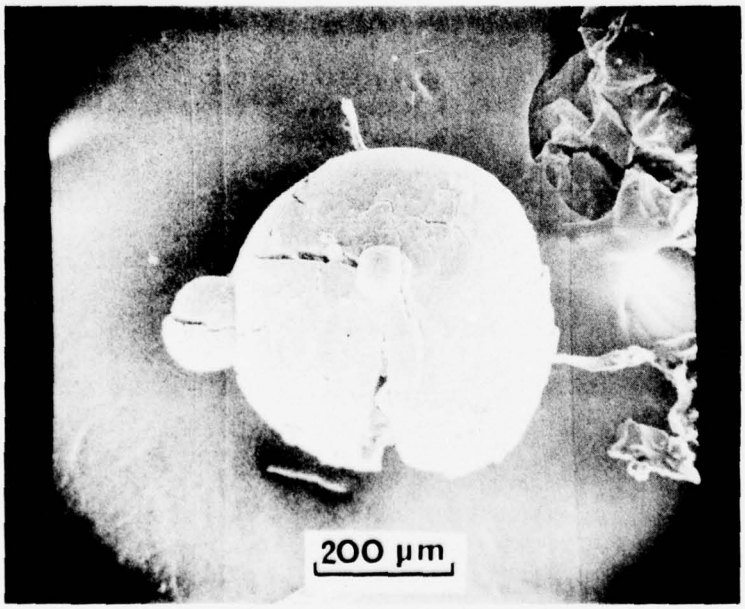

FIG. 29. MESOPHASE SPHERES SEPARATED BY EXTRACTION AND PHOTOGRAPHED USING A SCANNING ELECTRON MICROSCOPE

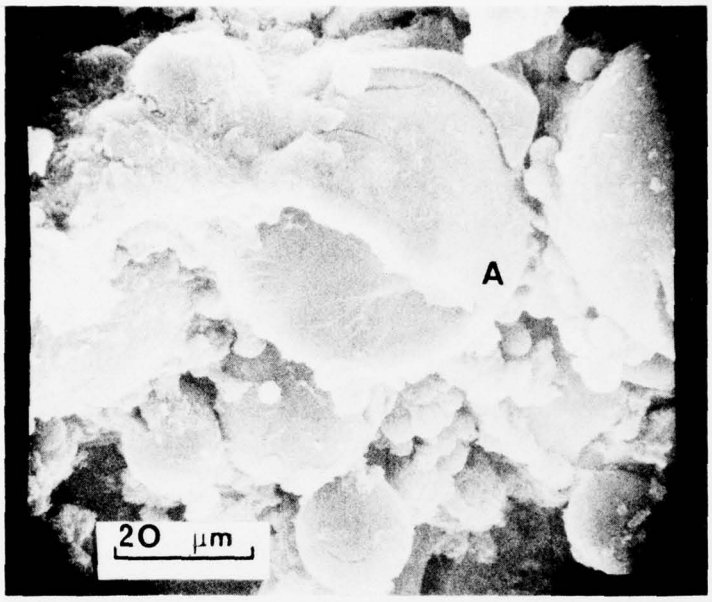

FIG. 30. SCANNING ELECTRON PHOTOMICROGRAPH OF MESOPHASE SPHERES ISOLATED BY EXTRACTING A SAMPLE OF ACENAPHTHYLENE WHICH WAS PYROLYZED TO 450°C

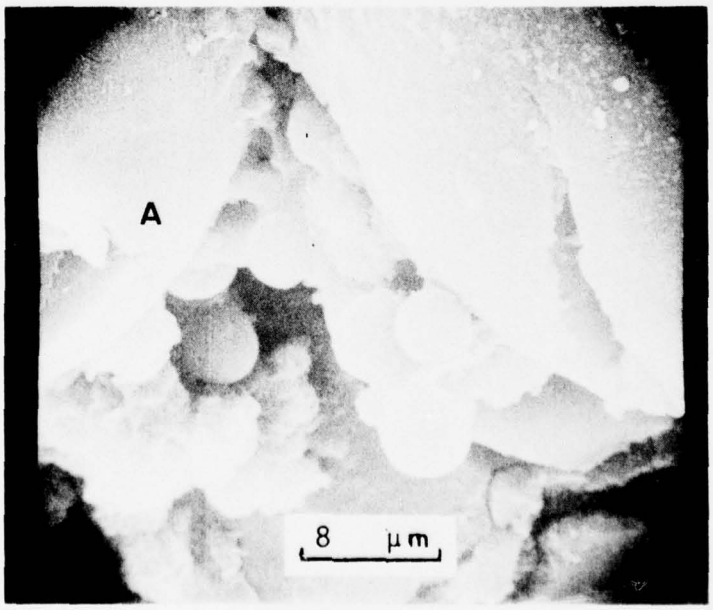

FIG. 31. HIGHER MAGNIFICATION OF REGION A IN FIGURE 30

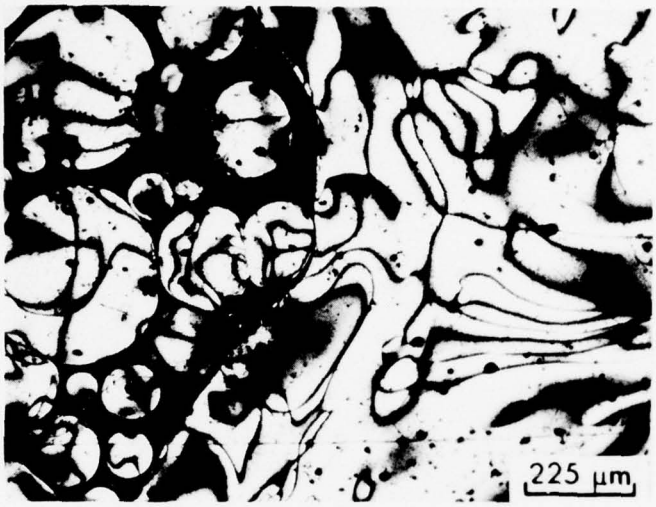

FIG. 32. MESOPHASE GROWTH AND COALESCENCE IN AN ACENAPHTHYLENE SAMPLE HEATED TO 466°C

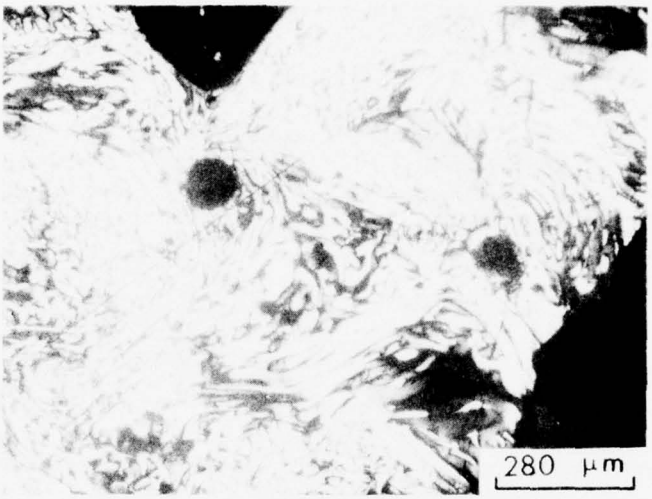

FIG. 33. COMPLETELY COALESCED MESOPHASE IN A SAMPLE OF ACENAPHTHYLENE HEATED TO 500°C

FIG. 34. ACENAPHTHYLENE COMPLETELY TRANSFORMED INTO THE COALESCED MESOPHASE AT 500°C

Several factors are considered noteworthy at this point. Acenaphthylene samples cooled rapidly to room temperature after pyrolysis first begin to show gas bubbles frozen in the residue at 450°C. Numerous bubbles were present in samples cooled rapidly from 462°C, 466°C, and 500°C. This is characteristic of viscosity increases as the degree of mesophase transformation increases. The regions around the gas bubbles or pores were more often than not composed of the fibrous microstructure (see Figures 35 and 36). In addition, the fine fibrous microstructure was not observed until acenaphthylene was heated above 466°C. (see Figure 36). However, only a small percent (<20%) of the total sample was transformed into regions showing the fine fibrous microstructure. White and Price[13,14] have reported that gas bubble formation stresses the coalesced mesophase formed during the pyrolysis of pitches. The stress deforms the coalesced mesophase and causes the formation of the fine fibrous structure which is characteristic of good needle cokes. This can happen only if the coalesced mesophase is sufficiently fluid to undergo extensive mechanical deformation just prior to solidification. Apparently, this same phenomenon produces the fine fibrous microstructure in the mesophase from acenaphthylene.

C. PYROLYSIS OF ACENAPHTHYLENE USING A MICROSCOPE HOT STAGE

A common method used to study liquid crystal formation is direct observation of the sample using a microscope hot stage. Since liquid crystals wet glass, their formation may be observed in liquid films between glass plates with a polarized light microscope. The carbonaceous mesophase is similar to a nematic liquid crystal and is known to wet mica, [9] carbon and graphite particles, [9,10] and metal oxide particles.[77] A simple microscope hot stage was built (see Figure 11, page 28) to observe mesophase formation in acenaphthylene in the 400°C to 500°C temperature range. The intent was to obtain direct information on the influence of gas bubble formation and percolation on the mesophase at the temperature of mesophase formation.

1. Preliminary Experiments

Preliminary experiments using the microscope hot stage revealed a number of technical problems. As reported earlier, 56% of the sample weight is removed during pyrolysis to 500°C as volatile by-products. These gases tend to condense on the microscope objective and prevent direct observation of the sample while it is being heated. The hot gases also have a corrosive effect on the objective. If a glass plate is placed between the objective and the cover glass on the hot stage, gaseous pyrolysis products condense on it immediately and also prevent direct observation of the sample using reflected polarized light.*

An attempt was made to remove the volatile by-products by passing an inert gas (argon) over the top cover glass and also directing a stream of gas across the tip of the objective. This technique prevented volatile by-products from obscuring the view; however, it caused a severe temperature gradient from the bottom glass slide to the top cover glass. As a result, the top cover glass was below the temperature

*Films of the black pitch-mesophase mixture as thin as 50 μm were not transparent to light, and the samples could be observed only with reflected polarized light.

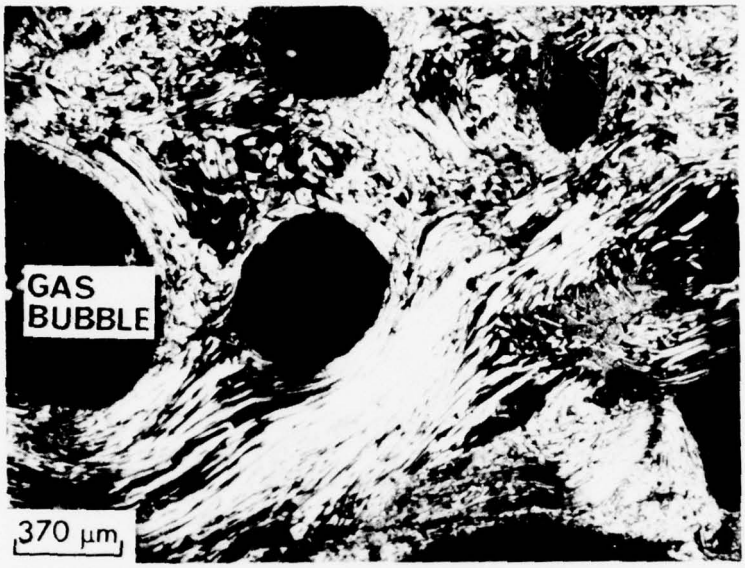

FIG. 35. FIBROUS MICROSTRUCTURE IN ACENAPHTHYLENE PYROLYZED TO 500°C

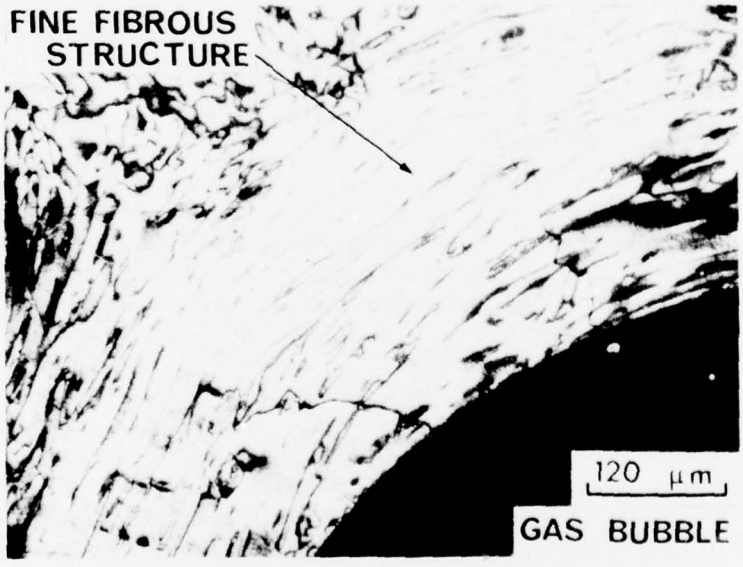

FIG. 36. FINE FIBROUS MICROSTRUCTURE AROUND A GAS PORE IN AN ACENAPHTHYLENE SAMPLE HEATED TO 500°C

required for mesophase formation (400°C) and the mesophase transformation could not be observed. Several experiments were conducted using the argon flow to sweep away the pyrolysis gases. No optical anisotropy was observed at elevated temperature even when the samples of acenaphthylene were heated on the hot stage to 460°C.*

Two experiments were conducted in which no argon was used to sweep away the volatile by-products. The objective was raised away from the hot stage to prevent gases from condensing on it. When the hot stage reached 440°C,* the objective was lowered and mesophase sphere formation and coalescence could be observed directly for one or two minutes before the objective tip was coated with condensate. Samples of acenaphthylene pyrolyzed in this manner were rapidly cooled to room temperature in two to three minutes by removing them from the hot stage with tweezers. Mesophase droplets were found to wet the glass slides. As a result, polarized light extinction contours which represent molecular ordering could be observed directly through either the top or bottom glass slides. Figures 37 through 40, pages 53 and 54, summarize the results of observations made at room temperature using reflected polarized light. A random distribution of mesophase droplets up to 16 μm in size was observed in several regions as shown in Figure 37. This photomicrograph gives many examples of extinction contours and crosses which indicate that the majority of the droplets have the same optical characteristics as observed in polished cross sections of samples containing ideal mesophase spheres. In other regions of the samples, strings of coalesced mesophase droplets were observed (see Figures 38-40, pages 53, 54). The coalesced droplets were found to be as large as 60 μm in size, indicating that several smaller spheres had coalesced to produce the strings of mesophase droplets. It is now known that these strings of coalesced mesophase droplets are formed by gas bubble percolation through the sample. This phenomenon will be described in detail in the following section.

The term mesophase "droplet" instead of mesophase sphere will be used in discussing the hot stage results. Since the mesophase must wet the cover glass to be observed, it does not form as a perfect sphere. The mesophase probably takes on a hemispherical shape in these experiments with the flat part of the hemisphere next to the cover glass. Therefore, the term droplet will be used to describe the mesophase particles formed initially during hot stage pyrolysis.

The microstructures illustrated by the photographs on pages 53 and 54, and all other photographs in Section C of Chapter IV, could be observed through either the top or bottom glass slide. Unless stated otherwise, all photographs were taken at room temperature using reflected polarized light which passed through the glass slide. Careful separation of the glass slides frequently caused the pyrolysis residue to cleave away from the glass surface. In such cases the surface of the pyrolysis residue which had wet the glass slide could be examined directly using reflected polarized light. The microstructure of the sample surface was the same when observed directly as it was when observed through the glass slide. In addition, no apparent differences were noted between the mesophase microstructure observed at 420°C to 450°C and that observed at room temperature. This indicates that the polarized light extinction contours observed in the hot stage microscopy part of this study were a result of molecular ordering, and not due to strain effects in the glass slides or the sample itself.

*No attempt was made to accurately program the temperature-time cycle in the preliminary experiments. The actual sample temperature was 20 - 30°C lower than that of the hot stage. A discussion on temperature measurement is given in section C.2 of this Chapter.

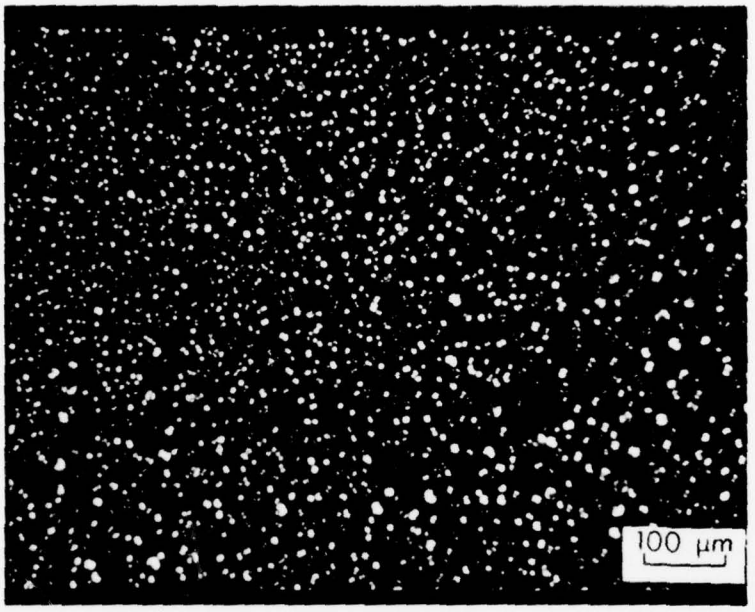

FIG. 37. MESOPHASE DROPLET FORMATION DURING HOT STAGE PYROLYSIS OF ACENAPHTHYLENE

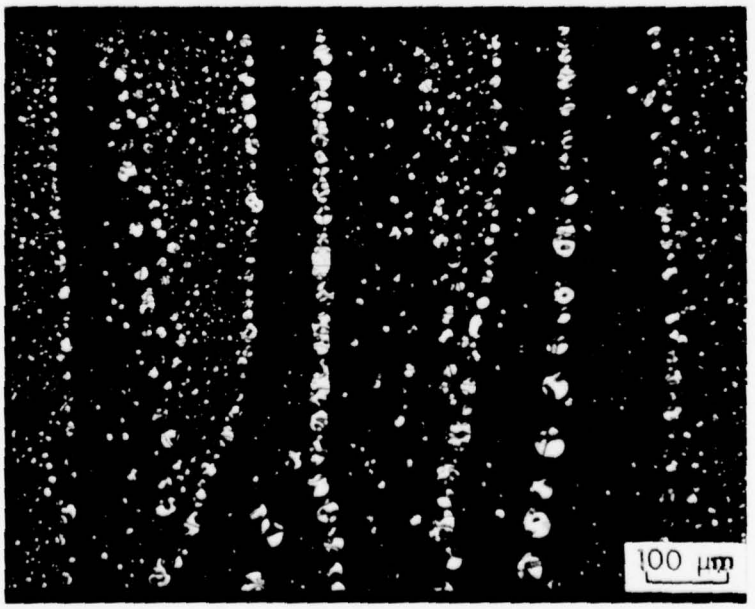

FIG. 38. STRINGS OF COALESCED MESOPHASE DROPLETS FORMED DURING HOT STAGE PYROLYSIS OF ACENAPHTHYLENE

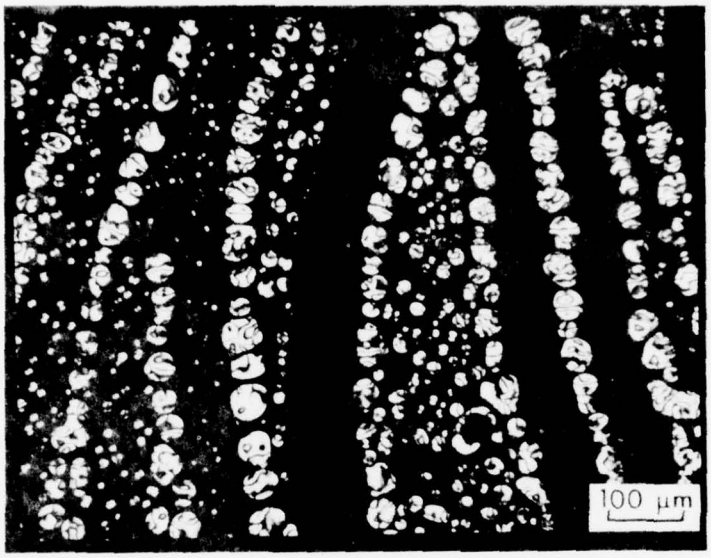

FIG. 39. GAS BUBBLE TRACKS IN THE MESOPHASE PRODUCED DURING HOT STAGE PYROLYSIS OF ACENAPHTHYLENE

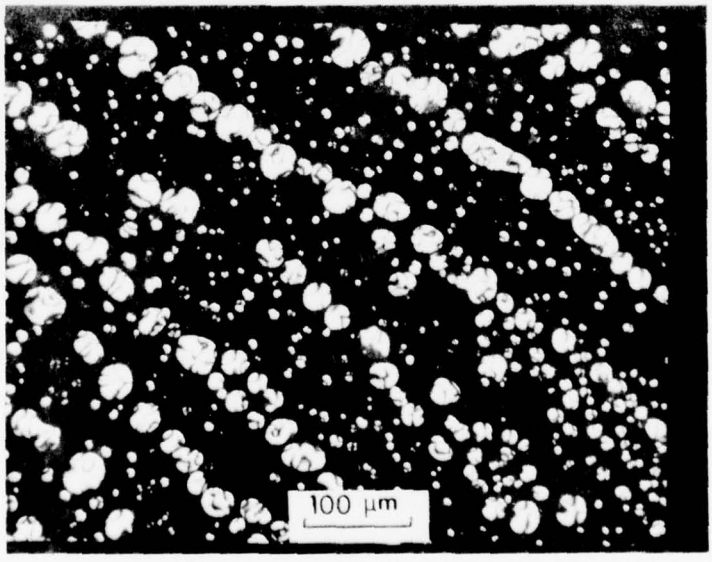

FIG. 40. MESOPHASE DROPLET COALESCENCE CAUSED BY BUBBLE PERCOLATION IN AN ACENAPHTHYLENE SAMPLE PYROLYZED ON A HOT STAGE

2. Influence of Gas Bubbles on Mesophase Formation

Changes were made in the hot stage pyrolysis technique to allow direct observation of the sample using reflected polarized light. The microscope and hot stage were positioned next to a large vent attached to an exhaust fan. This allowed efficient removal of the volatile pyrolysis gases without causing a large temperature gradient from the bottom glass slide to the top cover slide. As a result, mesophase formation, growth, and coalescence could be observed at the temperature of formation.

A thermocouple touching the bottom glass slide (see Figure 11, page 28) was used to measure the temperature. The actual sample temperature would be expected to be less than the measured temperature, since a temperature gradient probably exists from the bottom glass slide to the top cover slide. In order to better determine the sample temperature, melting point standards which melt at 206°C, 216°C, 258°C, and 318°C were used to calibrate the hot stage. The results indicate the measured temperature is 20°C to 30°C higher than the true temperature of the sample. A hole had been cut in the insulation covering the top of the sample (see Figure 11, page 43) in order to observe mesophase formation during pyrolysis. This probably caused a temperature variation of a few degrees across the sample in the horizontal direction from the center to the edge of the glass slides. Accurate temperature measurements would enable one to determine the temperature-time conditions necessary for mesophase formation. However, it is not essential to know the exact temperature in a study of the influence of gas bubble percolation on the mesophase. In this discussion of the hot stage pyrolysis of acenaphthylene, the sample temperatures reported are approximate and were determined by subtracting 25°C from the measured temperature of the copper heating block.

Figures 41 and 42, pages 56 and 57, give examples of the maximum and minimum heating rates for the hot stage. As indicated, samples were heated rapidly to about 370°C in 40 minutes. This temperature was held for approximately 25 minutes to allow removal of the large amounts of volatile acenaphthylene formed during pyrolysis. Mesophase formation was accomplished using heating rates of 0.6°C/min to 1.3°C/min. The slower heating rate produced mesophase formation at temperatures as low as 413°C compared to 421°C for the 1.3°C/min heating rate. Samples pyrolyzed in test tubes (see Chapter IV, Section B) at 0.3°C/min were heated for longer times near 400°C and produced sphere formation at even lower temperatures (about 400°C).

A total of seven experiments were conducted in which mesophase formation, growth, and coalescence was observed directly using reflected polarized light microscope during the pyrolysis of acenaphthylene on the hot stage. The discussion that follows is based on actual observations (at magnifications of 50 and 100) of mesophase formation and coalescence between 413°C and 455°C. Although no photographs were taken as the samples were being pyrolyzed, photographs taken after the heated samples were rapidly cooled to room temperature can be used to illustrate the results of these experiments. The results will be discussed in terms of the types of physical effects that gas bubbles have on the mesophase. These occur to some extent throughout the entire temperature range, even though increases in time or temperature gradually increase the percent of coalesced mesophase present in the sample.

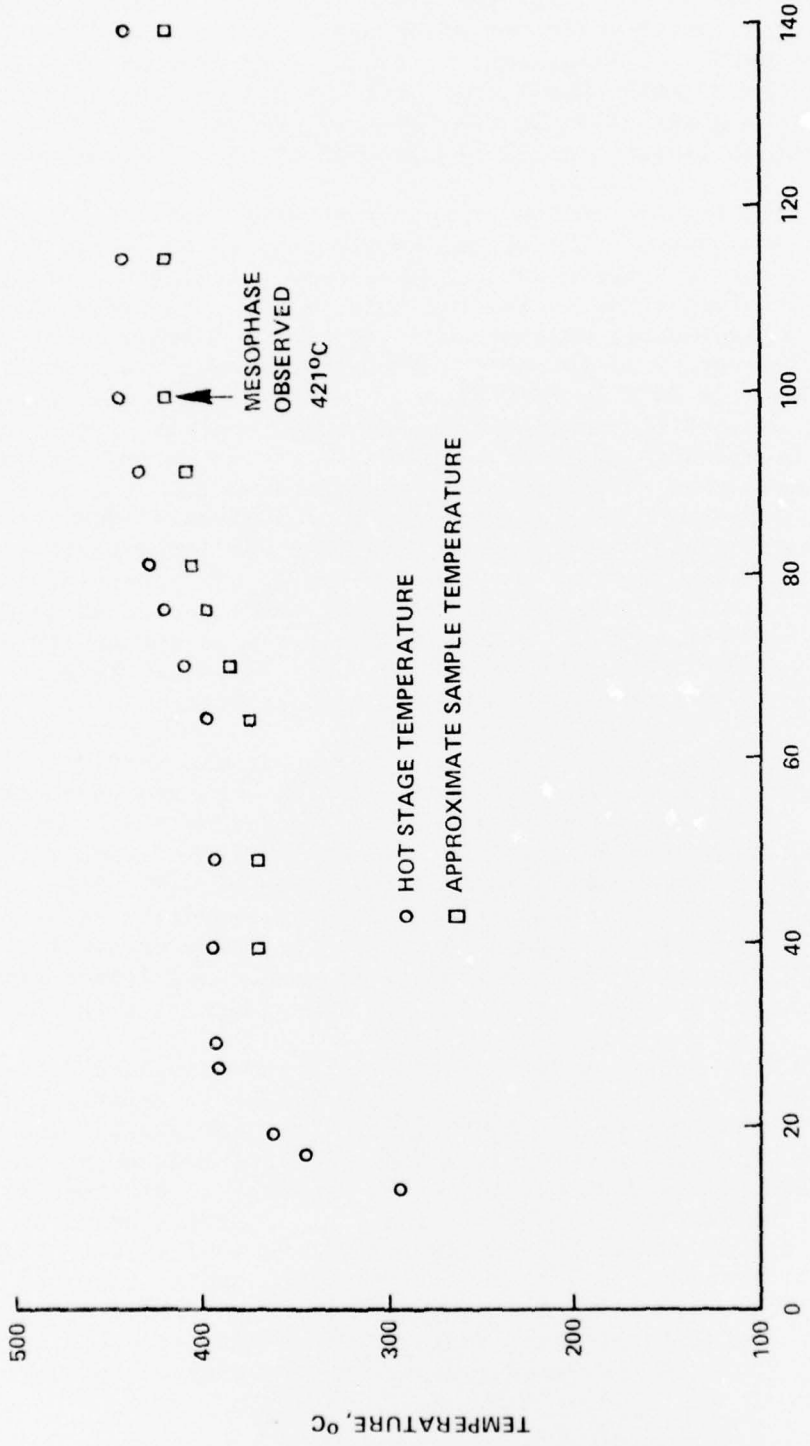

FIG. 41. TEMPERATURE - TIME CYCLE FOR HOT STAGE PYROLYSIS OF ACENAPHTHYLENE MAXIMUM HEATING RATE

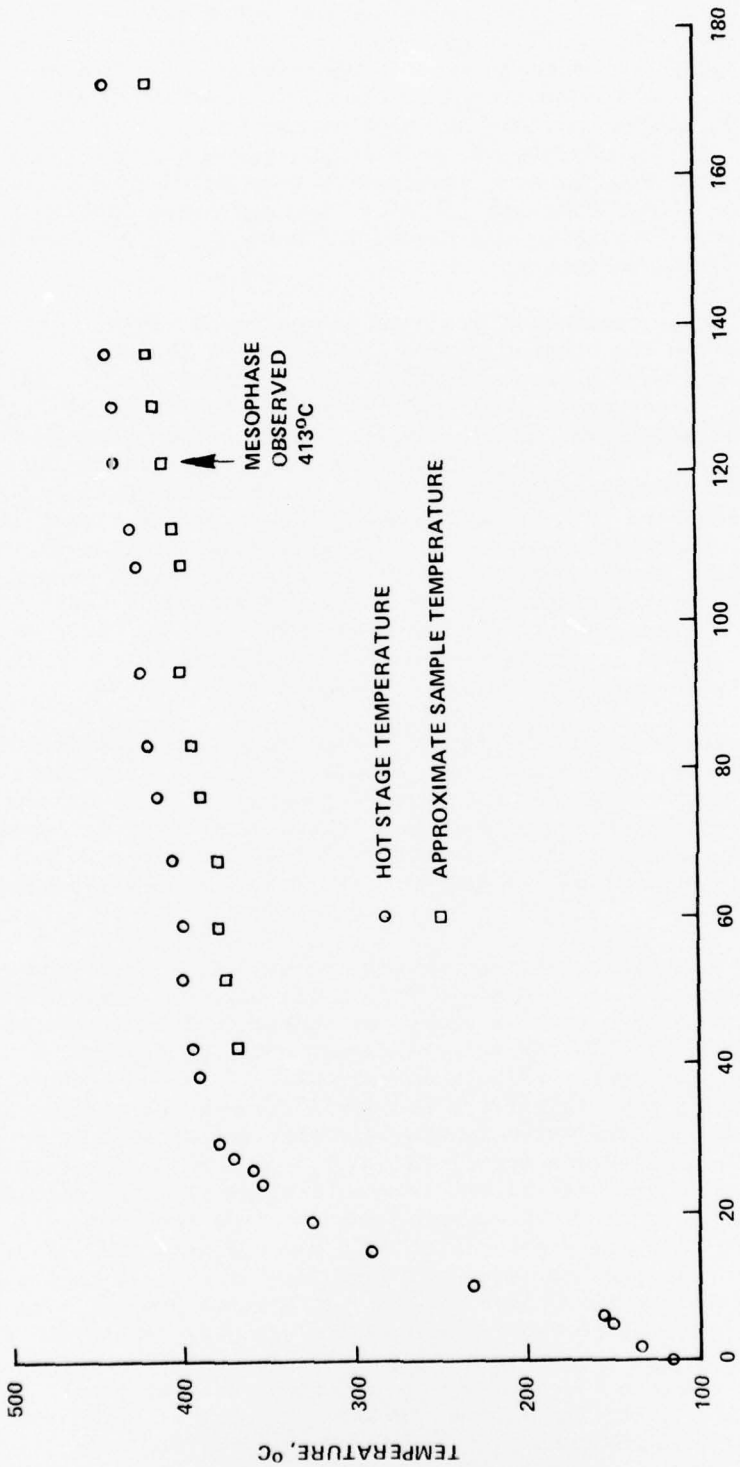

FIG. 42. TEMPERATURE - TIME CYCLE FOR HOT STAGE PYROLYSIS OF ACENAPHTHYLENE MINIMUM HEATING RATE

On melting at 86 - 90°C, acenaphthylene was converted into a light yellow liquid. The yellow liquid darkens and changes from yellow to orange to red-orange in the 300°C to 350°C temperature range. Soon afterwards a black pitch-like liquid forms and gas evolution becomes rapid in the 350°C to 400°C temperature range. This corresponds to the removal of gaseous by-products, primarily acenaphthene, which forms as a result of degradation of the acenaphthylene polymers. During this temperature range gas bubbles were observed to move across the field of view in a fraction of a second (at 100X, the field of view was about 1000 μm in diameter). The gas bubbles were usually in the range of 250 to 300 μm in diameter, but varied in size from a few micrometers to 1000 μm.

Above 400°C the formation of gas bubbles decreased rapidly and two to ten seconds were required for bubbles to travel 1000 μm in the sample. Bubbles were observed to form and move through the 1000 μm diameter field of view at 5 to 10 second intervals. After heating to temperatures in the range of 413°C to 421°C, mesophase droplets were found in all samples when observed through either the top or bottom glass slide. These droplets were usually less than 20 μm in diameter and were randomly dispersed throughout the liquid pitch as shown in Figure 43. Gas bubbles were observed to push the mesophase droplets around almost immediately after they were formed. Bubble formation in a region similar to that shown in Figure 43 pushed the mesophase droplets aside and forced them together, causing coalescence. Movement of gas bubbles through the same region caused coalescence of mesophase droplets along the front and sides of the gas bubble track. As a result, the bubbles produced a line or string of coalesced mesophase droplets along the boundary of the bubble path (See Figures 44 and 45, page 60).

Temperature increases or increased in time at a fixed temperature caused the mesophase droplets to grow in size and number. However, the primary mode of droplet growth was coalescence caused by gas bubbles pushing droplets together. Repeated bubble percolation through the same region formed strings of coalesced mesophase and coalesced droplets an order of magnitude larger in size than the mesophase droplets formed in regions of the sample with little or no gas bubble percolation (see Figures 46 and 47).

The influence of gas bubble percolation on mesophase formation in a large region of the sample is illustrated in Figure 48, page 62. Figure 48 is a composite photograph showing one-fourth of a sample of acenaphthylene heated to about 425°C and held at this temperature for forty minutes. This photograph shows several examples of strings of coalesced mesophase droplets formed by bubble percolation. Gas bubbles formed in the region at A and moved through the sample along the bubble tracks indicated at B. The white-spotted circular region at C is a gas bubble about 400 μm in size which was moving from A toward the large bubble at D. The bubble at C in Figure 48, page 62 was frozen in place by rapid cooling of the sample. During pyrolysis, about 10 to 15 seconds were required for bubbles to move from A to D. Gas bubbles repeatedly moved from A to D and pushed droplets of mesophase less than 20 - 30 μm in size to the sides of the bubble path where they became crowded together and were forced to coalesced. This pattern of droplet formation, followed by forced coalescence due to bubble percolation was observed in all seven experiments. At higher magnifications (see Figures 49 and 50, pages 63 and 65), it appears that the gas bubble at C in Figure 48, page 62 has undergone deformation from its normal circular shape due to a collision with a coalesced droplet of mesophase along the side of the bubble track. Apparently, coalesced droplets larger than about 100 μm in size resist being pushed aside by gas bubbles due to the increased contact between the glass slide and the droplet.

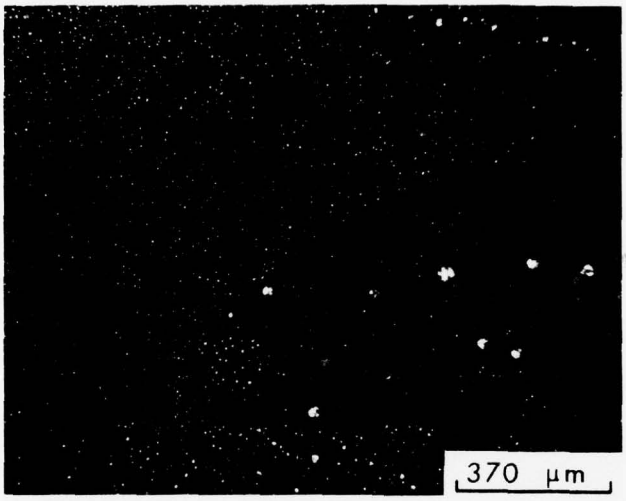

FIG. 43. INITIAL FORMATION OF MESOPHASE DROPLETS IN ACENAPHTHYLENE HEATED TO 421°C ON THE MICROSCOPE HOT STAGE

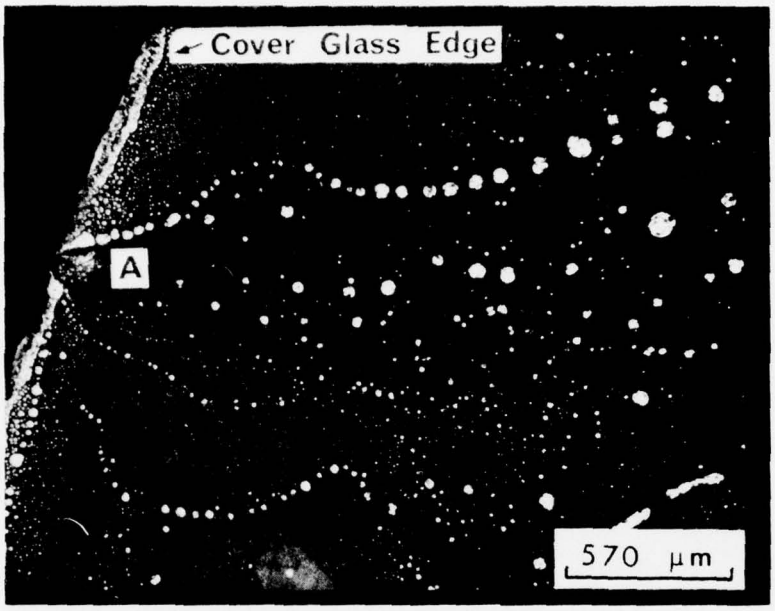

FIG. 44. STRINGS OF COALESCED DROPLETS OF MESOPHASE FORMED BY GAS BUBBLE PERCOLATION

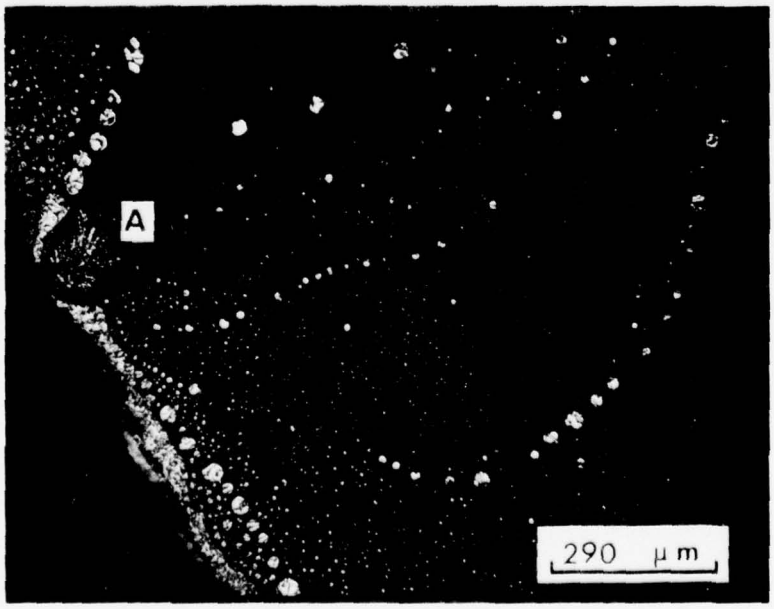

FIG. 45. HIGHER MAGNIFICATION OF REGION A IN FIGURE 44

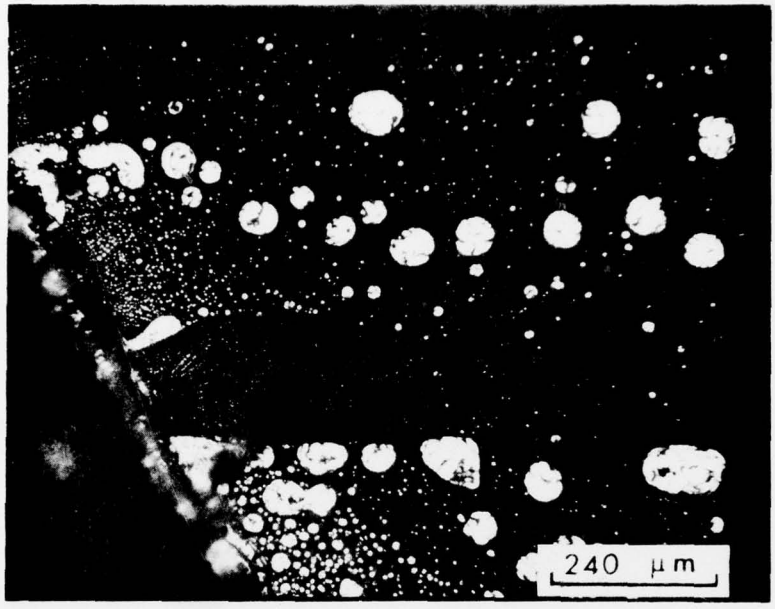

FIG. 46. ACCELERATED COALESCENCE OF MESOPHASE DROPLETS DUE TO GAS BUBBLE PERCOLATION DURING HOT STAGE PYROLYSIS OF ACENAPHTHYLENE

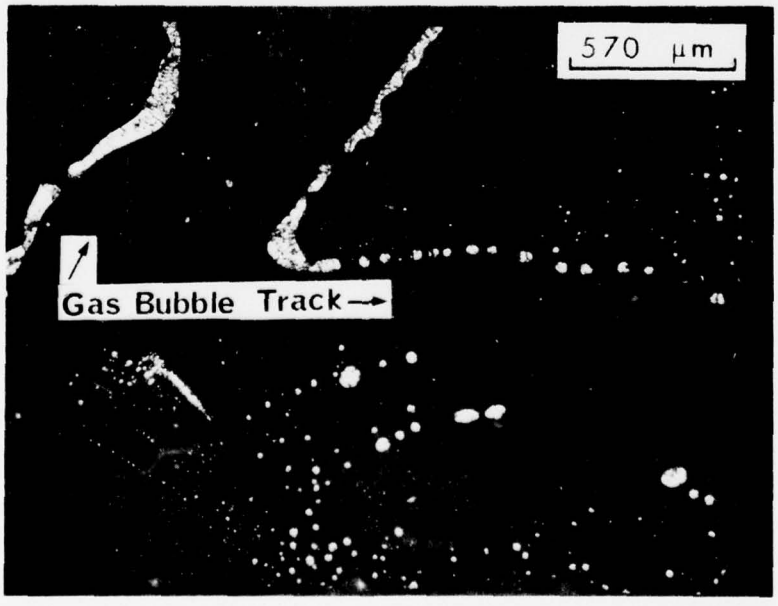

FIG. 47. COALESCED MESOPHASE DROPLETS OUTLING THE PATH OF GAS BUBBLES WHICH FORMED DURING ACENAPHTHYLENE PYROLYSIS

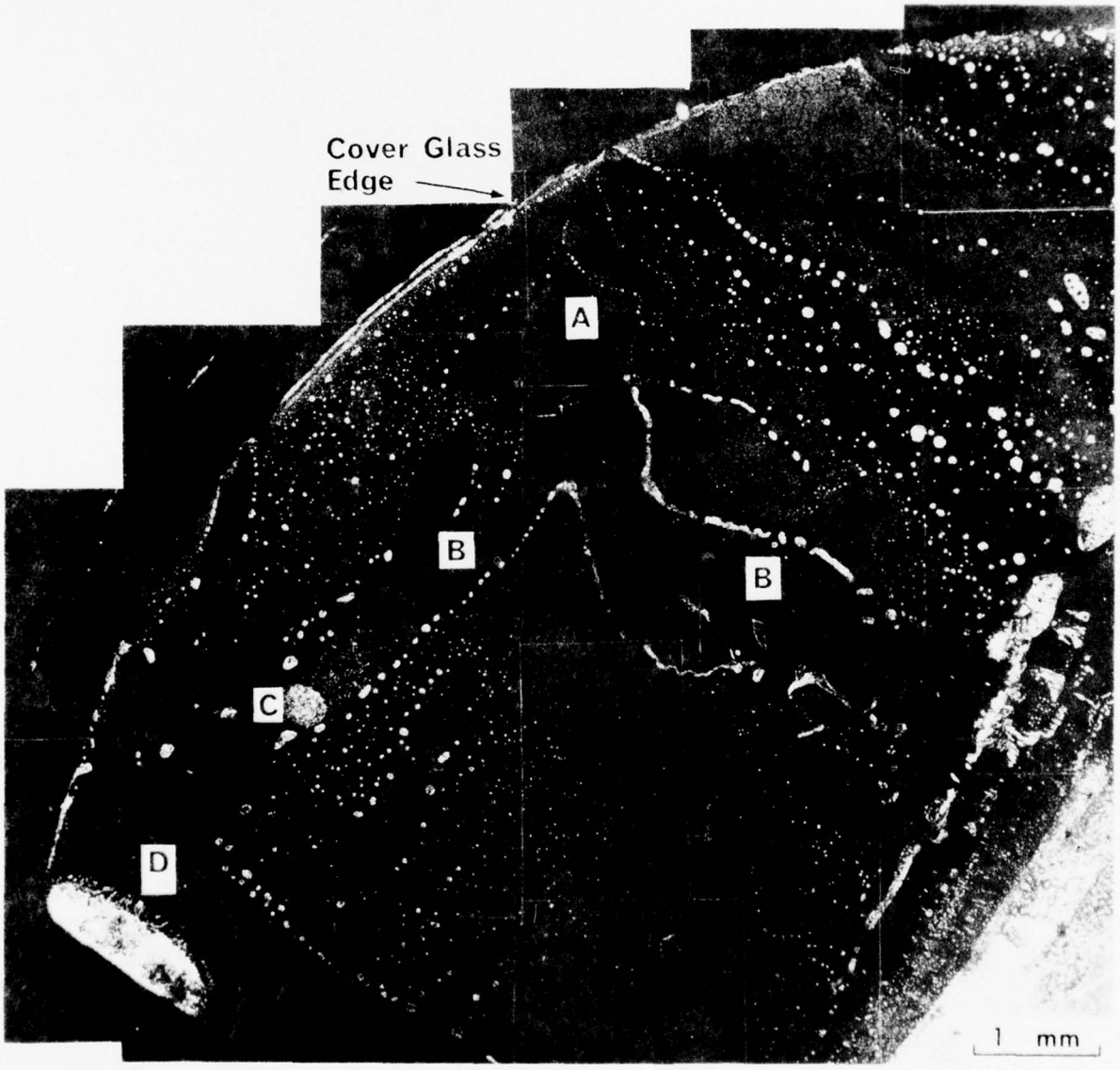

FIG. 48. COMPOSITE PHOTOGRAPH SHOWING STRINGS OF MESOPHASE DROPLETS FORMED BY GAS BUBBLE PERCOLATION DURING PYROLYSIS

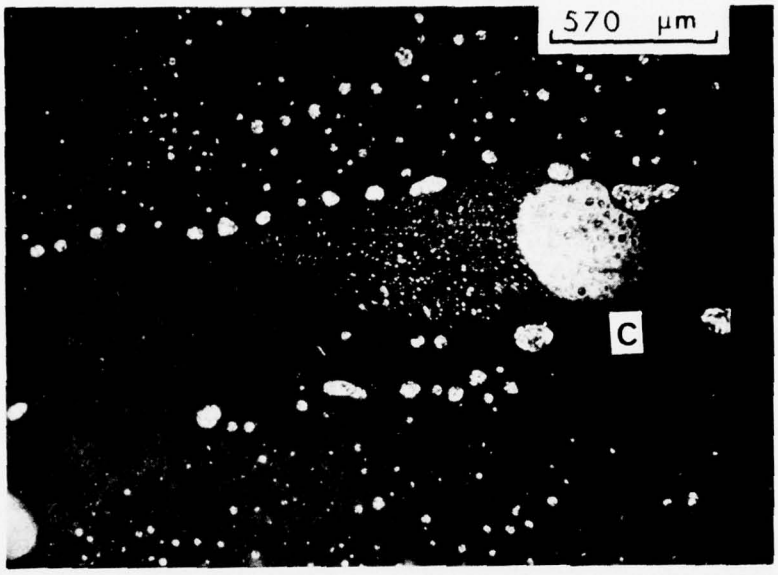

FIG. 49. GAS BUBBLE (C) TRAPPED IN A BUBBLE TRACK BY RAPID COOLING OF A SAMPLE OF ACENAPHTHYLENE PYROLYZED ON THE HOT STAGE

Figure 48, page 62 and Figure 50, page 65 illustrate another point. As discussed previously, most droplets of mesophase in the path of a gas bubble are pushed aside. Small droplets of mesophase not visible in front of a gas bubble were observed to be pushed against the top cover glass by the bubble. This caused the mesophase droplets to become attached to the top cover glass inside the gas bubble. As a result, the droplets became visible as white spots inside the bubble as shown at C in Figure 49, page 63 and Figure 50, page 65. After the gas bubble moved away, the droplets wetting the top cover glass slowly lost contact with the glass and disappeared into the liquid pitch. This phenomenon was not observed consistently. However, when it did occur, the trail of small mesophase droplets attached to the top cover glass disappeared a few seconds after the bubble moved away.

Another area of the sample described above shows long strings of coalesced mesophase almost one mm long (see Figure 51). These strings of completely coalesced mesophase were formed when a single gas bubble moved from A to B in the photo. Prior to the gas bubble movement, the entire region was composed of small mesophase droplets similar to region D. Repeated gas bubble percolation through a region causes a rapid increase in the size of the coalesced droplets but decreases the total number of droplets present.

When a gas bubble moved a mesophase droplet, the polarized light extinction contours were changed, indicating rearrangement of the molecular structure in the droplet. In most cases, at least part of the droplet lost contact with the glass surface and it was not possible to observe the entire droplet. The surface of mesophase droplets next to the cover glass became torn and disorganized if the droplets were repeatedly moved around. They could not maintain a smooth surface next to the cover glass, and it was not possible to distinguish the extinction contours as shown in Figure 52. The appearance of mesophase droplets in Figure 52 is in sharp contrast to the well defined extinction contours observed in droplets which remain stationary for 10 to 20 minutes as shown in Figure 46, page 60.

Coalescence of mesophase droplets was observed along the front and sides of gas bubbles moving through the sample. The actual coalescence process occured within five seconds after initial contact of two droplets. Coalescence in such a short period of time indicates that the mesophase droplets are very fluid at 410°C to 450°C. Polarized light extinction contours began to change in each droplet immediately after their initial contact, indicating rearrangement of the molecules in the mesophase droplet. Movement of the extinction contours continued until the two droplets grew together into an oblong shape. In samples pyrolyzed in test tubes spheres in contact with one another were sometimes observed to be deformed rather than coalesced. Coalescence would not be expected to occur if the molecular layers of each sphere are orientated at the point of contact in a manner that prevents interleaving of the layers. However, the stress applied to mesophase droplets by gas bubble percolation is apparently sufficient to force mesophase droplets to coalesce regardless of the orientation of molecules at the point of contact.

Other indications of the fluid nature of the acenaphthylene mesophase were found. Droplets of mesophase larger than approximately 200 μm in diameter tend to resist being moved by bubbles of about the same size. When a gas bubble hit on one of these large droplets, movement of the polarized light extinction contours in the droplet could be observed, even though the droplet itself did not move. A moving gas bubble can apparently apply a stress to the mesophase droplet, which tries to relieve the stress by rearrangement of the large planar molecules in the mesophase.

FIG. 50. COMPOSITE PHOTOGRAPH OF MESOPHASE DROPLETS ORDERED DURING PYROLYSIS BY GAS BUBBLE MOVEMENT

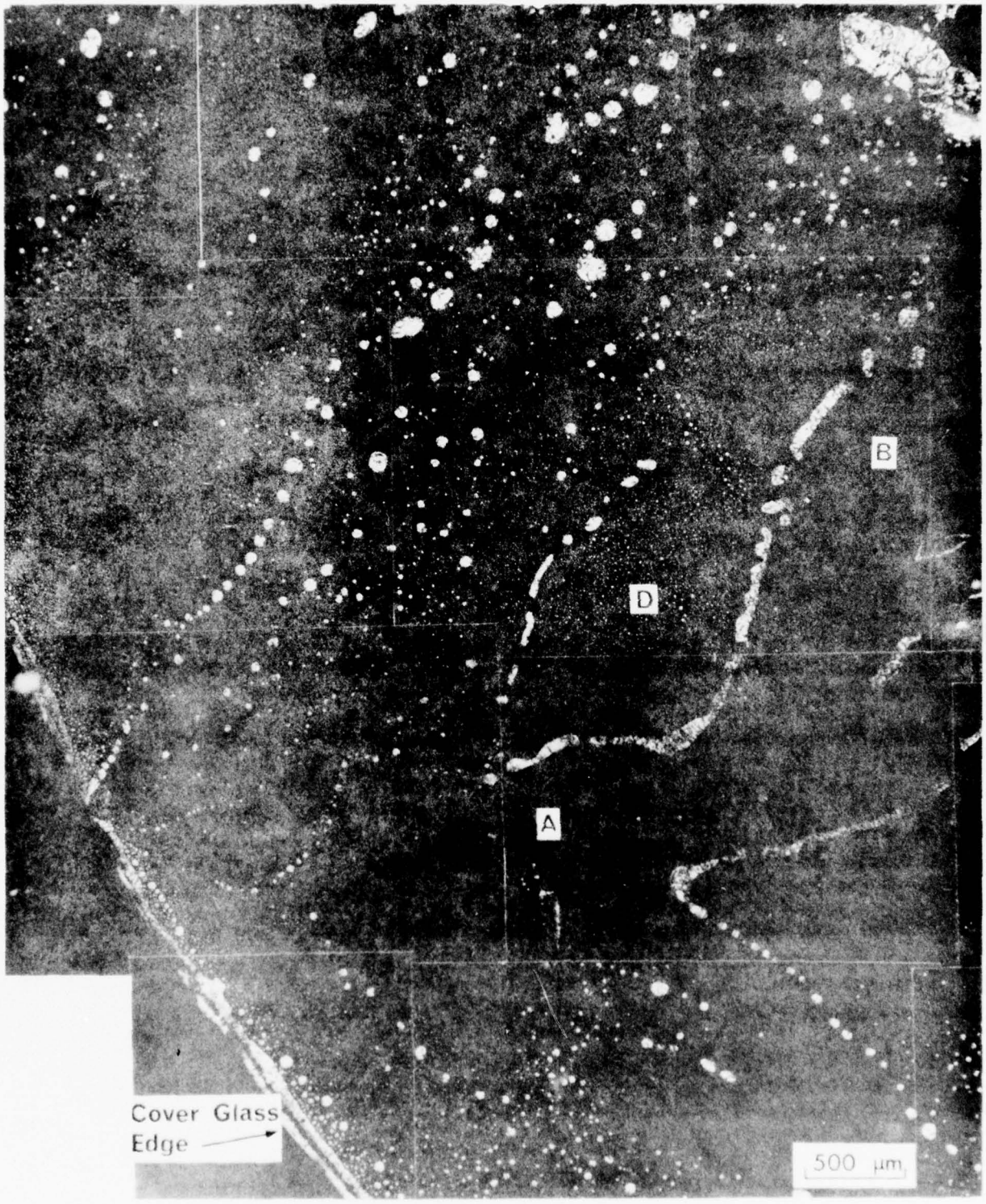

FIG. 51. HIGHER MAGNIFICATION OF REGIONS A AND B IN FIGURE 48

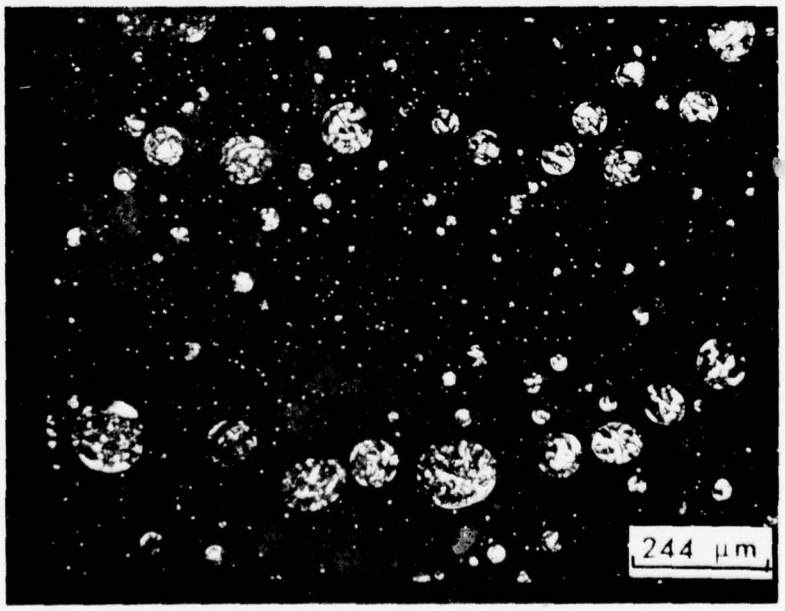

FIG. 52. MESOPHASE DROPLETS SHOWING A TORN SURFACE WITH ONLY PARTIAL CONTACT WITH THE COVER GLASS

Figure 53 gives an example of a curved string of coalesced mesophase droplets resulting from the slow formation of a large (1.5 - 2 mm) gas bubble in region A. Mesophase droplets were pushed along the gas-liquid interface as the gas bubble formed. The increasing size of the bubble crowded mesophase droplets together along the gas-liquid interface, causing them to coalesce. When the gas bubble collapsed as the volatile by-products escaped from the sample, the region occupied by the bubble was rapidly filled with untransformed pitch. The more viscous mesophase droplets remained in place, outlining the original liquid-gas interface. The photomicrograph shown in Figure 53, page 69 was taken through the top cover glass using reflected polarized light. Figure 54, page 69 shows the same area photographed through the bottom cover glass. These figures illustrate that once the mesophase droplets become as large in diameter as the sample is thick (about 50 - 60 μm) they wet the top and bottom glass slides. Droplets of this size show the same general characteristics when observed from either side of the sample. However, the molecular order in a single droplet, and therefore the polarized light extinction contours, is usually not the same at the top and bottom of the sample.

A band of coalesced mesophase was observed to some extent around the edge of all samples (see Figure 55). In general, the mesophase droplets next to this band of coalesced mesophase were larger in size than droplets a mm away from the edge of the cover glass (provided no bubble percolation had occurred in the region). There are several possible explanations for this observation. Since the sample and glass slides were placed in a recess in the heated copper block (see Figure 11, page 28), it is possible that the temperature around the edge of the sample was higher. This would cause a faster rate of mesophase growth near the sample edge. Oxygen present in amounts greater than about 5% by weight [14, 24] is known to cause formation of an isotropic coalesced mesophase (see page 32). These hot stage experiments were conducted in air, and one cannot rule out the possibility that the coalesced mesophase band along the sample edge is a result of reactions involving oxygen. However, in two experiments large gas bubbles were observed to repeatedly push mesophase droplets to the edge of the sample, where coalescence occurred to produce a band of coalesced mesophase. A similar effect is shown in Figure 56, region B, in which gas bubbles have pushed mesophase droplets from A to B. The result is a rapid build-up in the size of the coalesced mesophase droplets at the edge of the liquid in region B. Except in the case of the "edge effects" as illustrated in Figure 56, region B, strings of coalesced mesophase or droplets of mesophase are formed parallel to the direction of gas bubble movement.

The size of the coalesced mesophase regions near the edge of the glass slides grew larger with increases in temperature or time. At about 455°C, regions of coalesced mesophase larger than 1 mm were formed next to the sample edge. This coalesced mesophase had not been subjected to bubble percolation and as shown in Figure 57, page 72, produced a fine isotropic microstructure when observed under polarized light. Coalesced mesophase formed by bubble percolation had a much larger spacing between the polarized light extinction contours as illustrated in Figures 58 and 59, page 73.

Figures 58 and 59 also show that rapid forced coalescence of mesophase droplets due to bubble percolation leads in many cases to entrapment of untransformed pitch within the coalesced mesophase. Mesophase droplets will form inside these entrapped pools of untransformed pitch if the pyrolysis is continued.

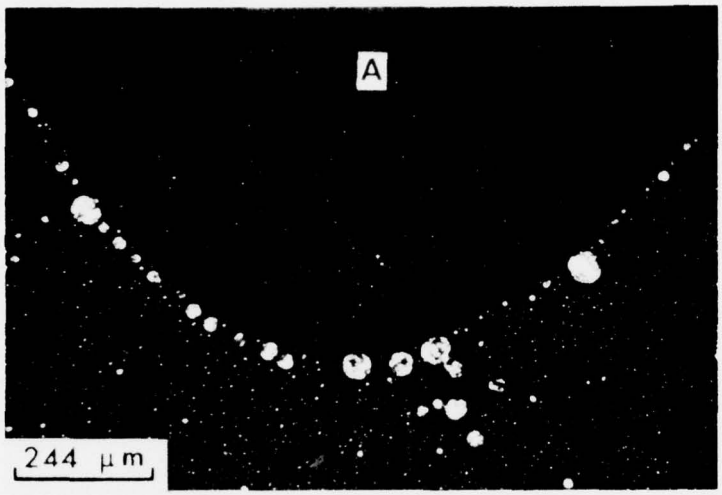

FIG. 53. COALESCED MESOPHASE DROPLETS OUTLINING ONE SIDE OF A GAS BUBBLE WHICH FORMED DURING HOT STAGE PYROLYSIS OF ACENAPHTHYLENE

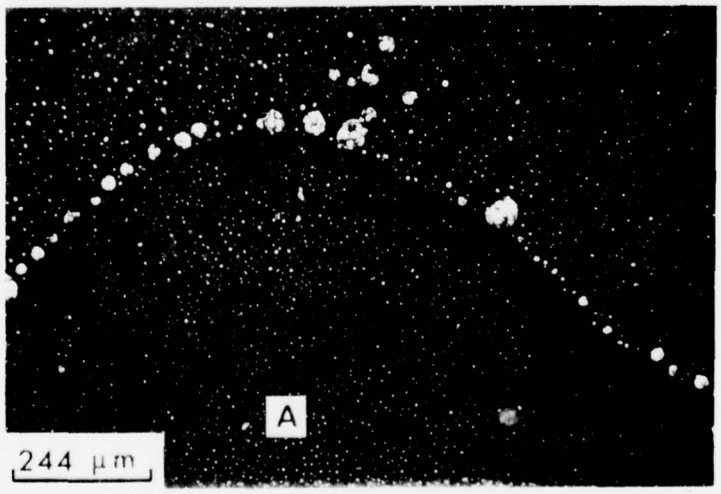

FIG. 54. PHOTOGRAPH OF THE BOTTOM SIDE OF THE AREA SHOWN IN FIGURE 53

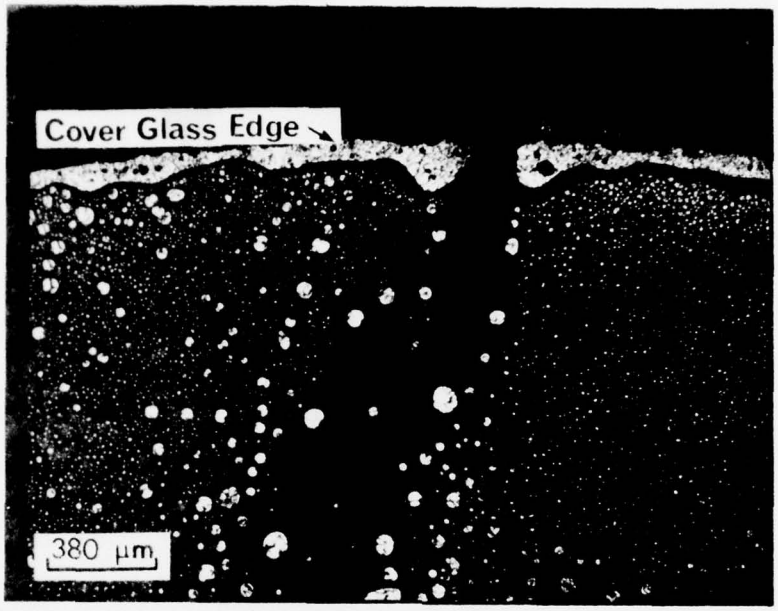

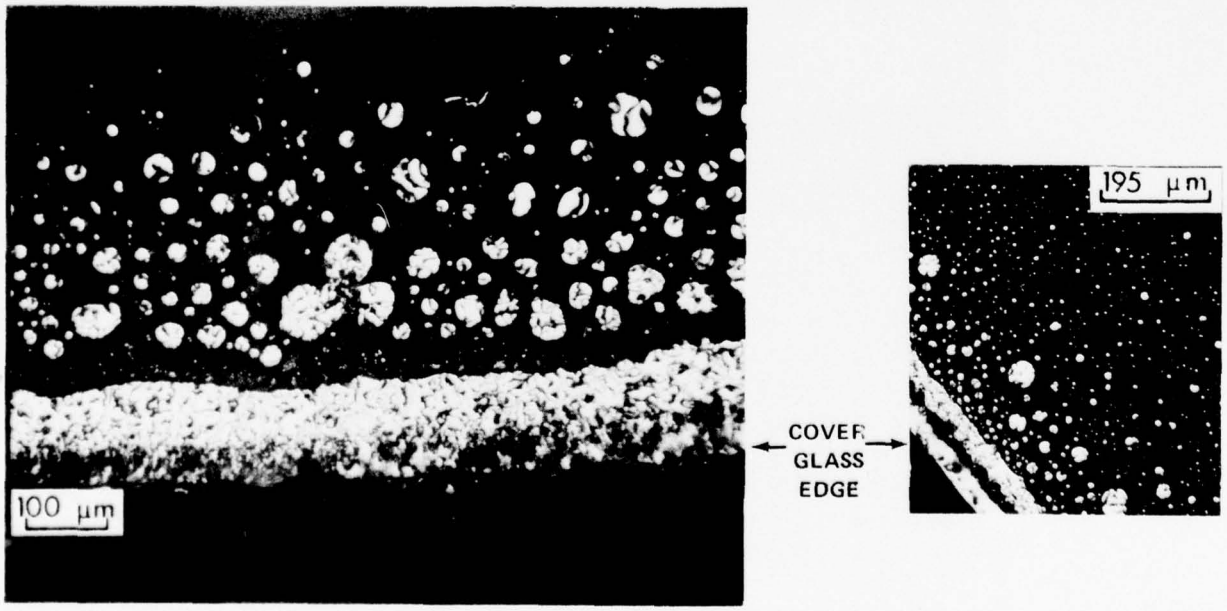

FIG. 55. BANDS OF COALESCED MESOPHASE AT THE EDGE OF THE SAMPLE COVER GLASS

FIG. 56 BANDS OF COALESCED MESOPHASE WHICH FORMED AT THE EDGE OF THE LIQUID SAMPLE DURING HOT STAGE PYROLYSIS OF ACENAPHTHYLENE

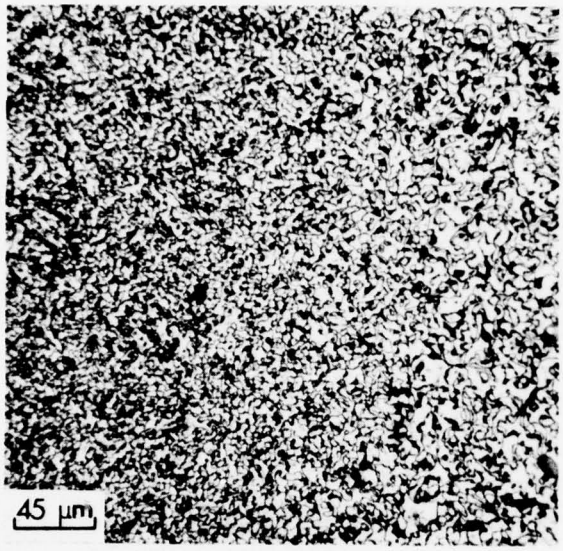

FIG. 57. COALESCED MESOPHASE WITH AN ISOTROPIC MICROSTRUCTURE FORMED DURING HEATING ACENAPHTHYLENE TO APPROXIMATELY 455°C ON THE MICROSCOPE HOT STAGE

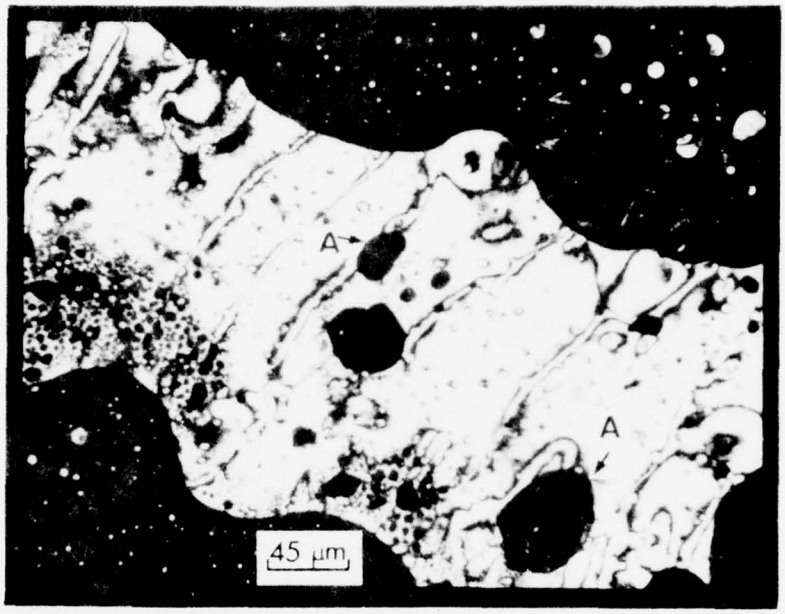

FIG. 58*. COALESCED MESOPHASE FORMED BY GAS BUBBLE PERCOLATION THROUGH AN ACENAPHTHYLENE SAMPLE PYROLYZED ON THE HOT STAGE

FIG. 59*. UNTRANSFORMED PITCH ENTRAPPED IN THE COALESCED MESOPHASE

*The black pools shown at A are regions of untransformed pitch which was entrapped as mesophase droplets were forced to coalesce rapidly due to gas bubble percolation during pyrolysis.

A wide variety of polarized light extinction contours was observed in the coalesced mesophase, and examples are given in Figures 60 through 63, pages 75 and 76. One feature common to all the examples of coalesced mesophase microstructure is the high concentration of extinction crosses. Extinction crosses are known[44] to be a result of the coalescence of mesophase spheres. The molecular arrangements which produce the extinction crosses when the sample is observed under polarized light (crossed polarizers) have also been determined by White, et al.[12] In this study, regions of coalesced mesophase larger than 500 μm in size which were formed as a result of bubble percolation were consistently found to have extinction crosses stretched out in one direction as shown in Figures 62 and 63, page 76. As illustrated at A in Figure 62, page 105, the polarized light extinction crosses took on an appearance which resembled parallel lines. It is not known if deformation due to bubble percolation causes the molecular rearrangements which produce the stretched out extinction crosses. Deformation and stretching of the coalesced mesophase by gas bubbles was so severe in some cases that the coalesced mesophase was torn apart as shown in Figure 64, page 77. Since this usually occurred in less than 10 seconds, it was not possible to determine how the polarized light extinction contours changed as the coalesced mesophase was being deformed by a gas bubble. However, deformation of the coalesced mesophase just prior to hardening has been reported by White and Price[14] to form the fine fibrous microstructure characteristic of needle cokes.

Although the usefulness of hot stage microscopy in studies of mesophase formation has been demonstrated in this work, the observations must be interpreted with caution. The behavior of a liquid crystal film between glass slides may be different from that which occurs in bulk samples. Some of the conclusions resulting from observations made during hot stage pyrolysis of acenaphthylene would be expected to be invalid for pyrolysis studies conducted on bulk samples. For example, the "edge effects" discussed on pages 69-71 would not occur during pyrolysis of bulk samples in large test tubes. Gas bubbles can move in only two dimensions in samples pyrolyzed between glass slides on the hot stage. As a result, mesophase droplets are pushed together and forced to coalesce by gas bubble movement. The coalesced droplets form an outline of the bubble path. Once these mesophase droplets become firmly attached to the glass slide, additional bubble movement in the same region will usually follow the previously established bubble path.

At some point after mesophase formation begins during pyrolysis of acenaphthylene in test tubes, the size and number of mesophase spheres becomes so large that gas bubble percolation could not occur without pushing numerous mesophase spheres together. Therefore, it is believed that bubble percolation in bulk samples leads to accelerated coalescence in a manner similar to that observed during the hot stage pyrolysis experiments. In bulk samples, gas bubbles produced during pyrolysis are free to move randomly in three dimensions and are less likely to repeatedly move along the same path as in the hot stage pyrolysis experiments. Therefore, one would not expect to see strings of coalesced mesophase spheres outlining bubble paths in samples pyrolyzed in bulk. As the mesophase transformation nears completion, the viscosity and percent of coalesced mesophase increases to an extent that any bubble percolation in bulk samples would cause stretching and tearing of the mesophase as observed during hot stage pyrolysis (See Figure 64, page 77).

FIG. 60. REGION OF COALESCED MESOPHASE CONTAINING A HIGH CONCENTRATION OF EXTINCTION CROSSES

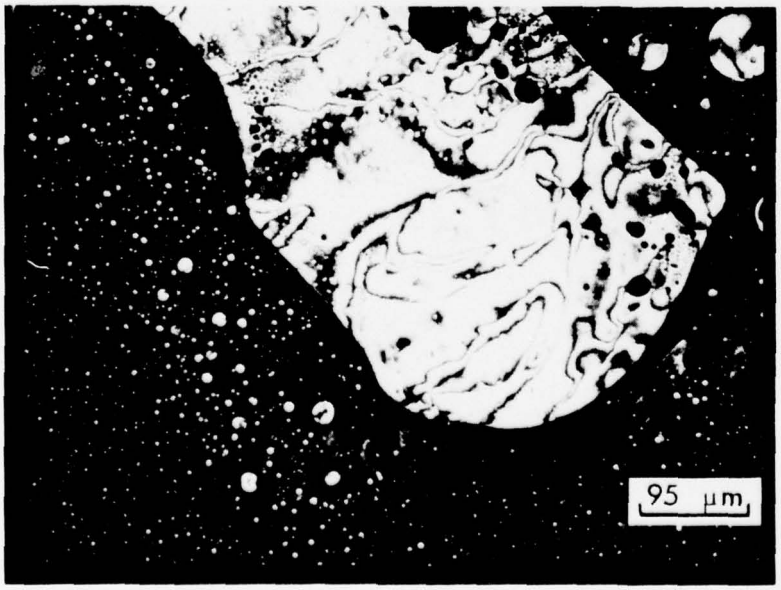

FIG. 61. LARGE DROPLET OF COALESCED MESOPHASE FORMED DURING HOT STAGE PYROLYSIS OF ACENAPHTHYLENE

FIG. 62. STRETCHED OUT EXTINCTION CROSSES IN THE COALESCED MESOPHASE

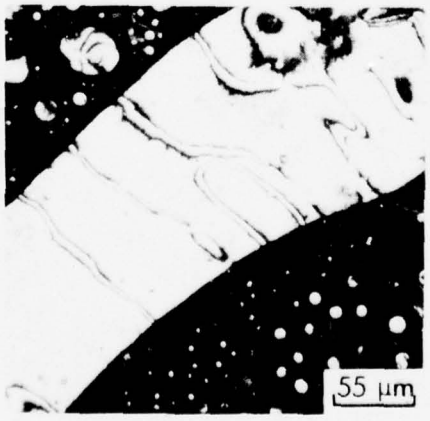

FIG. 63. EXTINCTION CROSSES DEFORMED TO PRODUCE NEARLY PARALLEL LINES IN THE COALESCED MESOPHASE FROM PYROLYSIS OF ACENAPHTHYLENE

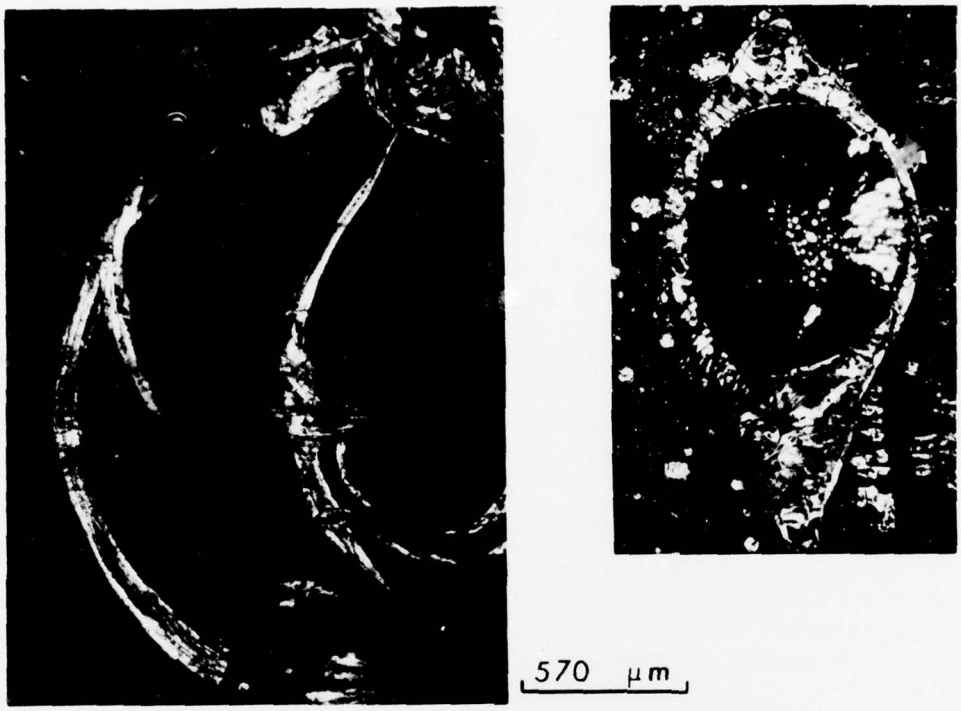

FIG. 64. MESOPHASE DROPLETS STRETCHED AND TORN APART DUE TO STRESSES CAUSED BY GAS BUBBLE FORMATION AND MOVEMENT

3. Formation of Fibrous Extinction Crosses

The type of microstructure illustrated by Figure 65 has been observed in six different samples of acenaphthylene pyrolyzed in the microscope hot stage at temperatures between 420°C and 450°C. However, it has never been observed in samples of acenaphthylene pyrolyzed in test tubes. As shown in Figure 65, regions as large as 1 mm have been observed in which only extinction crosses of various sizes are present. The crosses are all orientated in the same direction and have a fibrous or thread-like character. In one case (see Figure 66) an extinction cross of about 1 mm in diameter was observed in an acenaphthylene sample heated to about 450°C. This type of extinction cross observed using polarized light may be classified as a co-rotating cross[12] or a fixed type integral nucleus[83] since the brushes of the cross rotate clockwise as the plane of polarization of the incident light is rotated clockwise (see Figure 67, page 80). Regions composed of fibrous extinction crosses have been observed next to the top and bottom cover glasses using reflected polarized light. The same patterns were also observed using transmitted polarized light.

Some samples heated on the hot stage did not produce the fibrous extinction crosses. When present, the fibrous crosses were always observed to occur together in a cluster in only one region of the sample, and were near the edge of the liquid film between the glass slides. The fibrous extinction crosses were usually observed in a thin film attached to either the top or bottom cover glass. This film was thin compared to the thickness of the mesophase sample between the cover glasses. In some cases, droplets of coalesced mesophase are left attached to the glass slides when gas bubbles rapidly push the fluid, untransformed pitch material away. Since the bulk mesophase is opaque, regions of coalesced mesophase appear black when observed using transmitted light as in Figure 68. The white areas in Figure 68 represent regions where there is no pitch or mesophase, or regions where there is a thin film which is transparent. Gray areas surrounded by black in Figure 68 also represent thin film regions somewhat transparent to light. The same area observed using reflected polarized light is illustrated in Figure 69. Fibrous extinction crosses appear in those regions which were shown in Figure 68 to contain transparent thin films. If one were to illustrate this with a diagram, it would appear as given below:

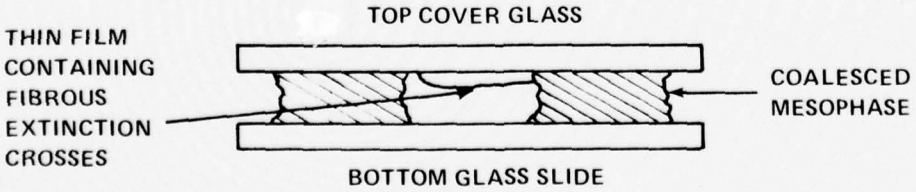

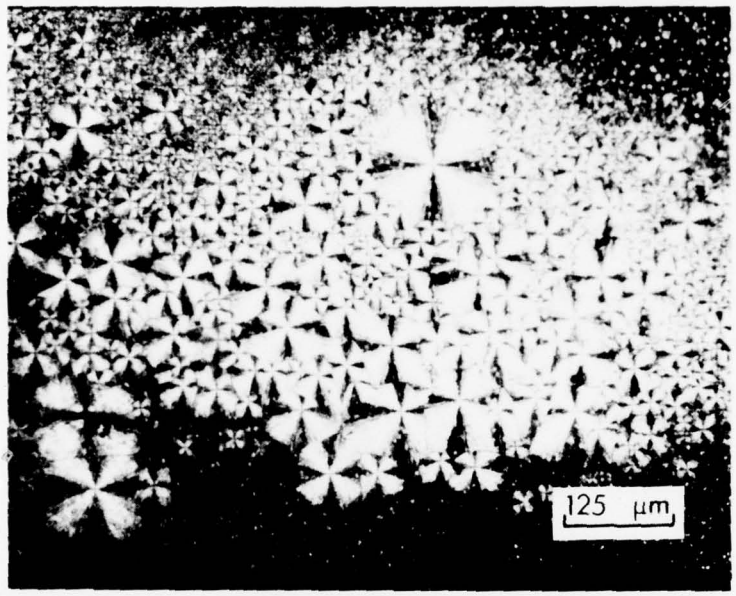

FIG. 65. FIBROUS EXTINCTION CROSSES OBSERVED IN A SAMPLE OF ACENAPHTHYLENE PYROLYZED ON THE MICROSCOPE HOT STAGE

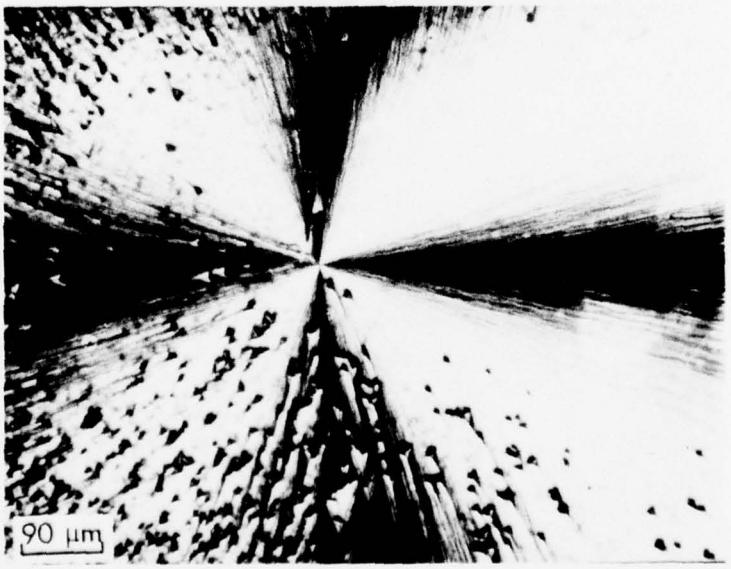

FIG. 66. SINGLE EXTINCTION CROSS ILLUSTRATING THE FIBROUS NATURE OF THE EXTINCTION CROSS BRUSHES

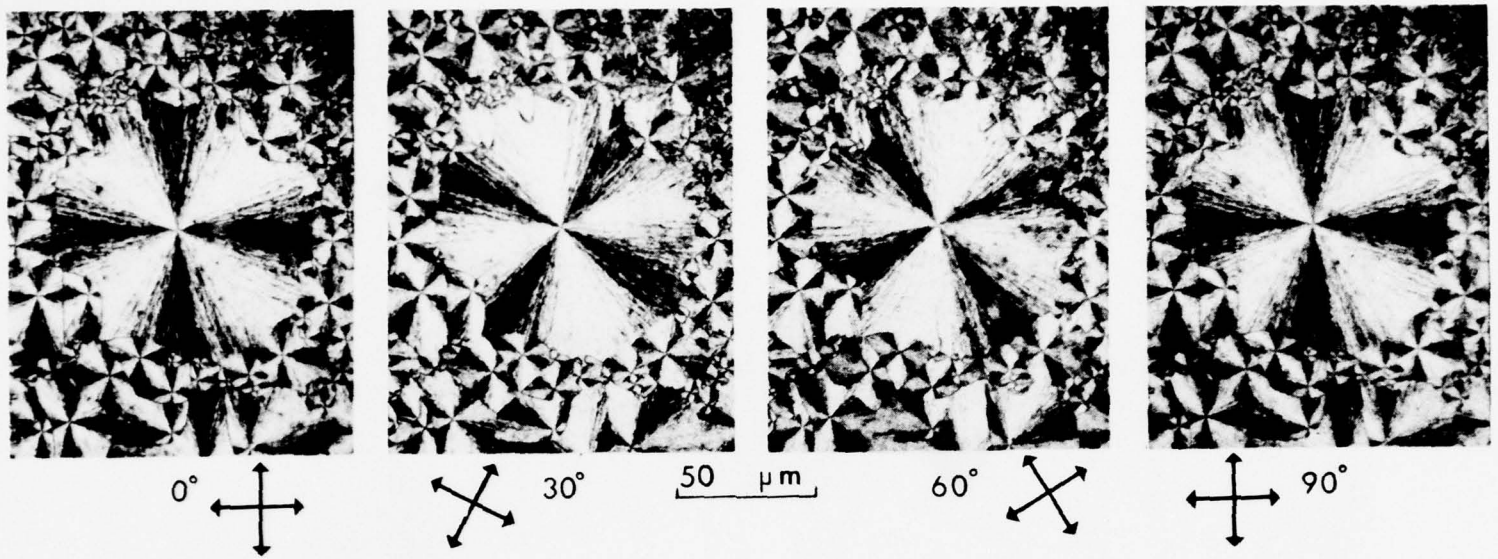

FIG. 67. CHANGES IN THE ORIENTATION OF FIBROUS EXTINCTION CROSSES DUE TO CLOCKWISE ROTATION OF THE PLANE OF POLARIZED LIGHT (CROSSED POLARIZERS)

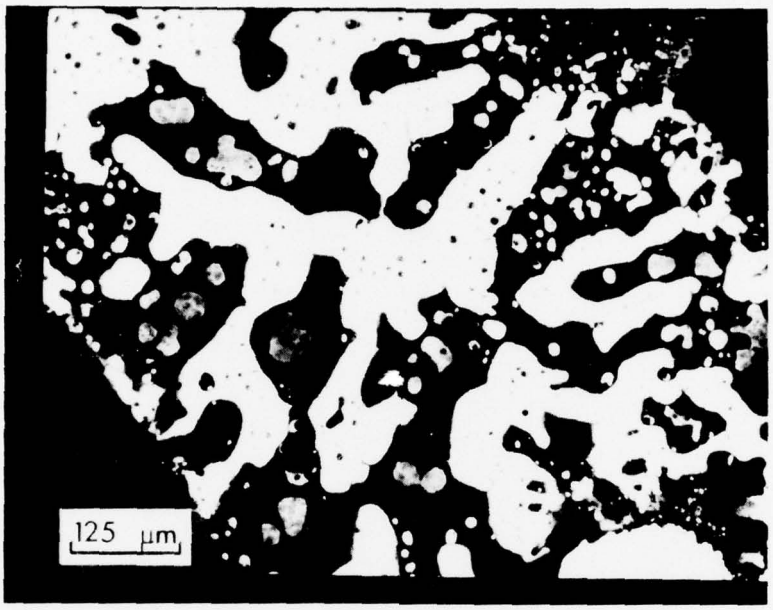

FIG. 68. TRANSMITTED LIGHT PHOTOMICROGRAPH OF ACENAPHTHYLENE PYROLYZED ON THE HOT STAGE

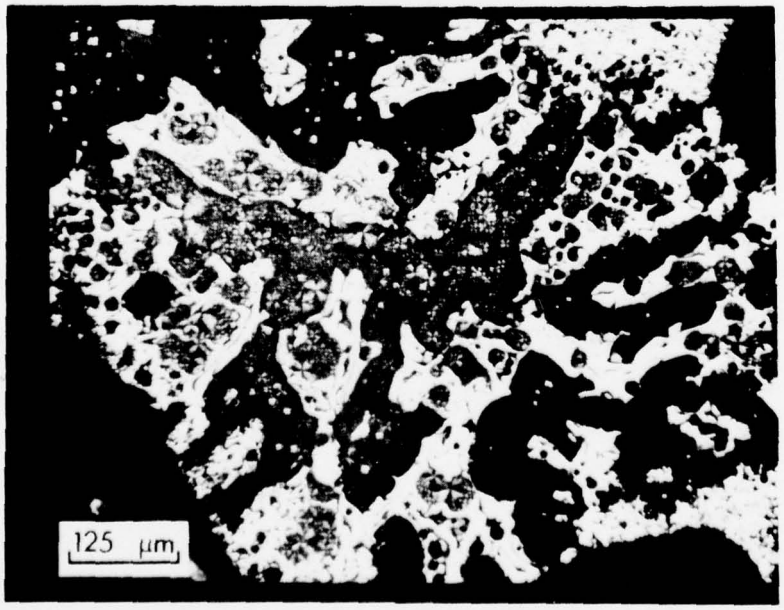

FIG. 69. REFLECTED POLARIZED LIGHT (CROSSED POLARIZERS) PHOTOMICROGRAPH OF THE SAME REGION SHOWN IN FIGURE 68

The glass slides containing pyrolyzed samples of acenaphthylene were separated in three instances. Fibrous extinction crosses were observed using reflected polarized light directed on the surface of the pyrolysis residue. The thin film on a cover glass containing the fibrous extinction crosses was easily scraped from the glass surface with a needle point.

Fibrous extinction crosses are different from the normal extinction crosses observed in cross sections of an ideal mesophase sphere (Figure 70), coalesced mesophase droplets (Figure 71, page 84), or large regions of coalesced mesophase formed between glass slides on the hot stage (Figure 72, page 85). Extinction crosses in the mesophase from acenaphthylene or any other organic have never been reported to have the fibrous brushes as shown in Figure 66, page 79. The fibrous crosses were observed in one sample of acenaphthylene heated to 380°C - 400°C on the hot stage. In this experiment, no mesophase was formed. These results indicate that the fibrous extinction crosses are a result of crystallization of some organic by-product produced during the pyrolysis of acenaphthylene. Since it forms in a thin film on the cover glasses near the edge of a pitch-mesophase region, it probably is a volatile by-product which condenses and crystallizes on rapid cooling of the sample to room temperature (possibly polyacenaphthylene). Microstructures similar to those shown in Figures 65-67, pages 79 and 80 are common in liquid crystal systems such as cholesteryl acetate,[84] and polymers such as polyethylene and polycarbonates crystallized from the melt.[85]

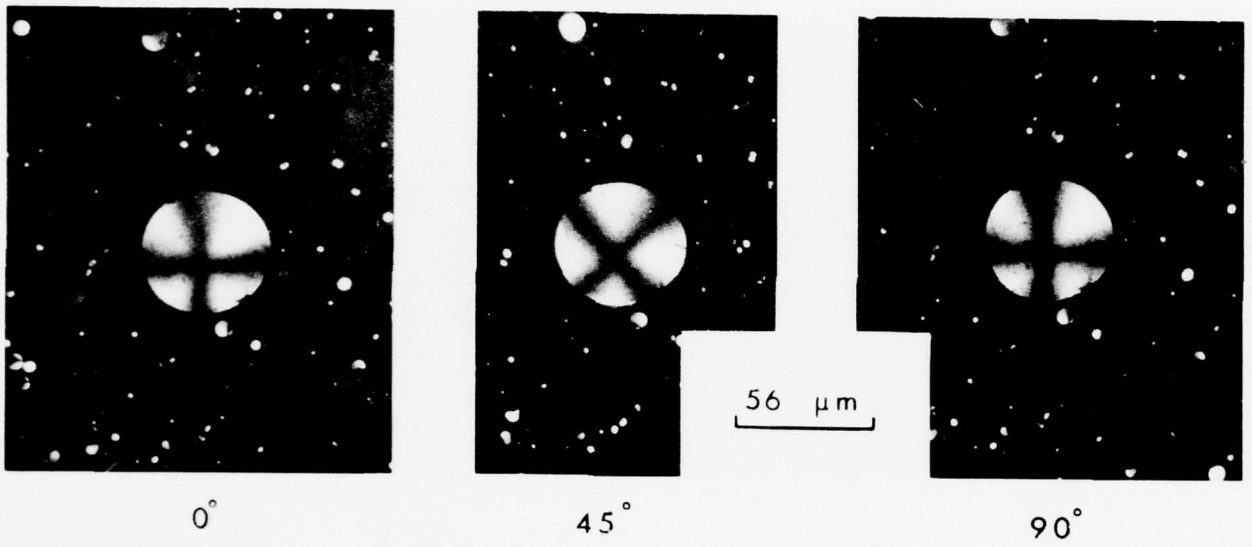

FIG. 70. POLISHED CROSS SECTION OF AN IDEAL MESOPHASE SPHERE SECTIONED PERPENDICULAR TO ITS AXIS ABOVE OR BELOW THE MEDIAN PLANE

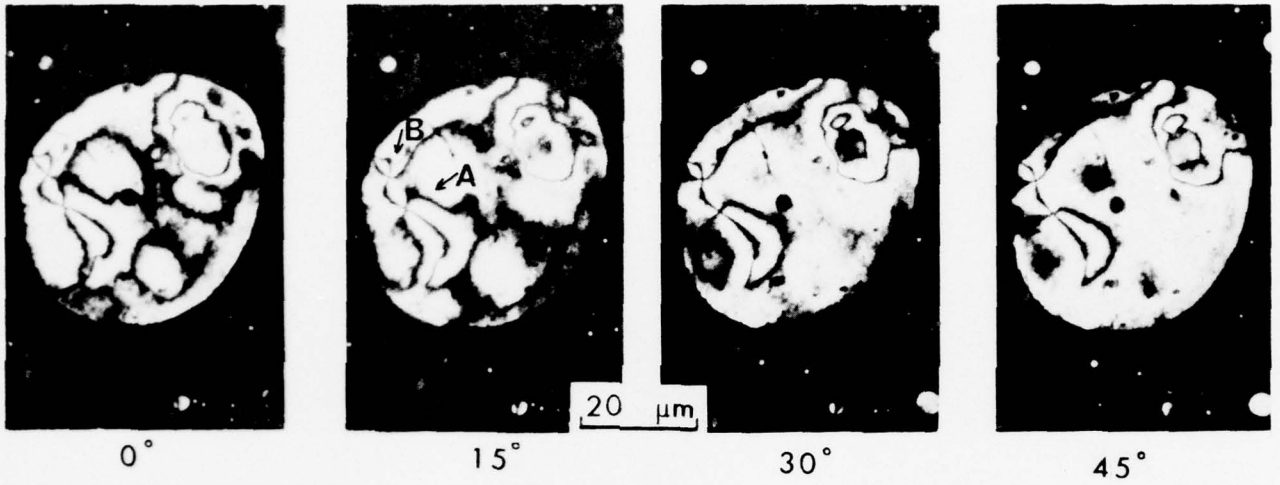

FIG. 71. CO-ROTATING (A) AND COUNTER-ROTATING (B) EXTINCTION CROSSES IN A DROPLET OF COALESCED MESOPHASE

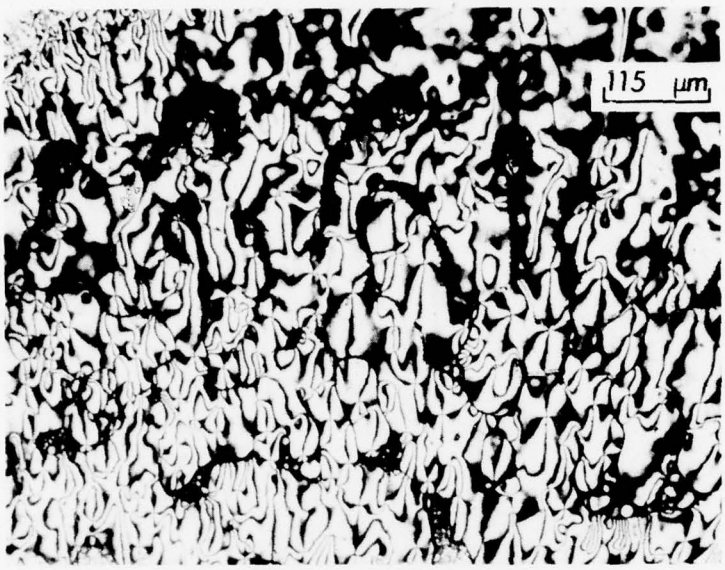

FIG. 72. EXTINCTION CROSSES IN COALESCED MESOPHASE FORMED DURING PYROLYSIS OF ACENAPHTHYLENE ON THE MICROSCOPE HOT STAGE

CHAPTER V

CONCLUSIONS AND RECOMMENDATIONS

Mesophase sphere formation, growth, and coalescence during pyrolysis of acenaphthylene is time-temperature dependent. For the particular heating cycle used in this study, mesophase sphere formation began at approximately 400°C. Sphere growth and coalescence continued during pyrolysis until the entire sample was transformed into the coalesced mesophase between 466°C and 500°C. The mesophase formed during acenaphthylene pyrolysis is fluid over a wide temperature range (from about 400°C to at least 466°C) and has a high solidification point (between 466°C and 500°C). Both of these characteristics is indicative of a highly graphitizing organic.[14] Above 450°C, a small percent (<20%) of the coalesced mesophase was observed to form the fine fibrous microstructure which is characteristic of highly graphitizing needle cokes. The fine fibrous microstructure was usually associated with gas bubbles. This provides additional evidence to support White's suggestion[14] that gas bubble percolation through a fluid coalesced mesophase just prior to mesophase solidification is responsible for formation of the fine fibrous microstructure.

The usefulness of hot stage microscopy as a technique for investigating mesophase formation was demonstrated in this study. Direct observation of mesophase formation in acenaphthylene during hot stage pyrolysis revealed that gas bubbles move mesophase droplets around, crowd them together along the gas bubble-liquid pitch interface, and cause the droplets to coalesce. Apparently, a mechanical stress such as that produced by gas bubble percolation increases the rate of coalescence compared to that which would normally occur in the absence of bubble percolation. Gas bubble formation and percolation also stresses the coalesced mesophase, which must constantly undergo rearrangement of the ordered molecules to relieve the applied stress. The physical action of gas bubble percolation must now be added to the list of factors which control the mesophase microstructure. In addition, the rate of gas bubble percolation and the temperature at which pyrolysis gases are formed must be considered as factors which may influence mesophase growth and coalescence.

In order to develop an improved understanding of how the various types of mesophase microstructure are formed during acenaphthylene pyrolysis, several areas of study should be pursued. The absence of the fine fibrous microstructure in samples pyrolyzed on the hot stage is believed to be due to the use of small samples and insufficiently low pyrolysis temperatures (455°C). Therefore, additional hot stage experiments should be conducted at temperatures up to 500°C in an attempt to observe directly the formation of the fine fibrous microstructure. The use of thicker samples (0.5 cm or more) would also allow one to obtain cross-sectional views of the phenomenon observed directly through the top cover glass. Improved methods of measuring sample temperature on the hot stage should be developed to provide an accurate method for determination of the temperature-time conditions necessary for mesophase formation during the pyrolysis of organic materials.

Since the fine fibrous microstructure of needle cokes is believed to result from deformation of a highly fluid coalesced mesophase by gas bubble percolation, it should be possible to increase the percent of the fine fibrous microstructural component by application of a mechanical stress to the coalesced mesophase just prior to its solidification. Such an approach may lead to the development of a new method to produce improved needle cokes for use in artificial graphite manufacture.

ACKNOWLEDGMENTS

Thanks are especially due to Mr. Frank Koubek and Mr. Leo F. Gowen of the Naval Surface Weapons Center, White Oak Laboratory, for financial support of this work. The assistance and interest of Dr. Raj K. Khanna in this research project and the numerous enlightening discussions with Dr. J. L. White of the Aerospace Corporation are also acknowledged. Finally, special appreciation is due to my wife, Carolyn, who endured much during this work and whose support and encouragement made this thesis possible.

REFERENCES

1. Mantell C. L., Carbon and Graphite Handbook, pp. 8-10, 32. Interscience Publishers, New York (1968).

2. Edstrom T. and Lewis I. C., Carbon 7, 85 (1969).

3. Improved Graphite Materials for High Temperature Aerospace Use, U. S. AFML Report No. ML-TDR-64-125, Vol. I. Air Force Materials Laboratory, Ohio (1964).

4. Lewis I. C., Polymer Preprints 14, 380 (1973).

5. Fitzer E. and Mueller K., Ber. Dtsch. Keram. Ges. 48, 269 (1971).

6. Brooks J. D. and Taylor G. H., In Advances in Chemistry Series (Edited by R. F. Gould), Vol. 55, pp. 549-563. American Chemical Society, Washington, D. C. (1966).

7. Brooks J. D. and Taylor G. H., Nature 206, 697 (1965).

8. Brooks J. D. and Taylor G. H., Carbon 3, 185 (1965).

9. Brooks J. D. and Taylor G. H., In Chemistry and Physics of Carbon (Edited by P. L. Walker, Jr.), Vol. 4, pp. 243-286. Marcel Dekker, New York (1968).

10. Dubois J., Agache C., and White J. L., Metallography 3, 337 (1970).

11. White J. L., Guthrie G. L., and Gardner J. O., Carbon 5, 517 (1967).

12. White J. L., Dubois J., and Souillart C. A., J. Chim Phys. Special Volume, 33 (1969); Available in English as EURATOM Report EUR 4094e (1969).

13. White J. L. and Price R. J., Abstracts of the 11th Biennial Conference on Carbon, p. 209. American Carbon Committee (1973).

14. White J. L. and Price R. J., Carbon 12, 321 (1974).

15. Horne O. J., Jr., Mesophase Formation in Polymers of Cinnamylideneindene and Acenaphthylene, Oak Ridge Y-12 Plant Report No. Y-1799. Union Carbide Corp. - Nuclear Division, Oak Ridge, Tn. (1971)

16. Lewis I. C. and Singer L. S., Abstracts of the 10th Biennial Conference on Carbon, p. 104. American Carbon Committee (1971).

17. Ramdohr P., Eisenhuttenwesen 1, 669 (1928).

18. Mackowsky M., Fortschr. Mineral 29/30, 10 (1951).

19. Martin S. W. and Shea F. L., Jr., Ind. Eng. Chem. 50, 41 (1958).

20. Kipling J. J., Sherwood J. N., Shooter P. V., and Thompson N. R., Carbon 1, 315 (1964).

21. Kipling J. J. and Shooter P. V., Proceedings of the Second Conference on Industrial Carbon and Graphite. Society of Chemical Industry, London (1965).

22. Kipling J. J. and Shooter P. V., Carbon 4, 1 (1966).

23. Kipling J. J. and Shooter P. V., Paper Presented at the 7th Biennial Conference on Carbon, Paper No. 48, Cleveland (1965).

24. Ihnatowicz M., Chiche P., Deduit J., Pregermain S., and Tournant R., Carbon 4, 41 (1966); Available in English as General Atomic Report GA-tr-7382 (1967).

25. Fitzer E., Mueller K., and Schaefer W., In Chemistry and Physics of Carbon (Edited by P. L. Walker, Jr.), Vol. 7, pp. 237-383. Marcel Dekker, New York (1971).

26. Taylor G. H., Fuel 40, 465 (1961).

27. Lewis I. C. and Edstrom T., Proceedings of the Fifth Conference on Carbon, pp. 413-430. Pergamon Press, Oxford (1963).

28. Marsh H., Dachille F., Melvin J., and Walker P. L., Jr., Carbon 9, 159 (1971).

29. Evans S. and Marsh H., Carbon 9, 733 (1971).

30. Evans S. and Marsh H., Abstracts of the 9th Biennial Conference on Carbon, p. 217. American Carbon Committee (1969).

31. Evans S. and Marsh H., Carbon 9, 747 (1971).

32. Singler L. S. and Cherry A. R., Abstracts of the 9th Biennial Conference on Carbon, p. 49. American Carbon Committee (1969).

33. Lewis I. C. and Singer L. S., Carbon 7, 93 (1969).

34. Lewis I. C. and Edstrom T., J. Org. Chem. 28, 2050 (1963).

35. Singer L. S. and Lewis I. C., Research and Development on Advanced Graphite Materials, U. S. AFML Report No. WADD TR 61-72, Vol. XVI. Air Force Materials Laboratory, Ohio (1963).

36. Singer L. S. and Lewis I. C., Carbon 2, 115 (1964).

37. Lewis I. C. and Edstrom T., Research and Development on Advanced Graphite Materials, U. S. AFML Report No. WADD TR 61-72, Vol. X. Air Force Materials Laboratory, Ohio (1962).

38. Lewis I. C. and Edstrom T., Research and Development on Advanced Graphite Materials, U. S. AFML Report No. WADD TR 61-72, Vol. XXVII. Air Force Materials Laboratory, Ohio (1963).

39. Singer L. S. and Lewis R. T., Abstracts of the 11th Biennial Conference on Carbon, p. 207. American Carbon Committee (1973).

AD-A044 631 NAVAL SURFACE WEAPONS CENTER WHITE OAK LAB SILVER SP--ETC F/G 7/3
THE EFFECT OF GAS BUBBLE PERCOLATION ON THE CARBONACEOUS MESOPH--ETC(U)
SEP 76 D O RESTER

UNCLASSIFIED NSWC/WOL/TR-76-113 NL

2 OF 2
ADA044631

END
DATE FILMED
10-77
DDC

40. Yamada Y., Imamura T., Kakiyama H., Honda H., Oi S., and Kukuda K., Carbon 12, 307 (1974).

41. Yamada Y., Imamura T., Kakiyama H., and Honda H., Abstracts of the 11th Biennial Conference on Carbon, p. 213. American Carbon Committee (1973).

42. Whittaker M. P. and Grindstaff L. I., Carbon 10, 165 (1972).

43. Foster J. M., Iley M., Marsh H., and Melvin J., Paper Presented at the International Carbon Conference, Paper No. Ch 1, Baden-Baden, W. Germany (1972).

44. Honda H., Kimura H., and Sanada Y., Carbon 9, 695 (1971).

45. Honda H., Yamada Y., Oi S., and Fukuda K., Abstracts of the 11th Biennial Conference on Carbon, p. 219. American Carbon Committee (1973).

46. Gray G. W., Molecular Structure and the Properties of Liquid Crystals, pp. 31-67. Academic Press, New York (1962).

47. Hüttinger K. J., Abstracts of the 10th Biennial Conference on Carbon, p. 100. American Carbon Committee (1971).

48. Honda H., Kimura H., Sanada Y., Sugawara S., and Furuta T., Carbon 8, 181 (1970).

49. Honda H., Kimura H., Sanada Y., Sugawara S., and Furuta T., Abstracts of the 9th Biennial Conference on Carbon, p. 173. American Carbon Committee (1969).

50. Sanada Y., Furuta T., Kimura H., and Honda H., Abstracts of the 10th Biennial Conference on Carbon, p. 335. American Carbon Committee (1971).

51. Price R. J. and White J. L., Abstracts of the 10th Biennial Conference on Carbon, p. 133. American Carbon Committee (1971).

52. Hüttinger K. J., Proceedings of the Third Conference on Industrial Carbon and Graphite, Society of Chemical Industry, London (1970).

53. Hüttinger K. J., Bitumen-Teere-Asphalte-Peche 24, 1 (1973).

54. Horne O. J., Jr., Smith W. E., and Napier B., Properties of Carbons Derived from Acenaphthylene and Cinnamylideneindene, Oak Ridge Y-12 Plant Report No. Y-1880. Union Carbide Corp. - Nuclear Division, Oak Ridge, Tn. (1973).

55. Horne O. J., Jr., Smith W. E., and Napier B., Properties of Carbon Derived from Petroleum Pitches, Oak Ridge Y-12 Plant Report No. Y-1875. Union Carbide Corp. - Nuclear Division, Oak Ridge, Tn. (1973).

56. Smith W. E. and Harper W. L., Abstracts of the 9th Biennial Conference on Carbon, p. 27. American Carbon Committee (1969).

57. Smith W. E., Napier B., and Harper W. L., Preparation and Characterization of Hydrocarbon Derivatives of Indene, Oak Ridge Y-12 Plant Report No. Y-1712. Union Carbide Corp. - Nuclear Division, Oak Ridge, Tn. (1970).

58. Smith W. E., Horne O. J., Jr., Napier B., Larson E. A., and Harper W. L., Properties of Carbon Derived from Indene Compounds, Oak Ridge Y-12 Plant Report No. Y-1790. Union Carbide Corp. - Nuclear Division, Oak Ridge, Tn. (1971).

59. Horne O. J., Jr., Abstracts of the 11th Biennial Conference on Carbon, p. 108. American Carbon Committee (1973).

60. Horne, O. J., Jr., Polymer Preprints 14, 416 (1973)

61. Walker P. L., Jr., Whang P., Dachille F., Hirano S., and Marsh H., Paper Presented at the International Carbon Conference, Paper No. Ch 2, Baden-Baden, W. Germany (1972).

62. Walker P. L., Jr. and Weinstein A., Carbon 5, 13 (1967).

63. Marsh H., Foster J., Hermon G., and Iley M., Carbon 11, 424 (1973).

64. Marsh H., Fuel 52, 205 (1973).

65. Marsh H., Foster J., Hermon G., and Iley M., Fuel 52, 234 (1973).

66. Marsh H., Foster J., Hermon G., Iley M., and Melvin J., Fuel 52, 243 (1973).

67. Marsh H., Dachille F., Iley M., Walker P., Jr., and Whang P., Fuel 52, 253 (1973).

68. Marsh H., Hermon G., and Cornford C., Fuel 53, 168 (1974).

69. Lewis I. C. and Singer L. S., Abstracts of the 9th Biennial Conference on Carbon, p. 120. American Carbon Committee (1969).

70. Kipling J. J., Shooter P. V., and Young H. N., Carbon 4, 333 (1966).

71. Brown H. R., Hesp W. R., and Taylor G. H., Carbon 4, 193 (1966).

72. Fitzer E., Hüttinger K. J., and Tillmanns H., Abstracts of the 11th Biennial Conference on Carbon, p. 112. American Carbon Committee (1973).

73. Fitzer E., Hüttinger K. J., and Tillmanns H., Paper Presented at the International Carbon Conference, Paper No. Ch 6, Baden-Baden, W. Germany (1972).

74. Walker P. L., Jr., Carbon 10, 369 (1972).

75. Whang P., Dachille F., and Walker P. L., Jr., Abstracts of the 11th Biennial Conference on Carbon, p. 114. American Carbon Committee (1973).

76. Hüttinger K. J., Paper Presented at the International Carbon Conference, Paper No. Ch 3, Baden-Baden, W. Germany (1972).

77. Fitzer E., Fritz W., and Megalopoulos A., Paper Presented at the International Carbon Conference, Paper No. Ch 5, Baden-Baden, W. Germany (1972).

78. Hüttinger K. J., Erdöl und Kohle 26, 21 (1973).

79. Gilliam H. K. and Whittaker M. P., Abstracts of the 11th Biennial Conference on Carbon, p. 211. American Carbon Committee (1973).

80. Ruland W., Carbon 2, 365 (1965).

81. Lang K. and Zander M., Chem. Ber. 94, 1871 (1961).

82. Sharkey A. G., Jr., Shultz J. L., and Friedel R. A., Carbon 4, 365 (1966).

83. Hartshorne N. H. and Stuart A., Crystals and the Polarizing Microscope, pp. pp. 503-555. American Elsevier Publishing Co., Inc., New York (1970).

84. McCrone W. and Johnson R., Techniques, Instruments and Accessories For Microanalysts, pp. 82-85. McCrone Associates, Inc., Chicago (1974).

85. Billmeyer F. W., Jr., Textbook of Polymer Science, pp. 148-152. Interscience Publishers, New York (1966).

DISTRIBUTION

	Copies
Office of the Secretary of Defense Director of Defense Research and Engineering Washington, D.C. 20301	
Attn: Mr. J. Persh (OAD/ET)	1
Dr. R. Ruffine (OAD/SW)	1
Mr. G. Barse (OAD/OS)	1
Assistant Secretary of the Navy (Research and Development) Washington, D.C. 20301	
Attn: Dr. S. Koslov	1
Office of the Chief of Naval Operations Department of the Navy Washington, D.C. 20350	
Attn: Mr. R. Blaise (OP-620E)	1
Office of the Chief of Naval Material Department of the Navy Washington, D.C. 20360	
Attn: (MAT-0342)	1
Office of Naval Research Arlington, Virginia 22217	
Attn: Dr. Art Diness (Code 471)	1
Commander, Naval Sea Systems Command Naval Sea Systems Command Headquarters Washington, D.C. 20362	
Attn: Mr. M. A. Kinna (SEA-0352)	1
Dr. J. H. Huth (SEA-03C)	1
Mr. G. Sorkin (SEA-035)	1
SEA-09G32 2 SEA-03B	1
Director, Strategic Systems Project Office (PM-1) Department of the Navy Washington, D.C. 20376	
Attn: Mr. M. Messerole (SP-272)	1
Dr. J. Kincaid, Consultant (SP-20)	1
Mr. D. R. Williams (SP-2720)	1
Mr. H. McMasters (SP-2723)	1

DISTRIBUTION (Cont.)

	Copies
Project Manager, Trident Systems Project (CNM-PM 2) Department of the Navy Washington, D.C. 20360 Attn: Mr. J. L. Crone (PM-2-001)	1
Director, Defense Nuclear Agency Washington, D.C. 20305 Attn: Dr. M. Atkins	1
Mr. D. Kohler	1
Mr. J. Moulton	1
Director, Naval Research Laboratory Washington, D.C. 20375 Attn: Dr. S. Freiman	1
Mr. P. Mast	1
Space and Missile Systems Organization (AFSC) Worldway Postal Center P. O. Box 92960 Los Angeles, California 90009 Attn: CAPT R. Engelbrecht, USN /RSN	1
COL L. Norris/RS	1
CAPT D. Jackson/RSSE	1
LTCOL McCormack/RSSE	1
CAPT H. Careway/RSSE	1
CAPT C. Jones/RSSE	1
Commander Naval Air Systems Command Department of the Navy Washington, D.C. 20361 Attn: Mr. R. Schmidt (AIR-52031A)	1
Air Force Materials Laboratory Wright-Patterson Air Force Base, Ohio 45433 Attn: Mr. D. Schmidt	1
Mr. C. Pratt	1
Air Force Weapons Laboratory Kirtland Air Force Base Albuquerque, New Mexico 87117 Attn: LTCOL David Ericson	1
Army Materials and Mechanics Research Center Watertown, Massachusetts 02172 Attn: Mr. J. F. Dignam	1
Plastics Technical Evaluation Center Department of Defense Picatinny Arsenal Dover, New Jersey 07801 Attn: Mr. A. M. Anzalone (Building 176)	1

DISTRIBUTION (Cont.)

	Copies
Aerospace Corporation P. O. Box 92957 Los Angeles, California 90009	
Attn: Dr. R. A. Meyer	1
Mr. R. Mortensen	1
Mr. S. Evangelides	1
Dr. J. White	1
Mr. J. Zimmer	1
Battelle Columbus Laboratories 505 King Avenue Columbus, Ohio 43201	
Attn: Mr. W. Chard	1
Lockheed Missiles and Space Company P. O. Box 504 Sunnyvale, California 94088	
Attn: Mr. A. Mietz	1
Mr. V. Mamoni	1
Los Alamos Scientific Laboratory University of California P. O. Box 1663 Los Alamos, New Mexico 87544	
Attn: Dr. J. Taylor	1
Sandia Laboratories Albuquerque, New Mexico 87115	
Attn: Mr. D. Northrup	1
AVCO Corporation AVCO Systems Division 201 Lowell Street Wilmington, Massachusetts 01887	
Attn: Mr. Paul G. Rolincik	1
Fiber Materials, Inc. Biddeford Industrial Park Biddeford, Maine 04005	
Attn: Mr. R. Burns	1
Franklin Institute Research Laboratories Physics of Materials Laboratory Material and Physical Sciences Department Benjamin Franklin Parkway Philadelphia, Pennsylvania 19103	
Attn: Mr. J. D. Meakin, Manager	1

DISTRIBUTION (Cont.)

	Copies
General Electric Company Re-Entry and Environmental Systems Division Valley Forge Space Center P. O. Box 8555 Philadelphia, Pennsylvania 19101 Attn: Mr. K. Hall	1
McDonnell Douglas Astronautics Company 5301 Bolsa Avenue Huntington Beach, California 92647 Attn: Mr. J. Jortner	1
Mr. R. Siebold	1
Great Lakes Carbon Corporation Graphite Products Division P. O. Box 667 Niagara Falls, N.Y. 14302 Attn: Dr. L. H. Juel	1
Science Applications, Inc. 201 W. Dyer Road, Unit C Santa Ana, California 92707 Attn: Mr. D. Eitman	1
Prototype Development Associates, Inc. 1740 Garry Avenue, Suite 201 Santa Ana, California 92705 Attn: Dr. J. McDonald	1
Southern Research Institute 2000 Ninth Avenue, South Birmingham, Alabama 35205 Attn: Mr. C. D. Pears	1
Mr. J. Koenig	1
Great Lakes Research Corporation Box 1031 Elizabethton, Tennessee 37643 Attn: Dr. L. Joo	1
Union Carbide Corporation Parma Research Laboratory P. O. Box 6116 Cleveland, Ohio 44101 Attn: Dr. J. Criscione	1
Mr. R. Mercuri	1
Mr. R. T. Lewis	1
Dr. I. C. Lewis	1
Mr. L. S. Singer	1

DISTRIBUTION (Cont.)

	Copies
Union Carbide Corporation Nuclear Division (Y-12 Plant) P. O. Box Y Oak Ridge, Tennessee 37830 Attn: Mr. G. Marrow	1
Oak Ridge National Laboratory P. O. Box X Oak Ridge, Tennessee 37830 Attn: Mr. R. Kennedy	1
Mr. W. Eatherly	1
Department of Material Sciences Pennsylvania State University University Park, PA 16802 Attn: Dr. P. L. Walker, Jr.	1
Ashland Petroleum Company P. O. Box 391 Ashland, Kentucky 41101 Attn: Mr. John Newman	1
Ashland Chemical Company P. O. Box 2458 Columbus, Ohio 42316 Attn: Dr. James E. Lewis	1
University of Maryland Department of Chemistry College Park, Maryland 20742 Attn: Dr. Raj K. Khanna	1
Thomas J. Watson Research Center P. O. Box 218 Yorktown Heights, N.Y. 10598 Attn: Mr. M. H. Brodsky	1

DISTRIBUTION (Cont.)

	Copies
Liquid Crystal Institute Kent State University Kent, Chio Attn: Dr. G. H. Brown	1
Defense Documentation Center Cameron Station Alexandria, Virginia 22314	12